U.PORTO

DOUTORAMENTO
BIOLOGIA BÁSICA E APLICADA

The role of YAP and TAZ in sprouting angiogenesis

Filipa Maia Neto

D
2018

U.PORTO

Filipa Maia Neto. The role of YAP and TAZ in sprouting angiogenesis

D.ICBAS **2018**

The role of YAP and TAZ in sprouting angiogenesis

Filipa Maia Neto

SEDE ADMINISTRATIVA

INSTITUTO DE CIÊNCIAS BIOMÉDICAS ABEL SALAZAR
FACULDADE DE CIÊNCIAS
FACULDADE DE MEDICINA

FILIPA FERREIRA MAIA NETO

THE ROLE OF YAP AND TAZ IN SPROUTING ANGIOGENESIS

Tese de Candidatura ao grau de Doutor em Biologia Básica e Aplicada submetida ao Instituto de Ciências Biomédicas Abel Salazar da Universidade do Porto.

Orientador – Doutor Holger Gerhardt

Categoria – Investigador principal

Afiliação – Max Delbrück Center for Molecular Medicine, Berlin

Coorientador – Doutor João Relvas

Categoria – Investigador principal

Afiliação – I3S Instituto de Investigação e Inovação em Saúde, Porto de Ciências Biomédicas Abel Salazar da Universidade do Porto.

Às minhas irmãs

The stone aims to be nothing but a stone. But in collaboration, it congregates and becomes a temple.

Antoine de Saint-Exupéry, Citadelle

Resumo

O funcionamento de cada célula no organismo depende do suprimento de oxigénio e nutrientes pelos vasos sanguíneos. Assim, a formação e manutenção de redes de vasos sanguíneos é fundamental para o desenvolvimento embrionário, crescimento, homeostasia e regeneração. Praticamente todas as redes de vasos sanguíneos são formadas por "sprouting" angiogénese, um processo que tem sido extensivamente estudado nas ultimas décadas. Ainda que muitos mecanismos celulares e moleculares tenham sido descobertos, ainda não é completamente entendido como é que as células endoteliais se dividem fornecendo números adequados para a formação de novos vasos sanguíneos e se arranjam convenientemente para dar forma a redes de vasos funcionais. Neste trabalho, eu investiguei a hipótese de que YAP e TAZ, as proteínas efetoras finais da via de sinalização Hippo, são necessárias para este processo.

YAP e TAZ são essenciais para o desenvolvimento de novos vasos sanguíneos. Em ratinhos sem YAP/TAZ nas células endoteliais os novos botões vasculares são em menor número, de forma arredondada e hemorrágicos, e as redes vasculares são mais pequenas e carecem de homogeneidade. Os novos botões vasculares contêm poucas protrusões celulares e mostram agregação de células endoteliais, denotando falência das células de se distribuírem devidamente.

Vários mecanismos contribuem para este fenótipo. YAP/TAZ promovem a proliferação das células endoteliais causada pela estimulação mecânica ao nível das junções celulares por estiramento cíclico. Além disso, YAP/TAZ aumentam a migração e os rearranjos das células endoteliais, ao mesmo tempo que reduzem a permeabilidade entre as células. Assim, YAP/TAZ mantêm a integridade vascular enquanto permitem os aumentados movimentos celulares que acontecem durante a brotação de novos vasos sanguíneos. O referido efeito na migração celular e na permeabilidade é pelo menos parcialmente explicado pelo papel que YAP/TAZ exerce nas junções celulares. Aí, YAP/TAZ aumenta a rotatividade das moléculas de VE-Caderina e promove a formação de lamelipodias intermitentes associadas a junções, o tipo mais dinâmico de junções aderentes. Isto é conseguido pelo menos em parte através da redução de sinalização BMP pela transcrição de inibidores de BMP.

Juntos, estes resultados sugerem um novo modelo no qual YAP/TAZ coordenam estímulos mecânicos e sinalização BMP e mantêm a flexibilidade e integridade das junções celulares ao mesmo tempo que promovem a migração e rearranjos celulares nos novos botões vasculares

Abstract

The functioning of every cell in the organism depends on the reliable supply of oxygen and nutrients by blood vessels. Because of this, the formation and maintenance of blood vessel networks is critical for embryonic development, tissue growth, homeostasis and regeneration. Virtually all the vessel networks in the organism form by sprouting angiogenesis, a process that has been extensively studied in the past decades. Although many cellular and molecular mechanisms have been discovered, it is still poorly understood how endothelial cells arise in adequate numbers and arrange suitably to shape functional vascular networks. In this work, I investigated the hypothesis that YAP and TAZ, the final downstream effectors of the Hippo signaling pathway, are required for this process.

YAP and TAZ are critical for the development of new blood vessels. In mice lacking endothelial YAP/TAZ nascent vessel sprouts are fewer, blunted and hemorrhagic, and blood vessel networks are smaller and lack homogeneity. Nascent vessel sprouts show little cellular protrusions and aggregations of endothelial cells are found, denoting failure to distribute properly. Several mechanisms account for this phenotype. YAP/TAZ promote endothelial cell proliferation downstream of mechanical stimulation at cell-cell junctions by cyclic stretch. Moreover, YAP/TAZ increase cell migration and rearrangements of endothelial cells, at the same time that it decreases endothelial permeability. Thus YAP/TAZ are able to maintain vessel integrity while allowing the dynamic cellular movements take place during sprouting of new blood vessels. The referred effect of YAP/TAZ on cell migration and permeability at least in part depends on their role at cell-cell junctions. There, YAP/TAZ increase the turnover of VE-Cadherin molecules and promote the formation of junction associated intermediate lamellipodia, the more dynamic type of adherens junctions. This is achieved in part by lowering BMP signaling via the transcription of BMP inhibitors.

Together, these results suggest a new model in which YAP/TAZ coordinate mechanical signals and BMP signaling and maintain junctional compliance and integrity whilst balancing endothelial cell rearrangements in angiogenic vessels.

Results presented in this thesis were published in the paper

NETO, F., KLAUS-BERGMANN, A., ONG, Y. T., ALT, S., VION, A. C., SZYMBORSKA, A., CARVALHO, J. R., HOLLFINGER, I., BARTELS-KLEIN, E., FRANCO, C. A., POTENTE, M. & GERHARDT, H. 2018. YAP and TAZ regulate adherens junction dynamics and endothelial cell distribution during vascular development. *Elife,* Feb 5;7

Acknowledgements

This thesis would not have been possible without the logistical, financial, technical, scientific and moral support of so many people and institutions!

First and foremost, I would like to thank my thesis supervision, Dr. Holger Gerhardt, for the opportunity he gave me to do my PhD in his lab, for his constant support and guidance. I thank you especially for the trust you put in me and for the freedom - to make mistakes, learn, correct, become better. You have been the best role model I could ever have asked for, and I leave your lab as a better scientist, colleague and person, and for all that I am in debt to you. I will mostly miss our one-to-one meetings and science discussions.

I thank my thesis co-supervisor, Dr. João Relvas, for allowing me to play around in his lab before my PhD, for guiding and inspiring my science decisions, and for always being available to discuss my project.

I thank my PhD program, GABBA, for accepting an outsider as I was and opening me the doors of science. A special thank you to Catarina Carona. I thank the IBMC and I3S in Porto for hosting the GABBA students. I thank the Portuguese Foundation for Science and Technology (FCT) for financially supporting me and so many Portuguese scientists in and out of Portugal.

I thank my host institutions, the London Research Institute (LRI) in London and the Max Delbruck Center for Molecular Medicine (MDC) in Berlin for taking me as one of your own PhD students. This work would not be possible if not for your support. In particular I would like to thank the PhD office, the mouse facility, the equipment park and the light microscopy facility in the LRI and PhD office and the mouse facility in the MDC.

I thank my lab, the integrative Vascular Biology Lab, and our sister lab in Leuven, the Vascular Pathology Lab, for having provided the best working place. I thank all the technicians, post-docs, PhDs and master students – I have learnt so much from all and each one of you! You have taught me how to be a better scientist, colleague, communicator, and team member. Especially I would like to thank Dr. Alexandra Klaus for all the enthusiasm and determination you always brought to the lab and to the YAP/TAZ project, and to Irene Hollfinger for helping me managing my mice colony, in the most light hearted and graceful way I encountered.

I would like to thank my collaborators. Dr. Cláudio Franco and his lab for receiving me in Lisbon for a short lab stay, and Dr. Michael Potente and Yu-Ting Ong for the collaboration in the YAP/TAZ project and manuscript preparation.

I thank my GABBA family for all the fun and continuous support. Ana Catarina, Bruno, Daniel, Filipinha, Inês, Lindo, Mariana, Milene, Pedro and Renáyou are the best PhD program colleagues one could imagine!

I thank the friends I made in the labs of London and Berlin. You made work more fun, victories more joyful and challenges more bearable, and your words supported me then and still do it today. I could not have made it without you! Thank you André, Anne-Clemence, Benni, Cláudio, Elena, Martina, Raquel, Véronique and Silvanus. I thank Niamh and Pedro for the friendship, science and life discussions, constant support, and for the curiosity and wonder of all things. Thank you also to my long time friend Delfim for being there and sharing a love for science and medicine and many other things.

Finally, I would like to thank my family for always being there and supporting me in all my choices. You are the ground from which I feel safe to take off, and joyful to come back to.

Declaration of originality

The data presented in this thesis represents my own work, generated at Doctor Holger Gerhardt's lab first at the London Research Institute in London and then at the Max Delbruck Center for Molecular Medicine in Berlin.

When data was generated by or in collaboration with other people, I acknowledge it here:

Dr. Silvanus Alt developed the following scripts (Chapter 4): measurement of number, size and circularity of vascular loops; patching images to analyse VE-Cadherin morphological classification; patching images to analyse VE-Cadherin turnover analysis of cell coordination in the monolayer.

Dr. Anne-Clémence Vion ran the flow cytometer and analysed the data regarding the proliferation measurement after VEGF treatment in HUVECs (Chapter 4).

Dr. Anna Szymborska cloned the VE-Cadherin mEOs 3.2 construct, performed the set up and optimization for the fluorescence loss after photoconversion experiments and analyzed the data (Chapter 5). Additionally, Dr. Anna Szymborska implemented the pipeline to analyze the subcellular location of YAP and TAZ in cultured cells (Chapter 4 and 5)

Dr. Alexandra Klaus-Bergmann acquired the microscopy images and quantified the proliferation of cells upon application of mechanical stretch (Chapter 4). Moreover, Dr. Alexandra Klaus-Bergmann independently started the analysis of signalling pathways downstream of YAP/TAZ. For this reason, the data presented in Chapter 5 is truly the result of a very close collaboration between Dr. Alexandra Klaus-Bergmann and me. Dr. Alexandra Klaus designed and performed the following experiments: luciferase assays, RT- qPCR and screening for a BMP inhibitor in YAP/TAZ knockdown cells.

Eireen Bartels-Klein performed WBs to confirm the knockdown of YAP/TAZ proteins in Chapters 4 and 5.

Table of contents

List of figures

List of tables

Abbreviations and Acronyms

AJ: adherens junctions
bFGF: basic fibroblast growth factor
BMPs: bone morphogenetic proteins
ECM: extra-cellular matrix
ECs: endothelial cells
EdU: 5'ethynyl-2'-deoxyuridine
EMT: epithelial mesenchymal transition
EndoMT: endothelial-mesenchymal transition
F-actin: filamentous actin
FLAP: fluorescence loss after photoconversion
FRAP: fluorescence recovery after photobleaching
HIF: hipoxia-inducible factor
HUVECs: human umbilical vein endothelial cells
IB4: Isolectin B4
IP: intraperitoneally
JAIL: junction associated intermediate lamellipodia
KO: knockout
MMPs: matrix metalloproteinases
NICD: Notch intracellular domain
P1: postnatal day 1
P3: postnatal day 3
P6: postnatal day 6
ROI: region of interest
siRNAs: small interfering RNAs
TAZ: transcriptional co-activator with PDZ binding motif
TJ: tight junctions
VEGF: vascular endothelial growth factor
WT: wild-type
WWTR1: WW domain containing transcriptional regulator 1
YAP: Yes-associated protein

Chapter 1 - Introduction

My thesis is about sprouting angiogenesis, the process through which the majority of blood vessels in the organism develop. At the start of my PhD the homologous proteins YAP and TAZ, the main effectors of the Hippo pathway, had drawn significant attention as key regulators of cell behaviour and organ morphogenesis in many tissues and organs, however their role during the formation of blood vessels had not been investigated. My work thus started with the hypothesis that YAP and TAZ are necessary for the formation of blood vessels, and aimed to understand their role in endothelial cells during sprouting angiogenesis.

In this chapter I will introduce necessary information for the understanding of my work. I will start with an overview of the cardiovascular system and blood vessels, their macroscopic and histologic structure and how they develop through sprouting angiogenesis. Next, I will describe YAP and TAZ: their position within the Hippo pathway, regulation, roles on cell biology and morphogenesis in general and what was known on the role of YAP and TAZ in vascular biology. Finally, I will finish this chapter by presenting my research questions and aims.

1. PART1. The cardiovascular system and sprouting angiogenesis

1. The cardiovascular system

A fundamental characteristic of life, from the most simple to the most complex, is that of converting nutrients and gases from the environment into energy, and on doing so, sustaining growth, survival and reproduction. In order to achieve this all organisms rely on the process of diffusion, which although energetically inexpensive is also very slow and only works over small distances. While very simple organisms achieve such exchange directly through the cell membrane, the increase in body size required new strategies as a means to overcome the time-distance constraints of diffusion. Although variable in design, these strategies are invariably based upon internal transport and exchange systems that provide delivery of substances and removal of waste products to and from all cells in the body

(Monahan-Earley et al., 2013). These are called circulatory systems, and their complexity grew in parallel with that of organisms. In mammals, the circulatory system is a vascular system in which blood is propelled by the contraction of a muscular pump: the cardiovascular system.

1.1. Functions of the cardiovascular system

In addition to the already described role of transportation of nutrients, oxygen and metabolic waste products throughout the body, the cardiovascular system serves several other functions. As a transportation system, it also ensures the circulation of hormones and immune cells which allow respectively for long distance communication leading to whole body integration and for immune defence. Moreover, the cardiovascular system is not simply a passive conduit for blood and substances. Instead, it functions as a dynamic interface between the circulation and tissues. By adjusting vascular tone and cardiac output the amount of blood flowing to different organs and cells is adjusted to their energetic needs, as illustrated by the increased flood flow to the splanchnic, muscular or cerebral vasculature during digestion (Matheson et al., 2000), exercise (Joyner and Casey, 2015) or mental activities (Attwell et al., 2010). The regulation of blood flow also allows for body temperature control by adjusting skin perfusion, where heat can be dissipated. Finally, the cardiovascular system also performs important perfusion independent roles, as the instruction of development (Lammert et al., 2003) and regeneration of other organs (Ramasamy et al., 2015).

Given the aforementioned, it is not surprising that the functioning of blood vessels directly impacts the health of every tissue and organ in the body. This is readily illustrated by the contribution of the vasculature to the pathogenesis of cardiovascular diseases and cancer, the two main mortality causes in western societies. Cardiovascular diseases are mostly secondary to the narrowing of blood vessels caused by atherosclerosis, which leads to tissue ischemia and loss of organ function. Moreover, insufficient reperfusion of injured organs caused by deficient formation of new blood vessels further maintains or aggravates the disease. Cancer, on the other hand, stimulates the formation of new blood vessels in order to supply its energetic demands and support its growth, and uses the vessel network to metastasize. Moreover, I would argue that due to the prevailing paradigm in western medicine that separates diseases into organ systems, the true impact of the

vasculature in the etiology and pathogenesis of most diseases has not been fully considered, questioned and investigated. Thus, understanding how blood vessels work holds enormous potential into understanding health and disease and improving human lives.

1.2. Macroscopic and histological organization of the cardiovascular system

The concept that blood circulates in a closed loop propelled by the action of a centrally located pump was not established until the 17th century. Galen, the famous 2nd century Greek physician, proposed that nutrient and oxygen rich blood constantly originated in the liver and in the heart, respectively, after which it travelled inside propelling blood vessels to all tissues in the body where it was consumed. This long-standing view was challenged in 1628 by William Harvey, who by using observation and experimentation correctly described how blood circulates in a closed circuit from arteries to veins propelled by the beating of the heart. The link between arteries and veins, predicted by but elusive to Harvey, was finally closed by Marcello Malphighi in 1661, who for the first time observed capillaries under a light microscope. These fundamental discoveries have laid the grounds to our current - more sophisticated yet still evolving - understanding of the cardiovascular system.

Blood flows from the heart into arteries, which progressively branch into smaller arteries and arterioles until reaching capillaries, one-cell layered vessels where the diffusion of gases, nutrients and metabolic waste products takes place (**Figure 1.1**). From capillaries, blood returns to the heart through progressively larger venules and veins. Two separate but communicating blood vessels loops are recognised: the pulmonary and the systemic circulation. Deoxygenated blood is transported from the right heart to the lungs, where it is oxygenated in the lung capillaries before returning to the left heart – pulmonary circulation. From there, oxygenated blood is carried to all the other tissues of the body, finally returning to the right heart as deoxygenated blood – systemic circulation. It is in the systemic circulation that nutrients enter the blood (from the splanchnic and liver capillaries) and metabolic waste products are discarded from the blood (in the kidney capillaries). A complementary network of lymphatic vessels exists in close proximity to blood vessels, draining excess interstitial fluid back into the blood circulation. As this thesis is about particular aspects of the development of blood vessels, I will exclusively focus on the blood vessel network.

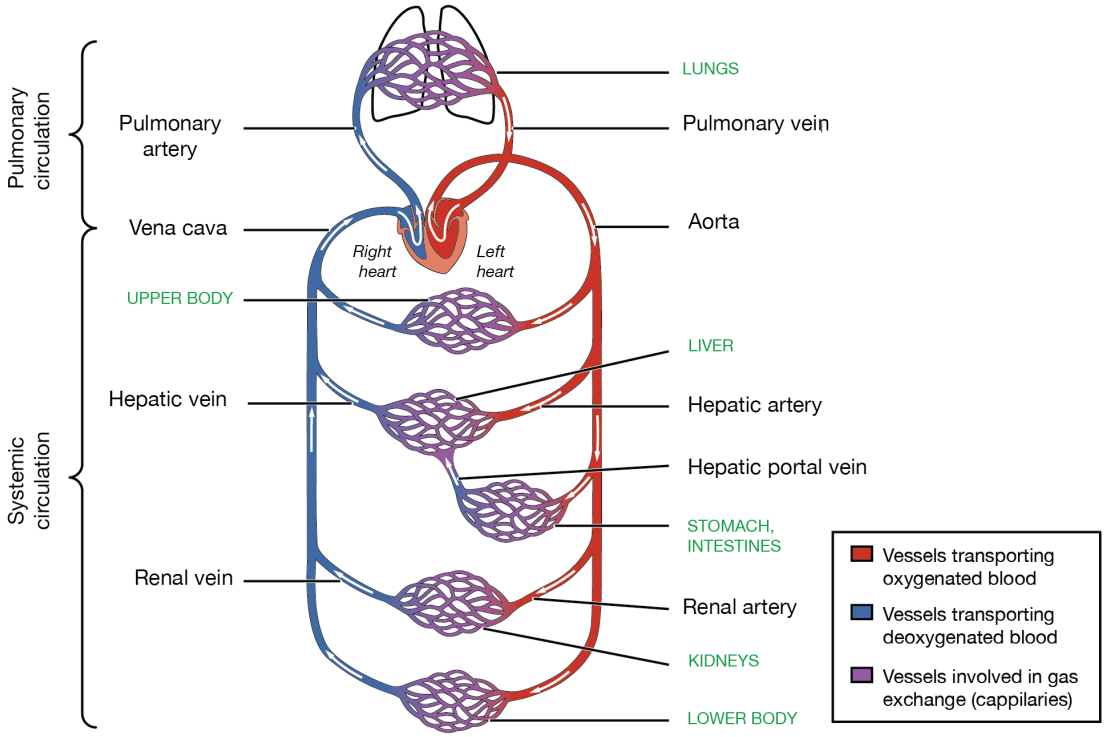

Figure 1.1. The vertebrate cardiovascular system

The vertebrate cardiovascular system is a closed vascular system in which the blood is set in movement by the contractions of the heart. From the heart, blood is transported to all tissues through arteries and arterioles (distributing vessels), and returns to the heart in venules and veins (collecting vessels). Exchange of gases, nutrients and metabolic waste products takes place in capillaries. Image adapted from OpenStax, Anatomy & Physiology. OpenStax CNX.

The functioning of the cardiovascular system is dependent on its hierarchical organization with vessels of different sizes and nature, which relate to their histological makeup. Capillaries, where exchange takes place, are composed of a single layer of **endothelial cells** (ECs) that provide a smooth contact surface with the blood, surrounded by a continuous basement membrane and by isolated pericytes. Arteries and veins, on the other hand, ensure the distribution and collection of blood. Arteries are exposed to high-pressure blood, and display thicker walls that include many layers of vascular smooth muscle cells and elastic fibres. Veins collect blood and return it to the heart, constituting a high capacity reservoir of low-pressure blood. Thus, veins have larger lumens and thinner walls in comparison to arteries, with fewer smooth muscle cells. A surrounding layer of connective tissue, mostly constituted by collagen fibres, supports and holds in place both arteries and veins.

2. Development of blood vessels

2.1. Vasculogenesis and angiogenesis

The cardiovascular system is one of the first functional organ systems to develop in the vertebrate embryo. Soon after gastrulation, before the onset of a heart beat or blood circulation, individual mesoderm-derived endothelial precursor cells named angioblasts migrate, differentiate and coalesce into solid cords of cells that are subsequently lumenised forming patent vessels and networks. This process of *de novo* formation of blood vessels is referred to as vasculogenesis **(Figure 1.2)**. It takes place only during early embryogenesis and leads to the formation of the major arteries and veins of the vertebrate embryo – which include the heart - as well as the formation of a primitive, homogeneous capillary network. Subsequently, this initial vessel network is expanded and remodelled into a highly stereotypical and hierarchical branched vessel network (where larger vessels ramify into smaller ones) covering the whole body. This occurs by a different process of blood vessel formation named angiogenesis, **(Figure 1.2)** a blood flow dependent process through which new blood vessels form from previously established ones.

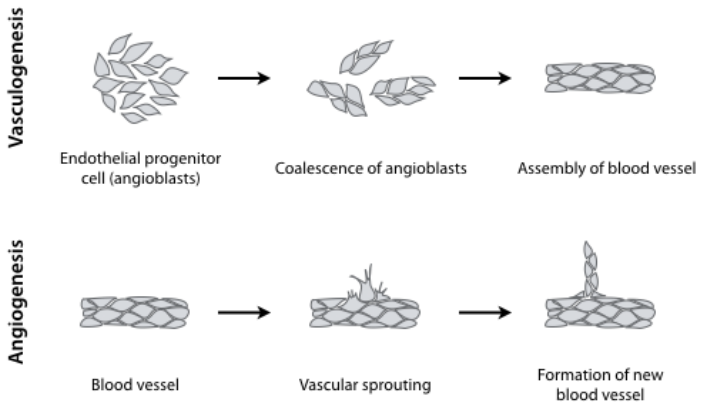

Figure 1.2. Blood vessel formation through vasculogenesis and angiogenesis

During development, the first and major blood vessels or the organism are formed through vasculogenesis. Subsequently, this initial vasculature is expanded to the whole organisms through angiogenesis.

Angiogenesis is the process by which the vast majority of blood vessels are formed during development and growth. By the time adulthood is reached the vasculature is formed and ECs are in a state of quiescence. Little to no angiogenesis takes place. Nevertheless, the ability to turn angiogenesis on is maintained throughout the entire life. Angiogenesis happens in the adult during the physiological processes of female reproductive cycles and pregnancy, tissue repair and regeneration, and also during pathological processes such as the growth of solid tumours. Therefore, angiogenesis plays fundamental roles not only during embryonic development and growth into adult size, but also during adult homeostasis and disease. During the past decades, largely because of more sophisticated genetic tools, a boom of discoveries started to uncover the cellular and molecular mechanisms driving angiogenesis.

2.2. Cellular and molecular mechanisms of sprouting angiogenesis

Although more than one mechanism of angiogenesis has been described, the most frequent one is **sprouting angiogenesis** (Risau, 1997), a process by which new blood vessels sprout out of established vessels and form new vascular loops. It is a multi-step morphogenic process triggered by the release of pro-angiogenic factors from hypoxic tissues, which on binding to quiescent ECs cause their activation. ECs loosen their cell-cell contacts, acquire a migratory phenotype and re-enter the cell cycle. Sprouts of ECs emerge from the parental vessel elongating towards the source of pro-angiogenic factors, and new vessel loops are formed by the fusion of neighbouring sprouts. As my thesis focuses on sprouting angiogenesis I will now present in more detail the cellular and molecular mechanisms driving this process.

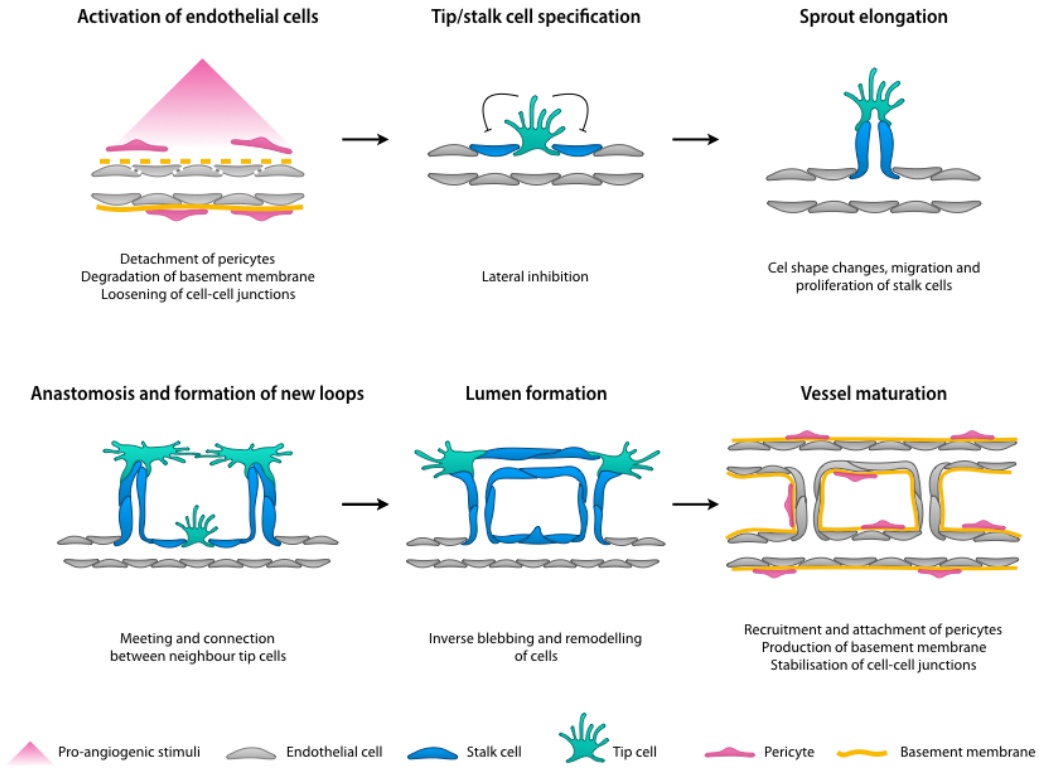

Figure 1.3. The steps of sprouting angiogenesis
Image adapted from (Potente et al., 2011).

2.2.1.Hypoxia and the release of pro-angiogenic factors

Sprouting angiogenesis is the appropriate response of the healthy vasculature to the presence of hypoxia – a state in which tissues do not receive enough oxygen to supply their metabolic needs. Hypoxia emerges as a result of increased oxygen demands or decreased oxygen delivery. Tissue growth increases the oxygen needs and drives angiogenesis during embryonic development and physiological growth, as well as during tumour growth. On the other hand, decreased oxygen delivery is caused by vascular dysfunction due to vessel narrowing, occlusion or rupture, and is for example the cause for the formation of collaterals during chronic heart ischemia.

Cells adapt to oxygen levels by regulating the transcription of specific genes. Central to this mechanism are the transcription factors HIF (hypoxia-inducible factors), which are regulated by oxygen dependent enzymes (Krock et al., 2011). HIF-hydroxylases require molecular oxygen for their catalytic activity, and under normal oxygen levels, add hydroxyl groups to HIF-α subunits. This modification

causes HIF-α to be degraded by the proteasome, so that no transcriptional activity is performed. In contrast, under hypoxic conditions HIF-hydroxylases have no catalytic activity and do not modify HIF-α, which can bind to HIF-β making a functional transcriptional complex. In the nucleus, the HIF-α/HIF-β complex induces the expression of genes required for the cell's adaptation to low oxygen levels. Among these are genes coding for pro-angiogenic molecules, such as *vegfa*, *Angiopoetin-1*, *Angiopoetin-2*, *tie2*, *pdgf* and *fgf2*. Hypoxic cells secrete pro-angiogenic molecules that bind to cell-surface receptors on ECs. This leads to their exit from the quiescent state and the start of sprouting of new vessels. The different factors play different roles during angiogenesis, which include all stages of the process from the initial breaking free from the parental vessel to the actual formation of new vessels and vessel maturation.

2.2.2. Endothelial activation: degradation of the basement membrane, detachment of pericytes and loosening of cell-cell junctions

Quiescent ECs in mature vessels are enveloped in their basal side by a continuous layer of basement membrane composed of extracellular matrix (ECM) proteins. Embedded in the basement membrane are pericytes, mural cells that surround microvessels to different extents depending on the vascular bed (Armulik et al., 2011). Both the basement membrane and the pericytes give structural support to the vessel and contribute to the maintenance of endothelial quiescence – both physically and chemically, by means of cell signalling. Because of this, they impede the sprouting of ECs out of the parental vessels once activated. Therefore, the degradation of the basement membrane and the detachment of pericytes are required steps for ECs to exit quiescence. This takes place in response to pro-angiogenic factors induced signalling in ECs. VEGF (vascular endothelial growth factor) and bFGF induce the expression, activation and secretion of matrix metalloproteinases (MMPs) that degrade the ECM proteins of the basement membrane, decreasing the physical barrier constraining ECs. Moreover, pro-angiogenic signalling is promoted as previously inaccessible cell-surface receptors are exposed and pro-angiogenic factors previously bound to ECM proteins are released. Moreover, the adhesive junctions (tight and adherens junctions) that maintain ECs connected to their neighbours and regulate the permeability of the endothelium are loosened upon the sensing of pro-angiogenic factors, which allows for increased degrees of mobility of the individual cells.

2.2.3.Sprouting

Once ECs are less constrained by physical barriers, a number of multicellular sprouts emerge from the parental vessel elongating in the direction of the hypoxic tissue. Individual cells within emerging sprouts show distinct phenotypes relating to their position (Gerhardt et al., 2003). The heading cells, named **tip cells**, are characterised by being highly migratory and invasive and by displaying numerous filopodia that probe the surrounding tissue for directional molecular cues (Gerhardt et al., 2003). Following cells, or **stalk cells**, trail behind the tip cells while maintaining the connection to the parental vessel, and contribute to the growth of the sprout by undergoing proliferation (Gerhardt et al., 2003, Dejana et al., 2009) and cell elongation (Sauteur et al., 2014). These morphological and behavioural differences between tip and stalk cells are accompanied by differences in gene expression (Gerhardt et al., 2003, Claxton and Fruttiger, 2004, Lu et al., 2004, Tammela et al., 2008). Interestingly, the tip/stalk cell phenotype, initially thought to be unchangeable once specified, was later shown to be dynamic. The position of ECs in the sprout is not fixed in a head to tail fashion, but instead ECs can swap positions with their neighbours and the tip position can be overtaken by cells that were previously following (Jakobsson et al., 2010).

The reason why neighbouring ECs respond to the same pro-angiogenic stimuli with different phenotypes lies in the mechanism of lateral inhibition. This mechanism is at the core of the **Notch signalling pathway**, which is extremely important in morphogenesis as it allows for the emergence of heterogeneity in a homogenous population of contacting cells (Lai, 2004). In ECs, the specification of tip/stalk phenotypes involves the cooperation of the Notch and the VEGF signalling pathways. The binding of VEGF to its cell-surface receptor in ECs leads to the transcription of genes that confer to that cell a tip phenotype. Among those genes is *dll4*. DLL4 is a transmembrane receptor of the Notch signalling pathway that binds the extracellular domain of the NOTCH1 protein in a neighbouring, contacting cell. This binding promotes the cleavage of the NOTCH1 protein and the release to the cytoplasm of the Notch intracellular domain (NICD). NICD translocates to the nucleus where it drives the transcription of Notch target genes that confer to that cell a stalk phenotype while supressing the tip phenotype. The latter is achieved by a decrease in sensitivity to VEGF caused by downregulation of the VEGF receptor and

upregulation of a decoy receptor for VEGF (that binds to the ligand without inducing downstream signalling, thus acting as an inhibitor). In summary, high VEGF signalling “makes” tip cells while high Notch signalling “makes” stalk cells, and “tip” cells inhibit neighbouring cells from also acquiring a tip phenotype. The specification of tip/stalk phenotypes here described is highly simplified, and many more layers of regulation exist that allow for the precise control of tip/stalk cell numbers and for their dynamic regulations.

2.2.4.Anastomosis and formation of new loops

In addition to their role in sensing molecular cues and guiding cell migration, filopodia in tip cells carry cell-cell junction molecules that recognise filopodia in the tip cells of neighbouring sprouts (Lenard et al., 2013). This is the first step in the fusion of sprouts leading to the formation of new vascular loops. While the initial contacts between neighbouring filopodia are unstable and short lived (Lenard et al., 2013), this is followed by the establishment of stable cell-cell junctions initially between filopodia and later involving the cell body. The migration and rearrangement of the contacting tip cells further causes the elongation of the cell-cell junction. A *de novo* lumen opens between the cell-cell junctions, while the lumens of both sprouts expand in the direction of the connection. Finally, the lumens connect and the new vascular loop is perfused and connected to the circulation of the plexus.

2.2.5.Formation of a vascular lumen

The formation of a continuous lumen is a critical step in forming functional, perfusable blood vessels. The initial model of lumen formation in blood vessels derived from observations of 3D cultured ECs (Davis and Bayless, 2003) and of blood vessels undergoing lumenisation in live zebrafish embryos (Kamei et al., 2006). These experiments proposed that the lumen in blood vessels arises from the formation and coalescence of intracellular vesicles in single cells, which than fuse with the lumens of neighbouring cells. More recently, the increase in time and space resolution during live imaging in the zebrafish embryo contradicted the previous model and showed that lumens in ECs form already in tip cells by inverse blebbing of the luminal membrane (Gebala et al., 2016). This mechanism is blood flow

dependent and involves a tight balance between flow-induced pressure pushing the lumen into the cell, and the response of the cell's actomyosin cytoskeleton.

2.2.6.Vessel maturation

The formation of a new functional vasculature requires final steps that ensure the stabilisation of blood vessels. Cell-cell junctions become more stable. ECs produce and deposit ECM proteins forming a continuous basement membrane that provides structural support for the vessel and promotes endothelial quiescence. Finally, mural cells are recruited to the vessels wall, also providing structural and signalling functions that help maintaining the vessel.

2.2.7.Vessel remodelling

Sprouting angiogenesis leads at first to the establishment of a primitive plexus in which an excess of vascular loops is present. With time, this primitive plexus is extensively remodelled into a more mature, hierarchically branched and functional network ideally suited to accommodate the metabolic demands of the tissue in the most efficient way. Critically, what happens during this process is the regression (or pruning) of a number of superfluous vessel segments. The mechanisms behind vessel regression are likely dependent on the vascular bed in case. In vascular networks that completely regress during development endothelial apoptosis plays a role in this process (Lobov et al., 2005, Meeson et al., 1999). However, the mechanism of vessel regression in vascular beds that persist does not rely on apoptosis but on endothelial migration and rearrangements in response to blood flow, in a cellular mechanism reminiscent of anastomosis in reverse (Franco et al., 2015). While vessel segments experiencing high blood flow are reinforced, those experiencing low blood flow are more likely to regress. While this explains how blood flow shapes the development of a more mature vasculature, it does not explain why some low flow segments are kept. Interestingly, recent work (Vion et al., 2018) showed that the endothelial primary cilia prevent the regression of low flow segments, thus proposing a mechanism in which ECs autonomously balance the effect of blood flow towards the achievement of a mature, functional network.

2.2.8.Specification of arteries and veins

The establishment of separate but interconnected arterial and venous vessel networks is imperative for the functioning of the cardiovascular system as a closed loop. Thus, it is critical that during the maturation of the vasculature immature vessels are specified into arteries or veins.

While arteries transport high speed and pressure blood from the heart to capillaries, veins carry the blood back to the heart in low speed and pressure conditions, and in most cases against gravity. These differences are appropriately reflected by the distinct structure of their walls. Arteries have thick and elastic walls with numerous layers of vascular smooth muscle and elastin fibers. Veins, on the other hand, have relatively thin walls with less smooth muscle and bear valves that help maintaining the unidirectionality of blood flow. In addition to the functional and morphological differences, arteries and veins also show molecular differences, the first identified being the ligand ephrin-B2 marking arteries and its receptor Eph-B4 marking veins (Wang et al., 1998).

The mechanism underlying the acquisition of an arterial or venous identity has for long been a subject of debate in vascular biology. It was initially thought that the hemodynamics of blood flow played a determinant role, as vessels are subjected to different speeds, pressure and directionality of flow depending on their position in the plexus. However, the fact that the major arteries and veins of the embryo are formed before the onset of a heartbeat and blood flow led to the idea of artery-venous identity being genetically programmed (Swift and Weinstein, 2009). Grafting experiments in avian embryos have shown that the identity of ECs as arterial or venous is plastic and can be reversed (Moyon et al., 2001, Othman-Hassan et al., 2001), suggesting that local cues instead of a genetic pre-programming drive arterial-venous identity. Soon after that, manipulation of blood flow in avian embryos proved able to regulate arterial-venous differentiation and expression of arterial-venous markers (le Noble et al., 2004), supporting the view that hemodynamic forces are instrumental in the specification of arteries and veins. Still, strong evidence supports a model in which the specification of arteries and veins is molecularly determined. Notch activity has been shown to promote arterial fate (Zhong et al., 2001, Lawson et al., 2001, Lawson et al., 2002, Geudens et al., 2010), while COUP-TFII, a transcription factor, induces venous specification (You et al., 2005). Unpublished data (Geudens et al., 2018) suggest that both mechanisms may in fact be correct and complementary, with blood flow being able to change the fate of arteries and

veins that are primarily molecularly predetermined, to ensure a correct balance between arteries and veins.

3. The mouse retina model of angiogenesis

The current understanding of the mechanisms driving sprouting angiogenesis is largely derived from observation and experimentation in animal models. Of the many available models, the vascularization of the mouse retina is one of the most widely used.

Unlike most tissues that are vascularized during embryonic development, the vascularization of the mouse retina only starts at birth. The complete retina vasculature consists of three parallel layers of blood vessels that develop from birth until around the 3rd week of live. The first layer to be developed, the superficial layer, grows radially over the inner surface of the retina from the optic disc to the periphery of the retina, reaching the outer limit of the tissue at the end of the first week of life. After that, new vessels sprout downward from the superficial layer and invade the retina, forming the intermediate and deeper layers. Mostly, angiogenesis studies focus on the development of the superficial layer of the mouse retina vasculature.

Many advantages account for the popularity of this model. Because the retina vasculature develops post-natally, its spares the need to collect mouse embryos, which translates into fewer used animals. Technically, the retina is relatively easy to handle, and its structure and shape make it suitable for whole-mount immunostaining. The superficial layer of the vasculature develops in a highly stereotypical and robust manner. Moreover, the vessels are arranged in two dimensions in close proximity to the surface of the tissue, allowing for high-resolution imaging. In addition, the same sample allows for the observation of ECs undergoing different steps of the angiogenesis process: while ECs are sprouting new blood vessels at the periphery of the retina, in the center blood vessels undergo remodeling and arteries and veins can be distinguished. Finally, the model benefits from sophisticated genetic tools available for the mouse. In particular, cell-specific and time controlled gene deletion technology enables the study of cell autonomous gene requirements during the development of the retina vasculature without affecting the development of blood vessels embryonically.

As such, the mouse retina model is an excellent tool to uncover the role of a variety of genes during different steps of the vascularization process.

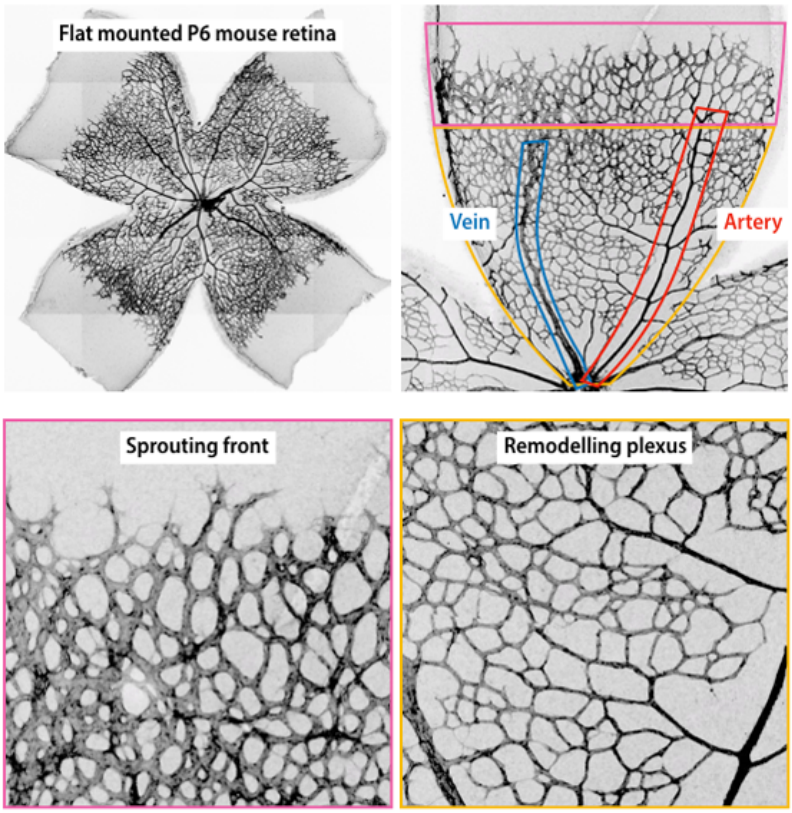

Figure 1.4. The mouse retina model of angiogenesis

A whole flat mounted retina from a P6 mouse, stained for blood vessels. The blood vessels correspond to the developing superficial layer of the vasculature. In the same preparation different steps of the angiogenesis process can be observed.

2. PART 2: YAP and TAZ

The past decades have uncovered many of the fundamental principles of sprouting angiogenesis, at the cellular and molecular level. Various signalling pathways regulating angiogenesis were discovered, and anti and pro-angiogenic molecules identified and applied in the clinical setting with a few successes. However, in the majority of cases the reality of angiogenic therapies eluded expectations, showcasing the need to understand in greater depth how this process works. In the meantime, a relatively new signalling pathway, the Hippo pathway, generated a lot of excitement in the developmental biology and cancer research fields. The final effectors of the Hippo pathway, the transcriptional co-activators YAP (Yes – associated protein) and TAZ (transcriptional co-activator with PDZ-binding motif), were shown to critically control many aspects of cell biology such as proliferation, apoptosis, migration and invasiveness. At the same time, multiple inputs regulating their activity were identified, not only of a chemical nature but interestingly also mechanical. This placed YAP and TAZ in the centre of a novel and complex intracellular hub for cell decisions. Sprouting angiogenesis requires the coordination of cell proliferation, apoptosis, migration and invasiveness, during which ECs integrate and are instructed by multiple cues from the environment, including mechanical signals from the flowing of blood. These reasons made YAP and TAZ very interesting candidates to investigate during sprouting angiogenesis, the more so that their role in ECs and vessels was virtually unknown at the start of this project.

1. YAP, TAZ and the Hippo pathway

YAP and TAZ (also known as WW domain containing transcription regulator 1, WWTR1) are two homologous transcriptional co-activators firstly identified as the final effectors of the mammalian Hippo signaling pathway, a highly conserved kinase cascade discovered as a master regulator of organ size (Huang et al., 2005, Dong et al., 2007). At its core, the Hippo pathway is a phosphorylation cascade comprising two kinases – MST and LATS – that inactivate the pro-growth transcriptional co-activators YAP and TAZ (Yu et al., 2015). Upon activation by upstream stimuli, MST phosphorylates and activates LATS, which then phosphorylates YAP and TAZ leading to their cytoplasmic retention (Kanai et al., 2000, Basu et al., 2003) and degradation (Liu et al., 2010, Zhao et al., 2010). When Hippo is not active, YAP and TAZ are not phosphorylated by LATS and are thus able to translocate to the nucleus

where, through cooperation with transcription factors, they increase the expression of pro-proliferation and anti-apoptosis genes(Yu et al., 2015) (**Figure 1.5**).

2. Upstream stimuli feeding into the Hippo pathway: from a kinase cascade to a complex signalling network

Since the discovery of the core components of the Hippo pathway a wide range of upstream regulators has been searched and identified (**Figure 1.5**). G-protein coupled membrane receptors (Yu et al., 2012, Miller et al., 2012, Mo et al., 2012), cell-cell junctions (Kim et al., 2011, Silvis et al., 2011, Schlegelmilch et al., 2011), apical-basal polarity complexes (Chen et al., 2010, Ling et al., 2010, Baumgartner et al., 2010, Genevet et al., 2010, Yu et al., 2010, Grzeschik et al., 2010, Hamaratoglu et al., 2006), planar cell-polarity complexes and cell-matrix interactions proteins (Elbediwy et al., 2016) all have been shown to regulate the Hippo pathway. Interestingly, to this extensive list of chemical inputs, also mechanical stimuli have been added. The location and activity of YAP and TAZ was shown to be sensitive to cell geometry and shape, ECM stiffness, intracellular tension dependent on actomyosin contraction, changes in the actin cytoskeleton and RhoGTPases (Dupont et al., 2011, Wada et al., 2011, Zhao et al., 2012).

In addition, further research evidenced that the Hippo pathway shows significant crosstalk with other signalling pathways, in a tissue and context depend manner, adding yet another layer of complexity to the kinase cascade. This intertwining of pathways has been observed with Wnt (Varelas et al., 2010, Heallen et al., 2011, Azzolin et al., 2012, Azzolin et al., 2014), Shh (Fernandez et al., 2009), TGF-β/BMP (Fujii et al., 2012, Beyer et al., 2013) and Notch signalling pathways (Totaro et al., 2017).

Finally, YAP and TAZ can also be directly regulated by LATS independent mechanisms (Dupont et al., 2011, Miller et al., 2012), which led some authors to suggest the terms canonical (through the kinase cascade) and non-canonical Hippo pathway. Regardless of the nomenclature, what has become clear is that unlike a conventional signal transduction pathway with dedicated receptors and molecules, the Hippo pathway is instead a complex signalling network, and YAP and TAZ a hub for cellular decision-making.

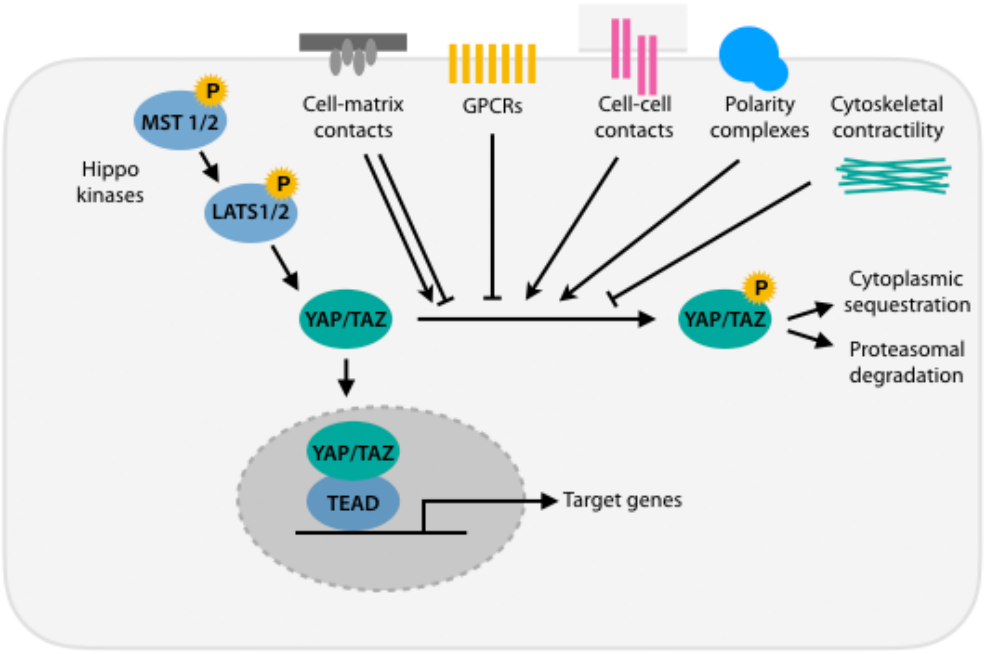

Figure 1.5. Regulation of YAP/TAZ

YAP/TAZ are regulated by several mechanisms. The phosphorylation of YAP/TAZ by the Hippo kinases MST1/2 and LATS1/2 leads to cytoplasmic retention and proteasomal degradation, impeding the binding to transcription factors in the nucleus. In addition to the Hippo kinases, YAP/TAZ are also regulated by cell-matrix contacts, GPCRs, cell-cell contacts, polarity complexus and cytoskeletal contractility. When YAP/TAZ are not phosphorylated they accumulate in the nucleus where they bind to transcription factors (as the TEAD family of transcription factors), resulting in transcription of target genes.

3. Downstream functions of the Hippo pathway

The discovery of the Hippo pathway took place during forward genetic screens in the fruit fly looking for tumor suppressor genes. There, the loss of the Hippo core kinases led to dramatic overgrowth phenotypes (Xu et al., 1995, Justice et al., 1995, Harvey et al., 2003, Jia et al., 2003, Pantalacci et al., 2003, Udan et al., 2003, Wu et al., 2003). Because of this, the first identified role of the Hippo pathway was that of controlling organ size through the regulation of cell proliferation and apoptosis. The Hippo pathway became recognized as the molecular mechanism explaining the phenomenon of contact inhibition of proliferation in epithelial tissues. Although this is also true for some mammalian tissues, some authors argue that the regulation of entry and exit from the cell cycle might be more relevant than organ size control in mammals (Halder and Johnson, 2011). Since these initial observations, an

abundance of data has attributed other critical functions to the Hippo pathway. The Hippo pathway was shown to regulate the maintenance and differentiation of stem cells (Ramos and Camargo, 2012, Hiemer and Varelas, 2013), cell migration, epithelial-mesenchymal transition (EMT) (Harvey et al., 2013, Moroishi et al., 2015, Yu et al., 2015), contractility and force generation(Lin et al., 2017) and even cell and body metabolism (Ardestani et al., 2018).

Because of described functions, the Hippo pathway plays fundamental roles during development, regeneration and homeostasis. Aberrant activation of YAP and TAZ has been extensively associated with increased cancer formation and aggressiveness, while inactivation of YAP and TAZ impairs tissue development, regeneration and maintenance of stem cell pools (Fu et al., 2017).

Molecularly, the Hippo pathway controls such cellular functions by regulating gene expression. Although YAP and TAZ lack DNA binding domains, they act as transcriptional co-activators by binding and promoting the activity of transcription factors once in the nucleus. The TEAD family of transcription factors, TEAD 1-4, are the best-known DNA partners of YAP and TAZ and mediate many of the described functions of the Hippo pathway (Vassilev et al., 2001, Zhang et al., 2009). In addition to TEAD, YAP and TAZ also interact with several other transcription factors such as the RUNX family of transcription factors (Passaniti et al., 2017) and p73 (Lapi et al., 2008). Importantly, although some common genes are regulated by YAP and TAZ throughout a wide number of cells, and thus considered as indicators for YAP and TAZ activity (as *Ctgf*, *Cyr61* and *Ankrd1*), most target genes are cell specific, emphasizing that the role of YAP and TAZ is highly cell context dependent (Halder and Johnson, 2011).

4. Similarities and differences between YAP and TAZ

While YAP orthologs are present from the earliest animal forms (Yorkie being the *Drosophila* YAP ortholog), TAZ proteins are only found in vertebrates. TAZ represent a late evolutionary novelty, and sequence analysis suggests that the *Taz* gene probably originated from gene duplication of *Yap* in early vertebrates (Hilman and Gat, 2011). With almost 50% amino acid identity, YAP and TAZ share many regulatory and structural domains, and bind similar proteins and transcription factors. However, the use of *Yap* and *Taz* knockout (KO) animals has revealed different *in*

vivo functions for both proteins. While the knockout of *Yap* leads to embryonic lethality around embryonic day 8.5 (Morin-Kensicki et al., 2006), *Taz* KO mice survive until adulthood but develop lung and kidney disease (Makita et al., 2008, Hossain et al., 2007). At the same time, the deletion of both *Yap* and *Taz* led to much earlier embryonic lethality, with embryos dying before the morula stage (Nishioka et al., 2009), which showcases a degree of redundancy between both proteins. While many cellular functions seem to be shared, the relative requirement of different tissues and organs for YAP and TAZ may differ, and the same is true for time sensitive demands throughout development, homeostasis and response to disease. Having said that, understanding the unique and redundant roles of YAP and TAZ will benefit from the use of tissue and cell specific genetic manipulation *in vivo*.

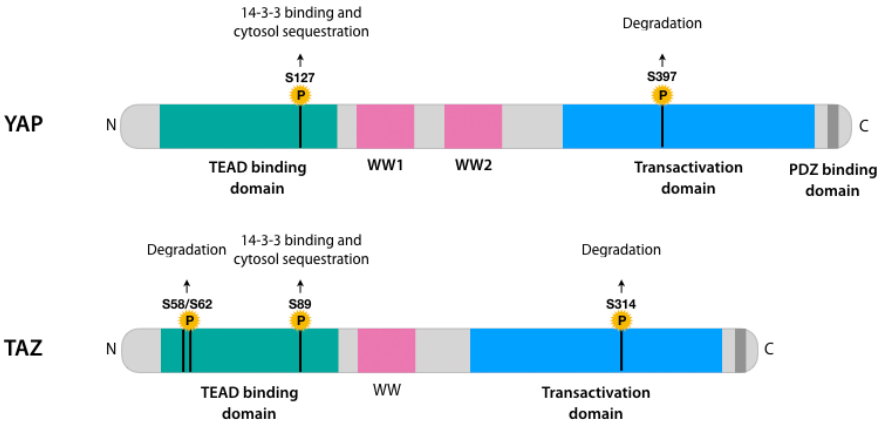

Figure 1.6: Amino acid structure of YAP and TAZ

YAP and TAZ are paralog proteins that share around 50% amino acid similarity, including many structural domains and regulatory regions. Both proteins display a transcription factor-binding domain that binds the TEAD family of transcription factors; two (YAP) or one (TAZ) WW domains that bind PPXY-containing transcriptional factors and are required for the interaction with LATS kinases; a transcription activation domain; and a PDZ binding domain that mediates the localization of YAP and TAZ to discrete nuclear foci, to the cell membrane or to the cytoskeleton. YAP and TAZ also have several serine residues that, upon being phosphorylated by LATS, mediate proteasome degradation or binding to 14-3-3 proteins leading to cytosol sequestration.

5. Yap and Taz in vascular biology

The first suggestion that the Hippo pathway was required for blood vessel formation came from the full deletion of *Yap* in mice. Among other critical defects that lead to developmental arrest, these embryos present defects in the vascularisation of the yolk sac (Morin-Kensicki et al., 2006). Later, an endothelial-specific deletion of

Yap in mice was generated using the constitutional Tie2-Cre transgenic line, which also targets endocardial cells. There, fatal heart valve defects caused by failed endothelial-mesenchymal transition (EndoMT) precluded the analysis of the blood flow dependent process of angiogenesis (Zhang et al., 2014). In a different study using small interfering RNAs (siRNAs) to decrease the expression of YAP in the post-natal mouse retina, YAP was shown to regulate vascular branching and density by promoting the transcription of *Angiopoetin-2* (Choi et al., 2015). While this study suggested an important effect during angiogenesis, the cell autonomous role of YAP could not be appreciated, as other cells could contribute to the phenotype. In the zebrafish, *Yap* mutants develop an initially normal vasculature but display increased vessel collapse and regression, suggesting a role for YAP during the maintenance of blood vessels. In contrast, *Yap/Taz* double mutant zebrafish fail to form the dorsal aorta and post cardinal vein (which are formed through vasculogenesis) and die before the onset of circulation with other severe developmental defects (Nakajima et al., 2017).

The cellular functions and molecular regulation of YAP and TAZ in ECs was also investigated using cell culture assays and live imaging in zebrafish embryos. A pro-proliferation effect of YAP on ECs was reported by some (Shen and Stanger, 2015), but not all (Choi et al., 2015) groups. In contrast, YAP was consistently found not to affect apoptosis in ECs (Shen and Stanger, 2015, Choi et al., 2015). While these initial studies did not extensively address the roles of endothelial YAP and TAZ, they did point towards important regulation of YAP in ECs. Similarly to other cell types, endothelial YAP is regulated by cell-cell contacts, specifically by the endothelial adherens junction molecule VE-Cadherin. Moreover, endothelial YAP was shown to sense blood flow (Wang et al., 2016, Nakajima et al., 2017).

While these studies suggest that YAP affects endothelial biology and plays a role during the formation of blood vessels, detailed analysis on the role of YAP and TAZ during developmental sprouting angiogenesis is missing. Likewise, the cellular functions of YAP and TAZ, their effectors and interplay with other relevant signalling pathways in ECs remain poorly understood.

3. PART 3: Project questions and aims

The recently discovered Hippo pathway has quickly gained its place in the restricted group of signalling pathways critically important for development. With reports suggesting that the Hippo pathway is required during vessel formation, a detailed picture of the cellular and molecular functions of endothelial YAP and TAZ is still missing. In this context, the aim of my project is to understand the role of YAP and TAZ in ECs during developmental sprouting angiogenesis. For that, I have focused on 3 main questions:

Are endothelial YAP and TAZ required for sprouting angiogenesis *in vivo*? (Chapter 3)

What are the cellular functions of YAP and TAZ in ECs? (Chapter 4)

What are the molecular mechanisms mediating the functions of YAP and TAZ in ECs? (Chapter 5)

To address these questions I took advantage of the mouse retina model of sprouting angiogenesis coupled with cell-specific inducible loss-of-function genetic tools. In addition, I complemented these techniques with *in vitro* culture of ECs to dissect specific cellular and molecular questions.

Having introduced the necessary background information in this chapter, I will in **chapter 2** describe in detail the material and methods used. In chapters 3, 4 and 5 I will present my results: in **chapter 3** I describe the phenotype of *Yap* and *Taz* endothelial cell mutants; in **chapter 4** I present the cellular functions of endothelial YAP and TAZ *in vitro* and *in vivo*; in **chapter 5** I show how YAP and TAZ affect endothelial behaviour by regulating BMP signalling. Finally, in **chapter 6** I conclude the thesis by discussing my results and present future perspectives.

Chapter 2: Material and Methods

1. Mice and treatments

For loss of function experiments the following mouse strains were used: *Yap* $^{fl/fl}$, *Taz* $^{fl/fl}$ (Gruber et al., 2016) and *Pdgfb-iCreERT2* (Claxton et al., 2008). Mice were maintained at the London Research Institute and at the Max Delbruck Center for Molecular Medicine under standard husbandry conditions. To induce Cre-mediated recombination 4-hydroxytamoxifen (Sigma, 7904) was injected intraperitoneally (IP) (20 µL/g of 1 mg/mL solution) at postnatal day 1 (P1) and day 3 (P3) and eyes were collected at P6. In all experiments control animals were littermate animals without Cre expression. Male and female mice were used for the analysis.

For EC proliferation assessment in the retina, mouse pups were injected IP 2 hours before culling with 20 uL/g of EdU solution (5-ethynyl-2'-deoxyuridine)(0.5 mg/mL; Thermo Fischer Scientific, C10340).

2. Cell culture

Human umbilical vein endothelial cells (HUVECs) from pooled donors (PromoCell) were cultured in EGM2-Bulletkit without antibiotics (Lonza) and used until passage 6. The manufacturers authenticated the identity of HUVECs by flow cytometry for cell-type specific markers (vWF, CD31, CD105) and by functional analysis (cells positive for acetylated low density lipoprotein uptake). All cells were tested negative for mycoplasma.

For knockdown experiments, HUVECs were transfected with SMARTpool: siGENOME siRNAs purchased from Dharmacon (Yap #M-012200-00-0005, Taz #M-016083-00-0005, VE-Cadherin #M-003641-01-0005 and non-targeting siRNA Pool 1 #D001206-13-05). Briefly, subconfluent (70-80%) HUVECs were transfected with 25 nM siRNA using Dharmafect 1 transfection reagent following the protocol from the manufacturer; transfection media was removed after 24h and experiments were routinely performed on the third day after transfection.

3. Immunofluorescence staining

3.1. Immunofluorescence in the mouse retina

Pups were culled by decapitation at P6, and eyes collected and fixed in 4% PFA in PBS for 1h at 4C. Retinas were dissected in PBS under a stereomicroscope. After that, retinas were permeabilised/ blocked for 1h at room temperature in 1% BSA, 2% FBS, 0.5% Triton X100, 0.01% Na deoxycholate and 0,02% Na Azide in PBS. Primary and secondary antibodies were incubated overnight at 4C and for 2h at room temperature, respectively, both in 1:1 PBS: blocking buffer. Isolectin staining was performed overnight at 4C in Pblec after retinas were equilibrated for 1h in Pblec at room temperature. Retinas were post-stained fixed in 2% PFA in PBS for 10 minutes. To mount the samples Vectashield mounting medium. (Vector Labs, H1000) or ProLong Gold (Thermo Fisher Scientific) was used. Imaging was done by laser scanning confocal microscopy (Carl Zeiss LSM700, LSM780 and Leica TCS SP8). Processing of samples was carried out in tissues from littermates under the same conditions. A list of the antibodies used can be found in Table 1.

3.2. Immunofluorescence in HUVECs

HUVECs were grown in #1.5 coverslips coated with poly-lysine and gelatin 0.2%. At the end of the experiment cells were fixed in 4% PFA for 10min, permeabilised in 0.3% Triton-X100 in blocking buffer for 5min and blocked in 1% BSA 20mM Glycine in PBS for 30 min. Primary and secondary antibodies were incubated for 2 and 1 hours, respectively, in blocking buffer. Nuclei labeling was performed by incubating cells with DAPI for 5 min (Life technologies, D1306). A list of the antibodies used can be found in Table 1.

	Reference	Dilution	Company	
Yap	46189	1:100	ThermoFisher Scientific	Retinas + HUVECs
Taz	HPA007415	1:100	Sigma	Retinas +

				HUVECs
Erg	sc-18136	1:100	Santa Cruz Biotechnology	Retinas
Erg	Ab92513	1:1000	Abcam	Retinas
VE-Cadherin	555289	1:100	BD Biosciences	Retinas
TER-119	MAB1125	1:100	R&D Systems	Retinas
PECAM-1	AF3628	1:200	R&D Systems	Retinas
Cleaved Caspase 3	AF835	1:200	R&D Systems	Retinas
Dll4	AF1389	1:100	R&D Systems	Retinas
pSMAD1/5/8	13820S	1:1000	Cell Signalling	Retinas
Phalloidin- Alexa-Fluor 488	A12379	1:100	ThermoFisher Scientific	HUVECs
Ib4-Alexa-Fluor 647 Conjugate	I32450	1:1000	ThermoFisher Scientific	Retinas + HUVECs
Ib4-Alexa-Fluor 488 Conjugate	I21411	1:1000	ThermoFisher Scientific	Retinas + HUVECs
Ib4-Alexa-Fluor 568 Conjugate	I21412	1:1000	ThermoFisher Scientific	Retinas + HUVECs

Table 1. Antibodies and dyes used.

4. Image analysis

4.1. Image analysis of retinal parameters

Analysis of radial expansion, capillary density, branching frequency, endothelial proliferation, apoptosis and sprouting numbers was done using Fiji (Schindelin et al., 2012). **Radial expansion** corresponds to the mean distance from the optic nerve to the sprouting front (8 measurements in tilescans of two whole retinas per animal). **Capillary density** corresponds to the vessel area (measured by thresholding IB4 signal) divided by the field of view area (6–8 images of (425 mm)^2 between artery and vein per animal). **Branching frequency** was measured by

manually counting all branching points in a field of view (4-5 images of (200 mm)^2 between artery and vein per animal). The **plexus regularity** was assessed through the standard deviation of the size and the circularity of the vascular loops in the plexus (using same images as for analysis of capillary density). Vascular loops were segmented by thresholding the IB4 signal, and in order to avoid artifacts loops with a size smaller than 86 um^2 were excluded from analysis. **Endothelial proliferation** was measured by manually counting the number of EdU positive endothelial nuclei (ERG positive) and dividing by the vessel area (measured by thresholding IB4 signal) (4 images of (425 mm)^2 containing the sprouting front and localized on top of arteries per animal). **Apoptosis** was measured manually by counting the number of cleaved caspase 3 positive figures and dividing by the vessel area (measured by thresholding IB4 signal) (tilescan of one whole retina per animal). The **number of sprouts** was measured manually (3 images of 425x850mm of the sprouting front per animal). To quantify **pSMAD1/5/8 status** the number of pSMAD1/5/8 positive endothelial nuclei was manually counted and dividing by the total number of endothelial nuclei (defined by being ERG positive) (3 images of (225mm)^2 containing the sprouting front were used per animal).

4.2. Image analysis in cell culture experiments

To analyse **YAP/TAZ subcellular localisation in HUVECs** a previously existing cytoplasm-to-nucleus translocation assay pipeline from Cell Profiler (Carpenter et al., 2006) was adapted. Briefly, YAP or TAZ staining intensity was measured both inside the nucleus of the cell and in a 12 pixels wide ring of cytoplasm grown radially from the nucleus. The nucleus localisation was determined using a DAPI mask.

Cell junction morphology analysis was done in confluent monolayers of HUVECs stained for VE-Cadherin. 5 morphological categories were defined: straight, thick, thick to reticular, reticular and fingers. 5 images of (160mm)^2 were acquired per condition per experiment. Each image was divided in (16 mm)^2 patches, and patches were randomly grouped using a script written by Dr. Silvanus Alt. The classification into categories was done manually and blindly for the condition.

To analyse **cell coordination** confluent cells labelled for DAPI were used. The nuclei were automatically segmented using a customized Python algorithm

relying on the Scikit Image Library written by Dr. Silvanus Alt. By fitting an ellipse to each nucleus its major and minor axis were obtained, and the angle of the major axis with the x-axis of the image was assigned to the nucleus as its orientation. This way each nucleus in the images was assigned a position given by its midpoint and an orientation. Next, the average alignment of the nuclei of two cells depending on their distance was analyzed. As the nuclei don not have a directionality (i.e. they are nematics as opposed to vectors), the angles between two nuclei range from 0 corresponding to the nuclei being parallel, to $\pi/2$ corresponding to them spanning a right angle. For any two cells in each image the angle and the Euclidean distance between them were calculated, and then the cells were binned depending on their distance. A parameter called 'alignment' was defined in which 1 corresponded to all cells being perfectly aligned and 0 corresponded to a completely random distribution of cell orientations.

5. VEGF treatment experiments

5.1. VEGF treatment and YAP/TAZ staining

Confluent HUVECs were maintained in VEGF free media for 24h. VEGF treatment was then performed for 30 min, 1h and 3h with 0 or 40ng/mL of VEGF-165 (PrepoTech, 450-32). Immunofluorescence staining and analysis of YAP and TAZ subcellular localisation was performed as above described.

5.2. VEGF treatment and proliferation assessment

Knockdown HUVECs were maintained in VEGF free media for 24h. VEGF treatment was then performed for 24h with 0ng/mL, 40ng/mL, 200ng/mL or 1000ng/mL of VEGF-165. Cells were pelleted, ressuspended in 90% cold Methanol and stored at -20C° before further processing. Cells were then ressuspended in Propidium Iodide/RNase staining solution (Cell signaling, 4087) for 30 minutes before cell cycle analysis by flow cytometry (LSRII, BD). Data was analysed using BD FACSDiva™ software.

6. Mechanical stretch experiments and proliferation assessment

HUVECs were plated on collagen I - 0.2% gelatine-coated Bioflex plates (BF-3001C, Flexcell International Corporation). Gene knockdown was preformed as previously described. Cells were incubated in transfection media for 24h, and allowed to recover in fresh complete media for 4h. Afterwards cells were incubated for 24h in serum starvation media (0,1%BSA in EBM2 pure media) to form a confluent, quiescent monolayer. Cyclic stretch (0.25Hz, 15% elongation) was then applied for 24h using a Flexcell® FX-5000™ Tension System. Control cells were placed in the same incubator but not on the Flexcell® device (static conditions). EdU pulsing was performed after 20h of the 24h stretch period. At the end of the experiment cells were fixed in 4% PFA and EdU staining was performed according to the manufacturer's protocol (Click-It EdU C10340 Life Technologies). Nuclei were labelled with DAPI. Three regions of interested were acquired per sample in a Carl Zeiss LSM700 scanning confocal microscopes (Zeiss, Germany). Quantification of proliferation was done using a CellProfiler pipeline. Percentage of S phase cells was determined as percentage of EdU positive nuclei over the total number of nuclei.

7. Assays on cells to investigate adherens junctions function and morphology

7.1. Permeability assay

24h after siRNA transfection cells were re-plated into fibronectin coated Transwell® membranes (Costar 3460) at confluence and incubated for 2 more days to stabilize cell junctions. On the third day after transfection 0.5mg/mL of 250kDa FITC Dextran in cell media (Sigma FD250) was added to the top well. Fluorescence on the bottom well was measured after 6h in a Gemini XPS fluorescent plate reader.

7.2. Pulse chase VE-Cadherin experiment for quantification of low, intermediate and high turnover junctions

Cells were labelled live with a non-blocking monoclonal antibody directed against extracellular VE-Cadherin and directly coupled with Alexa-Fluor647

(BD Pharmingen, #561567, 1:200) for 30 minutes. Cells were then washed 2x with PBS and incubated with complete media for additional 2 hours. Cells were fixed with 4% PFA and stained for VE-Cadherin (Santa Cruz Biotechnology, #6458, 1:200) with a secondary antibody coupled with Alexa-Fluor-488. 5 $(160mm)^2$ images per condition per experiment were acquired in a Carl Zeiss LSM700 confocal laser scanning microscope using the same acquisition settings. Max projection of z stack and merging of channels was done in Fiji. Images were divided in $(16\ mm)^2$ patches and the patches were randomly grouped. Patches were classified into a morphological category and into low, intermediate or high turnover categories, manually and blindly for the condition.

7.3. Live imaging of VE-Cadherin-EGFP expressing HUVECs

24h after siRNA transfection, knockdown HUVECs were transduced with VE-cadherin-EGFP adenovirus as described before (Bentley et al., 2014). Briefly, cells were incubated with the virus for 24 hours and then washed 3 times to remove viral particles. Cells were replated onto 2-well LabTek chambered coverslips (Nunc) coated with 10 ug/mL Fibronectin (Sigma, F1141). Imaging was performed 48 hours post-transduction. Cells were imaged at 37ºC under 5% CO_2 on LSM 780 (Zeiss) using a Plan-Apochromat 63x/1.4 oil objective. Images were acquired at a 260 sec time frame.

7.4. Fluorescent loss after photoconversion experiments using VE-Cadherin- mEos3.2 expressing HUVECs

7.4.1. VE-cadherin mEos3.2 cloning

mEos3.2 cDNA (Zhang et al., 2012) was cloned downstream of full-length human VE-cadherin with a short linker (ARDPPV) and inserted into pAc-GFP-N1 backbone (Clontech) using NEBbuilder HiFi Assembly mix (NEB).

7.4.2. Fluorescent loss after photoconversion

HUVECs double-transfected with YAP/TAZ or scrambled siRNAs and pN1-CMV-VE-cadherin-mEos3.2 were cultured to confluency in 2-well LabTek chambered coverslips (Nunc) coated with 10 ug/mL Fibronectin (Sigma, F1141) in EGM (Promocell) supplemented with EGM2 bulletkit (Lonza). Cells were imaged at 37ºC under 5% CO_2 on LSM 780 (Zeiss) equipped with Definite Focus stabilizer. Imaging was performed using the 488 nm (green mEos3.2 component) and the 561 nm (red component) lasers using Plan-Apochromat 63x/1.4 oil objective, 0.26 x 0.26 µm pixel size and 5.09 µs pixel dwell time, 16-bit image depth. A circular region of interest (ROI) of 21 μm^2 area was selected on straight junctions and photoconverted using the 405 nm laser. Mean fluorescence intensity in the ROI was monitored in the red channel for 15 min with 10s resolution, while the movement of the junction was followed in the green channel. Background signal in each frame was estimated by measuring mean intensity in non-photoconverted region and subtracted from the fluorescence-loss curves. The curves were further corrected for bleaching, using parameters estimated from fixed cells. The curves were normalized between the mean intensity in the frames before photoconversion and fluorescence intensity measured immediately after photoconversion. Normalized curves were smoothed using the moving average method; the half-time of redistribution and immobile fraction of VE-cadherin were estimated directly from the plots. Only junctions which did not substantially move or remodel during the observation time were considered for analysis. Analysis was performed using Fiji and Matlab (Mathworks).

8. Cell migration experiments

8.1. Scratch wound assay

24h after siRNA transfection cells were re-plated into a scratch wound assay device (IBIDI). On the following day a cell free gap of 500µm was created by removing the insert of the device. Images were taken immediately after removing the insert (0h) and after 16h. The cell free area was measured in Fiji and used to calculate the percentage of wound closure at 16h.

8.2. Cell coordination analysis

Described before in image analysis.

9. Biochemistry

9.1. RNA extraction and quantitative real time-polymerase chain reaction

RNA was extracted using the RNeasy Mini Kit (Qiagen) according to the manufacturer's instructions. 90ng of RNA were reverse transcribed using RevertAid First Strand cDNA Synthesis Kit (ThermoFisher Scientific). qRT-PCR was performed using TaqMan reagents and probes (Applied Biosystems) (listed in Supplementary File 3). qRT-PCR reactions were run on a StepOnePlus real-time PCR instrument (ThermoFisher Scientific) or Quant Studio 6 Flex (Applied Biosystems) and expression levels were normalised to human *ACTB* or human *HPRT1* using the 2deltaCT method.

9.2. Western blot

Protein was extracted from HUVECs using M-PER protein extraction reagent with Halt Protease and Phosphatase inhibitors (Pierce). Proteins concentration was assessed using a BCA protein assay kit (Pierce). Proteins were separated by SDS–PAGE and blotted onto nitrocellulose membranes (Bio-Rad). Membranes were probed with specific primary antibodies and then with peroxidase-conjugated secondary antibodies. The following antibodies were used: YAP 63.7 (Santa Cruz Biotechnology, sc-101199, 1:1000), GAPDH (Millipore, MAB374, 1:4000). The bands were visualized by chemiluminescence using an ECL detection kit (GE Heathcare) and a My ECL Imager (Thermo Scientific).

10. Dual luciferase reporter assay

Renilla-luciferase reporter assays for TEF-1 (Mahoney et al., 2005), RBPj (Jarriault et al., 1995), BRE (Korchynskyi and ten Dijke, 2002, Fritzmann et al., 2009) and FOPflash (Korinek et al., 1997)-Luciferase promoter activity were performed as follows: 48 hours after gene knockdown by siRNA HUVECs were cotransfected with

600 ng of Luciferase reporter gene construct and 300 ng of pRL-TK (Promega) using Lipofectamine2000 and incubated for 4 hours. Cell extracts were prepared 72 hours post siRNA transfection and 24 hours post Luciferase reporter transfection, and luciferase activity was measured using a dual luciferase system as described (Hampf and Gossen, 2006). Experiments were carried out in duplicates and results were normalized to the correspondent FOPflash/Renilla measurement.

11. Notch and BMP inhibition experiments

A list of the reagents used, together with duration of treatment, can be found in Table 2.

Reagent	Reference	Final conc.	Duration of treatment*	Reference
DBZ	14627, Cayman chemicals	0.1uM	20hrs/16hrs	(Ridgway et al., 2006)
Recombinant-hGremlin	5190-GR, R&D Systems	0.1ug/ml	20hrs	(Mitola et al., 2010, Grillo et al., 2016)
Recombinant-hEndoglin	1097-EN, R&D Systems	0.25ug/ml	20hrs	(Castonguay et al., 2011)
LDN-193189	19396, Cayman chemicals	1uM	20hrs/16hrs/24h/24h	(Sanvitale et al., 2013)
K02288	16678, Cayman chemicals	1uM	20hrs	(Sanvitale et al., 2013)
Recombinant hAlk1fc	370-AL-100, R&D Systems	25ng/ml	20hrs	(Mitchell et al., 2010, Larrivee et al., 2012)

Table 2: Reagents used for inhibition of Notch and BMP signalling

* Duration of treatment: Luciferase assay/ Scratch wound assay/ Permeability assay/ VE-Cadherin staining

12. Statistical Analysis

Statistical analyses were performed using GraphPad Prism software and *p* value was determined using unpaired Student *t*-test between the control and the knockout/ knockdown/ condition. Statistical significance was considered for $p<0.05$. Values shown are mean and standard deviation was used as the dispersion measure. Biological replicates refer to individual mice for *in vivo* experiments and different wells for *in vitro* cell culture experiments; independent experiments refer to experiments done in different days; technical replicates refer to repeated measurements taken from the same sample, both for *in vivo* and *in vitro*. Exclusion of outliers was done using “Robust regression and Outlier removal” from GraphPad Prism software, with a coefficient Q of 1%. A statistical method of sample size calculation was not used during study design. For *in vivo* experiments, we used an average of 6 animals per experiment, from different litters, with a minimum of 3 (detailed number of animals used in figure legends). For *in vitro* experiments, we did a minimum of 3 independent experiments (detailed number of experiments in figure legends and source data). When technically possible the investigators were blind to the genotype of the animal or cell culture condition during sample processing and data analysis.

Chapter 3: Sprouting vessels lacking YAP/TAZ are haemorrhagic and show abnormal endothelial cell organisation

1. Nuclear YAP and TAZ are found in sprouting endothelial cells of the mouse vasculature

1.1. YAP and TAZ show distinct and complementary staining patters in the developing mouse retina vasculature

To understand if YAP and TAZ are expressed in angiogenic blood vessels, I stained retinas from wild-type (WT) mice at P6 for YAP or TAZ protein by immunofluorescence. I chose this time point because at P6 the developing blood vessels reach approximately 2/3 of the radius of the mouse retina, and one can observe both the sprouting front and a more mature plexus, where arteries and veins are already specified and vessel pruning is taking place. YAP and TAZ staining revealed that these proteins are highly expressed in the developing vasculature of the mouse retina, interestingly with distinct and complementary patterns (**Figure 3.1**): while the expression of YAP is lower at the sprouting front than in the remaining vasculature, the expression of TAZ is higher at the sprouting front than in the remaining vasculature.

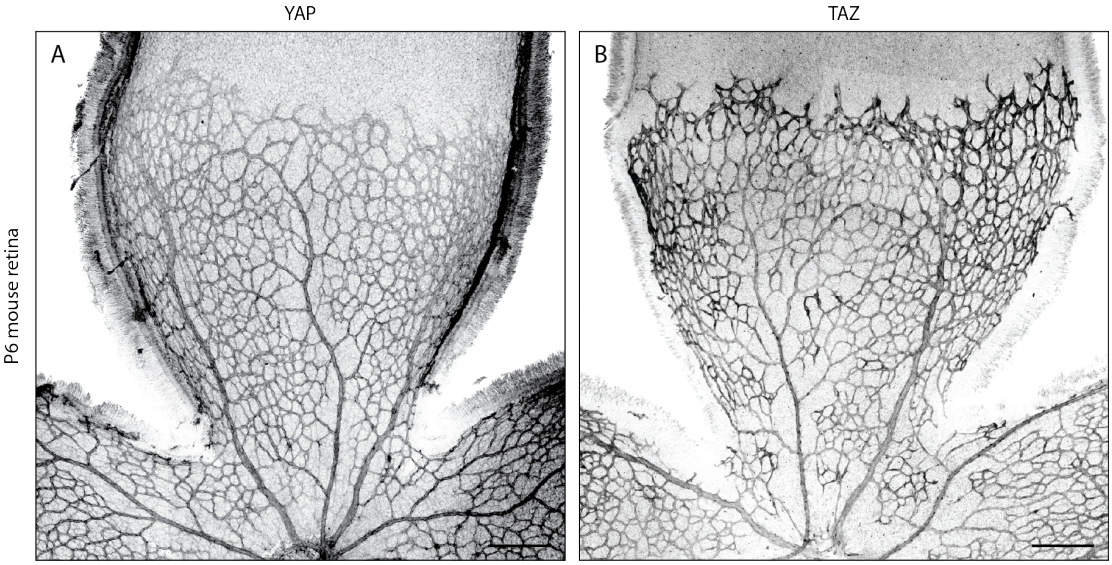

Figure 3.1. YAP and TAZ are differently expressed in developing blood vessels

Immunofluorescence staining of YAP (A) and TAZ (B) in WT mouse retinas at P6. Images correspond to maximum projection of z-stack. Scale bar: 200µm.

1.2. YAP and TAZ are expressed by endothelial cells and pericytes

ECs are not the only cell type in blood vessels, but share close contact with pericytes and smooth muscle cells. In order to investigate which cells in the retinal vessels express YAP and TAZ, I co-stained P6 WT retinas for YAP or TAZ with the endothelial membrane and cytoplasm marker Isolectin B4 (IB4), the endothelial nuclear marker ERG and the universal nuclear marker DAPI (**Figure 3.2**). Followed by high-resolution single plane confocal imaging, this allowed me to distinguish between endothelial signal (cells with ERG positive nuclei) and signal from mural cells (cells with ERG negative nuclei). Furthermore, pericytes could be distinguished as having ERG negative nuclei, but being also enveloped by a weakly IB4 positive membrane. By doing so, I observed that both ECs **(Figure 3.2 white arrowheads**) and pericytes (**Figure 3.2 yellow arrowheads**) expressed YAP and TAZ in the developing vasculature of the mouse retina.

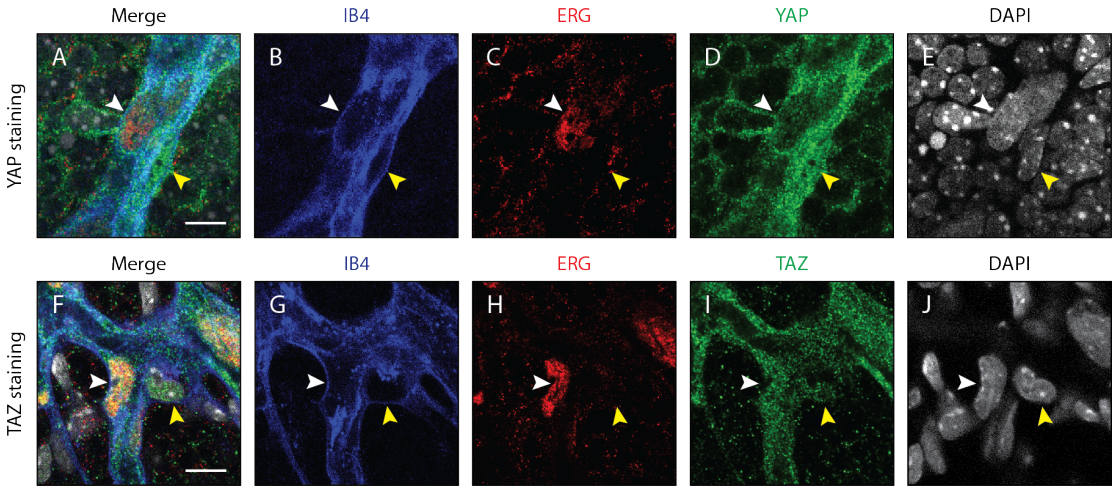

Figure 3.2. In blood vessels, YAP and TAZ are expressed in endothelial and perivascular cells

Immunofluorescence staining of IB4 (B,G, blue), ERG (C, H, red), YAP (D) or TAZ (I) (green) and DAPI (E, J, white) in WT mouse retinas at P6. Both ECs and pericytes are within IB4 staining, but only ECs are positive for the nuclear marker ERG. White arrowhead, endothelial nuclei. Yellow arrowhead, nuclei of pericyte. Images correspond to a single confocal plane. Scale bar: 10µm.

1.3. Nuclear YAP and TAZ is found in sprouting endothelial cells

As the activity of YAP and TAZ depend strongly on their relative presence in the nucleus or cytoplasm, I specifically looked for the subcellular localisation of YAP and TAZ in the developing vasculature of the mouse retina. For this, I further analysed the retinas co-stained for YAP or TAZ, for ERG – marking endothelial nuclei –, and labelled with IB4 – marking endothelial cytoplasm. Specifically in ECs (**Figure 3.3**), I observed that while the expression of YAP was comparable in all areas of the vasculature, the expression of TAZ was much higher in ECs at the sprouting front than in those in more mature vessels (remodelling plexus, arteries and veins), where little staining signal was observed. For both YAP and TAZ there was no variability of subcellular location in ECs in the mature plexus; there, YAP is exclusively cytoplasmic and TAZ is similarly nuclear and cytoplasmic. In contrast, the subcellular location of YAP and TAZ is variable in ECs at the sprouting front: for YAP, ECs show different amounts of nuclear protein, although in all cases less nuclear than cytoplasmic signal is seen; for TAZ, some ECs show preferential nuclear signal, others show similar signal between nucleus and cytoplasm and others show preferential cytoplasmic signal. This variable subcellular location of YAP/TAZ in sprouting ECs is present both in tip and stalk cells, suggesting that they are not primarily regulated by tip/stalk cell identities.

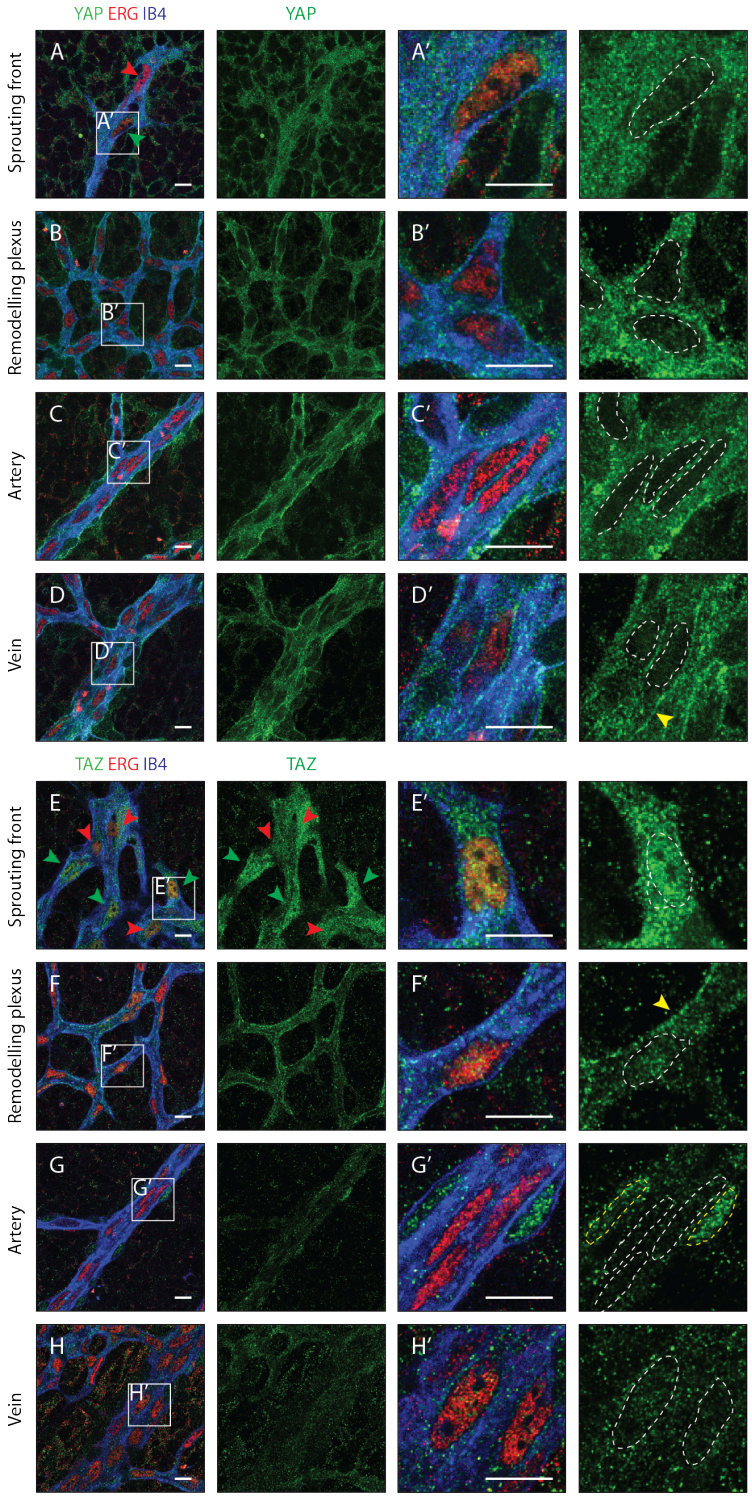

Figure 3.3. YAP and TAZ are nuclear in some sprouting endothelial cells

Immunofluorescence staining of YAP (green, A-D and A'-D') and TAZ (green, E-H and E'-H') in P6 WT mouse retinas. Retinas were co-stained with the endothelial membrane and cytoplasm marker Isolectin-B4 (IB4; blue) and with antibodies against the endothelial nuclei marker ERG (red). White dotted lines, outline of endothelial nuclei. Yellow dotted lines, outline of perivascular cells' nuclei. Green arrowheads, nuclear localisation of YAP and TAZ. Red arrowheads, cytoplasmic localisation of YAP and TAZ. Yellow arrowheads, junctional localisation of YAP and TAZ. Images correspond to single confocal planes. n>3 animals for each staining. Scale bar: 10µm.

1.4. YAP and TAZ also localise to endothelial adherens junctions in the mouse retina vasculature

My analysis further revealed a linear pattern of staining for YAP and TAZ not suggestive of nuclear or cytoplasmic location. The signal instead overlapped with that from VE-Cadherin staining, showing that YAP and TAZ also localise to adherens junctions in ECs (Figure 3.4). Interestingly, I found this junctional location to be mostly present in veins and in the remodelling plexus, and absent at the sprouting front and arteries. Furthermore, the presence of YAP at adherens junctions was stronger and broader than that for TAZ.

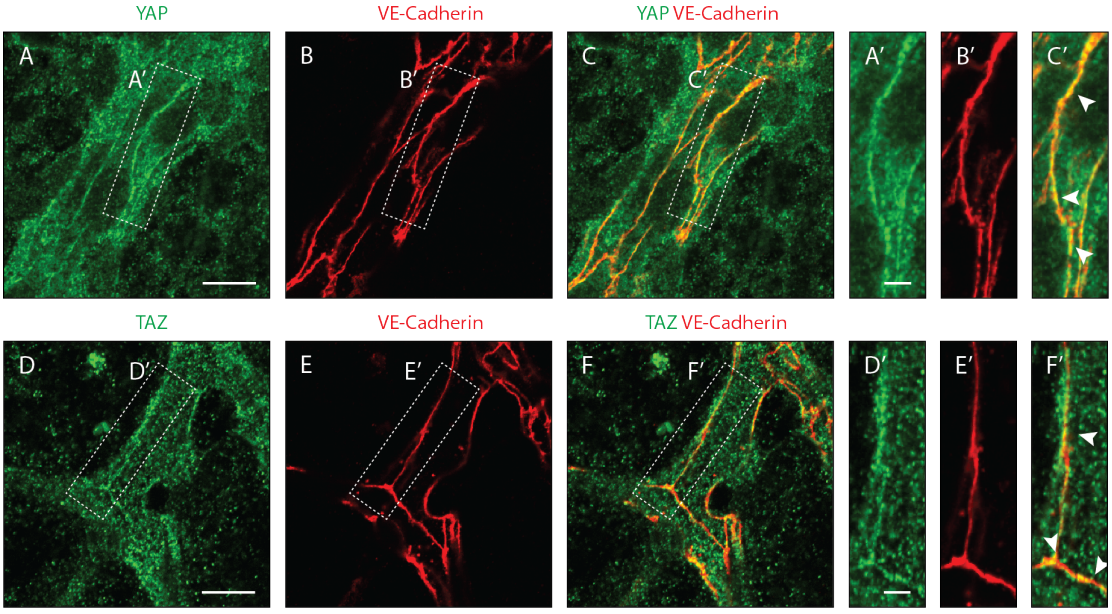

Figure 3.4. YAP and TAZ localise at endothelial adherens junctions in the mouse retina

Immunofluorescence stainings of YAP (green, A-C,A'-C'), TAZ (green, D-F, D'-F') and VE-Cadherin (red, B,E,B',E') were performed in WT mouse retinas at P6. Arrows, co-localisation of YAP or TAZ with VE-Cadherin. Images correspond to single confocal planes. n> 3 pups per staining. Scale bar A-C and D-F 10µm, A'-C' and D'-F' 3µm.

Together, these results suggest that:

1) YAP and TAZ do not have fully overlapping functions,

2) they are differently regulated in mature vs. sprouting ECs and

3) they may act as transcriptional co-activators in sprouting ECs.

2. Endothelial YAP and TAZ are required for vessel growth and density and for the formation of a homogeneous plexus

2.1. Endothelial YAP and TAZ are efficiently lost by tamoxifen injection using the PdgfbCreERT2 line

To understand the cell autonomous role of endothelial YAP and TAZ, I took advantage of the Cre-Lox technology to specifically delete YAP and TAZ from ECs during post-natal sprouting angiogenesis. In order to do so, I crossed mice carrying *Yap* and/or *Taz* floxed genes with mice expressing *PdgfbCreERT2.* In this line, the expression of the *Cre* recombinase is under the control of the endothelial specific promoter *Pdgfb,* restricting its expression to ECs. Furthermore, the CRE is fused to a mutated estrogen receptor, causing its sequestration in the cytoplasm until exposure to tamoxifen. By crossing females homozygous for the floxed gene(s) with males homozygous for the floxed gene(s) and heterozygous for the Cre, I obtained in the same litter both mutant (Cre positive) and control pups (Cre negative). To assess the efficiency of protein deletion, I injected pups with tamoxifen at P1 and P3 and performed immunostaining for YAP or TAZ in the mouse retina at P6. This protocol efficiently led to the deletion of endothelial YAP or TAZ (**Figure 3.5**).

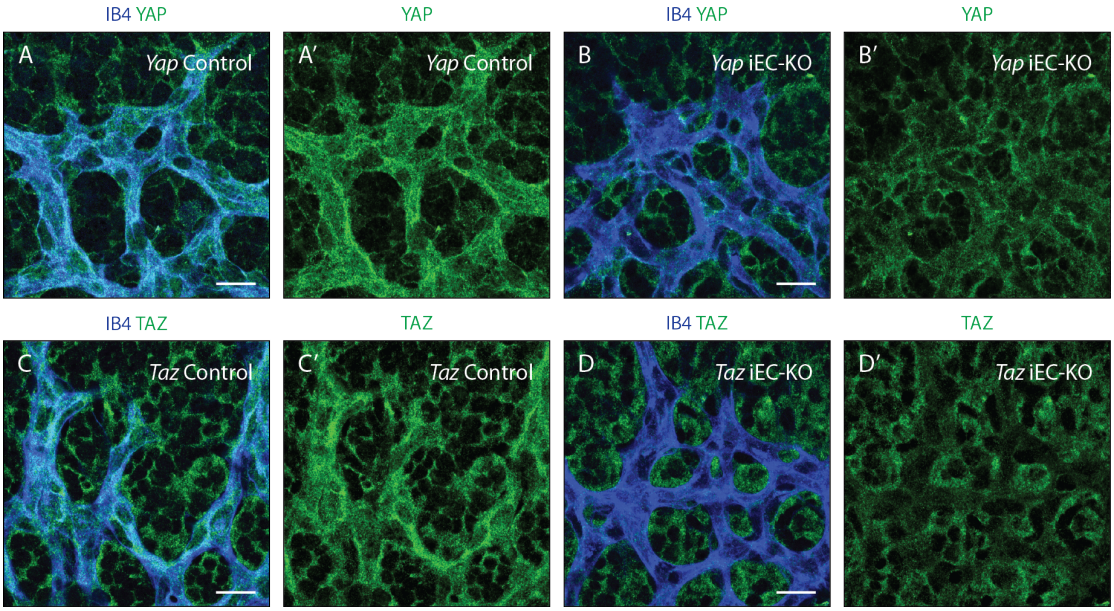

Figure 3.5. YAP and TAZ proteins are efficiently lost upon Cre-mediated genetic deletion

Yap iEC-KO (*Yap*$^{fl/fl}$ *Pdgfb-iCreERT2*+/wt), *Taz* iEC-KO (*Taz*$^{fl/fl}$ *Pdgfb-iCreERT2*+/wt) and respective littermate control mice were injected with tamoxifen at P1 and P3. At P6, retinas were stained

for YAP (green, A, A', B, B'), TAZ (green, C, C', D, D'), and with Isolectin B4 (IB4; blue, A,B,C,D). Scale bar: 20µm.

From here on, I will refer to $Yap^{fl/fl}$ PdgfbCreERT2 +/wt mice as Yap iEC-KO, $Yap^{fl/fl}$ mice as Yap Control, $Taz^{fl/fl}$ PdgfbCreERT2 +/wt mice as Taz iEC-KO, $Taz^{fl/fl}$ mice as Taz Control, $Yap^{fl/fl}Taz^{fl/fl}$ PdgfbCreERT2 +/wt mice as YapTaz iEC-KO and $Yap^{fl/fl}Taz^{fl/fl}$ mice as YapTaz Control.

2.2. YAP/TAZ are required for vessel extension and density in the developing mouse retina

To investigate the role of YAP and TAZ during vessel development, I collected retinas from *Yap* iEC-KO and *Taz* iEC-KO pups at P6 and stained the blood vessels using IB4. The single deletion of endothelial YAP or TAZ led to mild vascular defects (**Figure 3.6**). *Yap* iEC-KO retinas show an 8% reduction in the radial expansion of the vasculature (92+/-5% of the control, p=0.0123) and a 9% reduction in the vascular density of the plexus (91+/-4% of the control, p=0.0002). *Taz* iEC-KO retinas do not show a defect on the radial expansion of the vasculature but display a 7% reduction in the vascular density of the plexus (93+/-6% of the control, p=0.0214). Both *Yap* iEC-KO and *Taz* iEC-KO retinas show no defect in the branching frequency of the plexus. Unlike the single mutants, the deletion of both proteins in double mutant mice (*YapTaz* iEC-KO) causes a dramatic vascular phenotype. *YapTaz* iEC-KO retinas show a 21% reduction in the radial expansion of the vasculature (79+/-14% of the control, p=0.0012), a 26% reduction in the vascular density of the plexus (74+/-7% of the control, p<0.0001) and a 55% decrease in the branching frequency of the vessels (45+/- 15% of the control, p<0.0001). These results show that YAP/TAZ are required for vessel development, and suggest that they can functionally compensate for the loss of the other.

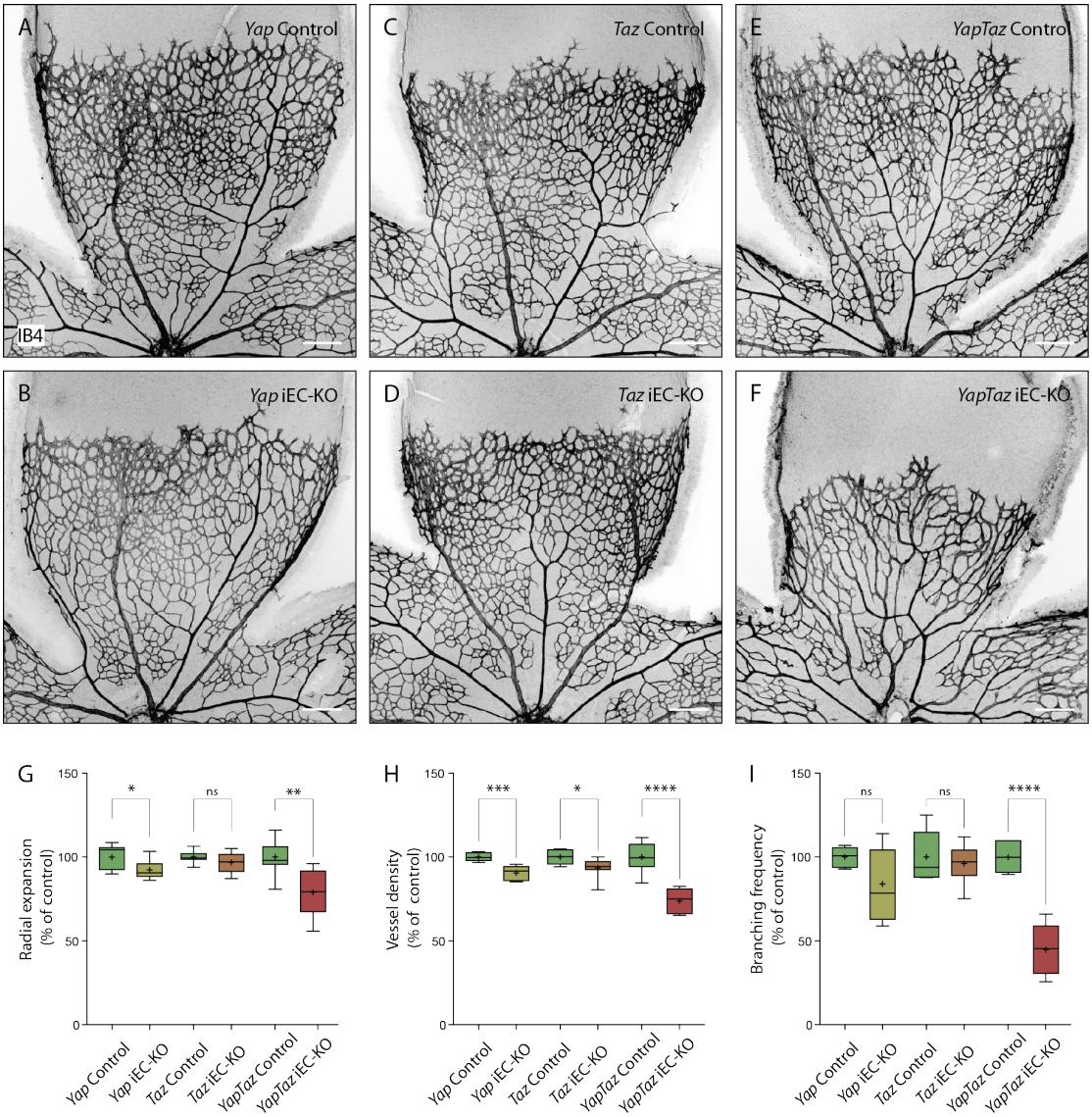

Figure 3.6. Endothelial YAP and TAZ are required for vessel growth and branching

A-F, Retinas from P6 *Yap* iEC-KO (B), *Taz* iEC-KO (D) and *YapTaz* iEC-KO (F), and respective control pups (A, C, E) were stained with Isolectin B4 (IB4). Scale bar: 200µm.

G-I, Radial expansion (G), vessel density (H) and branching frequency (I) in *Yap* iEC-KO, *Taz* iEC-KO and *YapTaz* iEC-KO. Results are shown as percentage of the respective controls. Box and whiskers plot: whiskers show minimum to maximum value; box extends from the 25th to 75th percentiles; line shows median; + sign shows mean. n≥ 5 pups. *p* values were calculated using unpaired *t*-test. *, $p<0.05$; **, $p<0.01$; ****, $p<0.0001$.

To look for evidence of compensation between YAP and TAZ at the protein level, I stained *Yap* iEC-KO retinas for TAZ and *Taz* iEC-KO retinas for YAP. *Yap* iEC-KO retinas show a clear increase in nuclear TAZ (**Figure 3.7**). This is true not only at the sprouting front, where normally some ECs have nuclear YAP, but interestingly also for the remaining vasculature, where normally all ECs express cytoplasmic YAP. In other words, the loss of YAP, regardless of its presence in the

nucleus or cytoplasm, leads in ECs to an increase in TAZ nuclear protein. In contrast, *Taz* iEC-KO retinas did not show increased nuclear YAP in any region of the vasculature, and also did not show a clear difference in YAP staining intensity (not quantified). These results show that TAZ compensates for the loss of YAP with increased nuclear shuttling.

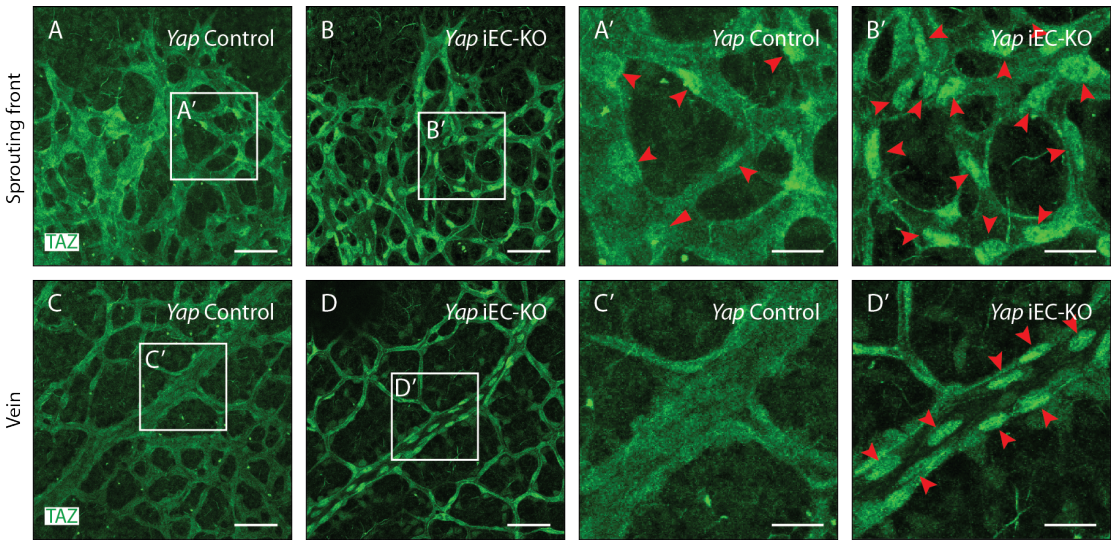

Figure 3.7. TAZ compensates for the loss of YAP in endothelial cells *in vivo*

Retinas from P6 *Yap* iEC-KO (B, D and B', D') and littermate controls (A, C and A', C') were stained by immunofluorescence for TAZ. Green arrowheads, nuclear Taz staining. A, B, A', B' images correspond to maximum projection of z stack. C, D, C', D' correspond to single confocal planes. Scale bar: A-D 50µm, A'-D' 20µm.

2.3. YAP and TAZ are required for the homogeneity of the vascular plexus

On closer observation, I noticed that the organisation of the capillary bed was affected on *YapTaz* iEC-KO mice (**Figure 3.8 A-F**). In control mice, the loops between blood vessels are of similar size and shape, reflecting the homogeneous distribution of ECs throughout space. *Yap* iEC-KO and *Taz* iEC-KO mice showed bigger vascular loops than control mice, but no difference in the variability of size and shape of these loops (**Figure 3.8 B, D, G-I**). In contrast, in *Yap/Taz* iEC-KO mice the loops were not only bigger but also more variable in size, and shape (**Figure 3.8 F, G-I**) than in control mice. These results indicate that endothelial YAP and TAZ are critical for the development of a homogeneous blood vessel network.

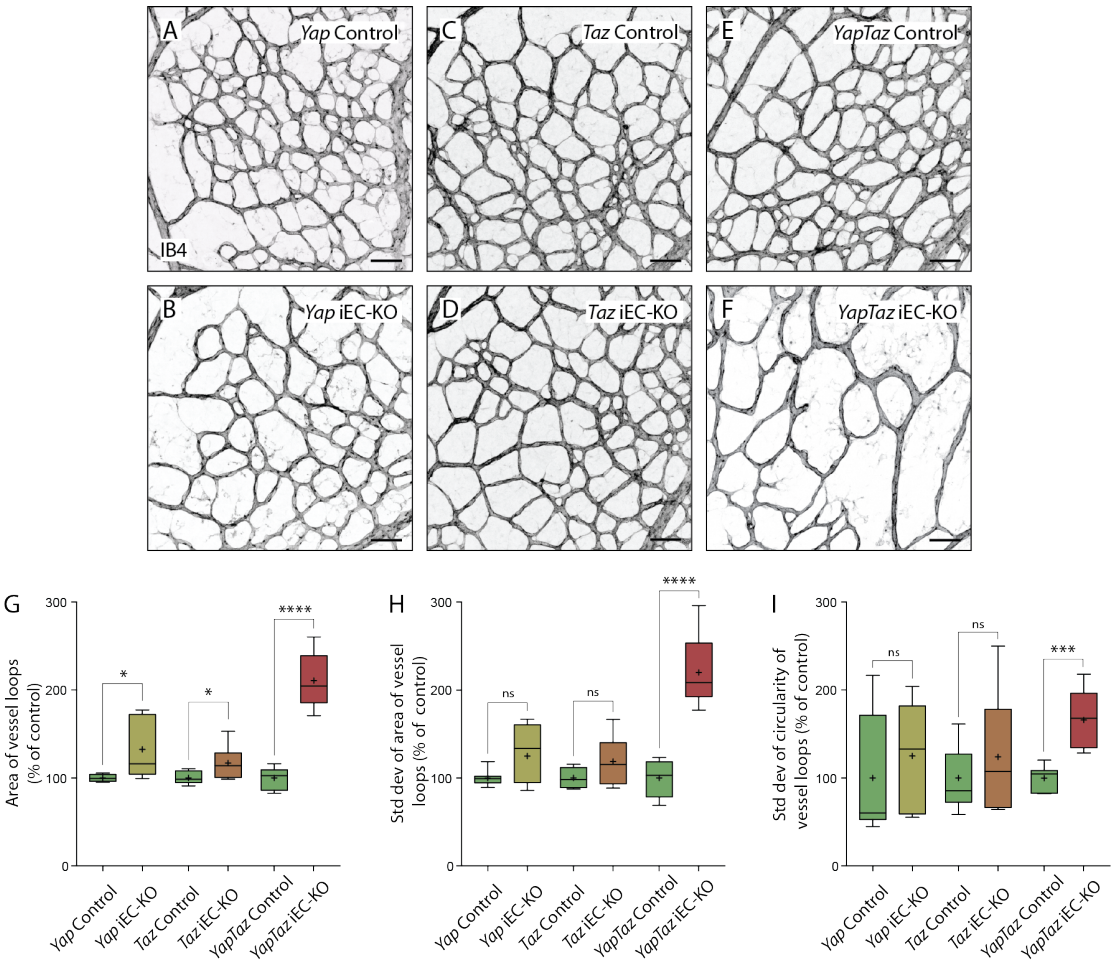

Figure 3.8. Endothelial YAP and TAZ are required for the homogeneity of the plexus

A-F, Retinal vascular plexus of P6 *Yap* iEC-KO (B), *Taz* iEC-KO (D) and *YapTaz* iEC-KO (F), and respective control pups (A, C, E) stained with Isolectin B4 (IB4). Scale bar: 50µm.

G, Area of vessel loops in the retinal vascular plexus of *Yap* iEC-KO, *Taz* iEC-KO and *YapTaz* iEC-KO. **H-I**, Standard deviation of the area (H) and circularity (I) of the vessels loops in *Yap* iEC-KO, *Taz* iEC-KO and *YapTaz* iEC-KO vascular plexus. G, H, I, Results shown as percentage of the respective controls. Box and whiskers plot: whiskers show minimum to maximum value; box extends from the 25th to 75th percentiles; line shows median; + sign shows mean. n≥ 5 pups. *p* values were calculated using unpaired *t*-test. *, $p<0.05$; **, $p<0.01$; ****, $p<0.0001$.

2.4. TAZ and YAP/TAZ mutants show crosses between arteries and veins

In addition to affecting the capillary network, the endothelial deletion of YAP and TAZ also impacted the organisation of arteries and veins (**Figure 3.9**). In control retinas arteries and veins run parallel to each other, separated by the capillary network, and do not normally cross (Figure 3.9 A, A'). In contrast, *Yap/Taz* iEC-KO retinas often show arteriovenous crosses (Figure 3.9 B, B' yellow arrowheads and D). Furthermore, some of these crosses occur in association with venous defects.

Normally in the mouse retina vasculature, arteries branch into smaller arteries in oblique angles, while veins run straight and receive blood from capillaries connecting in perpendicular angles (Figure 3.9A). *Yap/Taz* iEC-KO retinas however show veins that branch or split (Figure 3.9 B, B', C, C' yellow circles and E). In more severe cases, it is difficult to distinguish between arteries and veins in *Yap/Taz* iEC-KO retinas, as veins show multiple oblique connections with surrounding vessels (Figure 3.9 C, C' yellow circles). *Yap* iEC-KO retinas show no increase in arteriovenous crosses (Chapter 3 – Figure 9D) and vein defects (Figure 3.9 E), but interestingly, both were already present in *Taz* iEC-KO retinas (Figure 3.9 D and E).

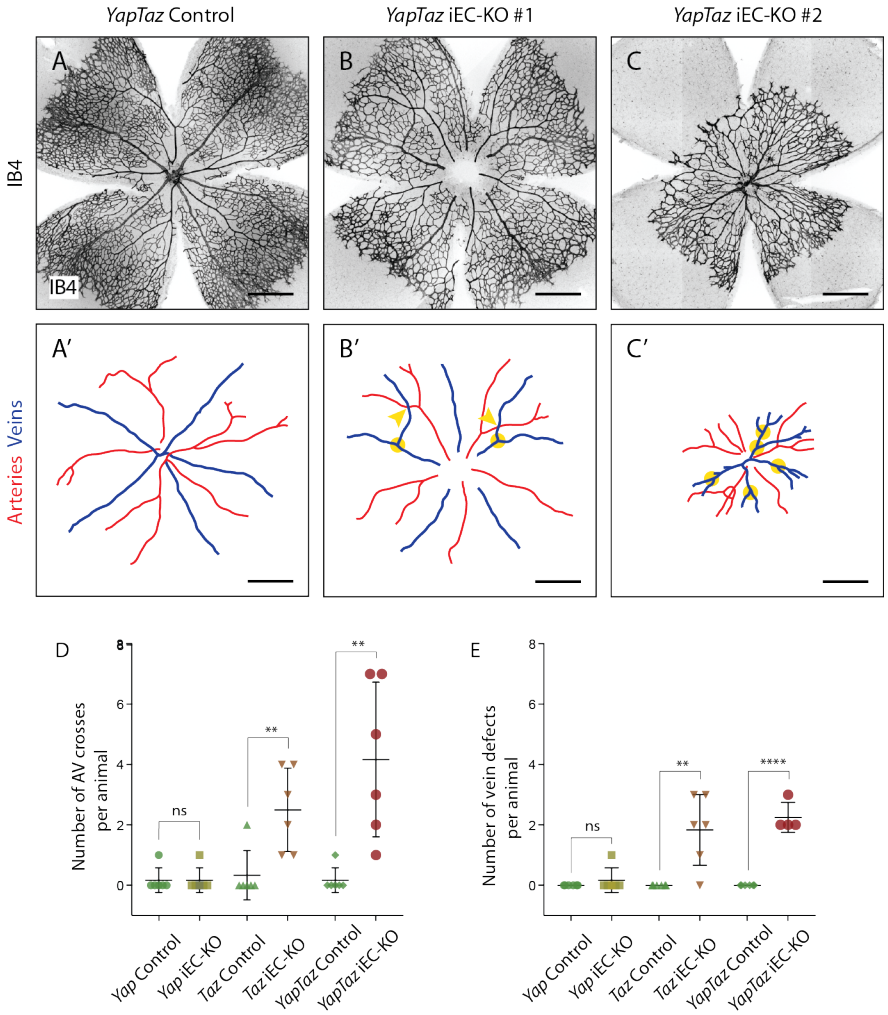

Figure 3.9. YAP and TAZ regulate the organisation of arteries and veins

A-C, Retinas from two P6 *YapTaz* iEC-KO mice (B,C), and one control mouse (A) stained with Isolectin B4 (IB4). A'-C', mask of arteries and veins from A-C respectively. Red, arteries; Blue, veins. Yellow arrowheads, arterio-venous crossover. Yellow circle, vein defect (splitting of branching). Scale bar: 500µm.

D, E, Number of AV crosses (E) and vein defects (E) per animal in *Yap* iEC-KO, *Taz* iEC-KO, *YapTaz* iEC-KO and respective controls. Scatter dot plot: each dot represents one animal. Data are

mean +/- SD. *p* values were calculated using unpaired t-test. *, $p<0.05$; **, $p<0.01$; ****, $p<0.0001$. n= 6 pups per condition except for quantification of vein defects in *YapTaz* iEC-KO (n=4).

3. At the sprouting front, YAP/TAZ maintain the integrity of the vascular barrier and promote the distribution of endothelial cells

3.1. YAP/TAZ are required for sprouting

To understand if the defects described above were related to a defect in sprouting of new vessels, I analysed with more detail the sprouting front of *Yap* and *Taz* single mutants and *Yap/Taz* double mutants (**Figure 3.10 A-F**). *Yap* iEC-KO retinas do not show a change in the number of sprouts per length of the sprouting front (106+/-8% of the control, $p=0.3085$) (**Figure 3.10 A, B, G**). In contrast, *Taz* iEC-KO retinas have an 18% reduction in the number of sprouts (82+/-5% of the control, $p=0.0127$) (**Figure 3.10 C, D, G**). As with previous parameters, the deletion of both proteins also increases the sprouting defect, so that *YapTaz* iEC-KO retinas show a 30% reduction in the number of sprouts (30+/-10% of the control, $p=0.0004$) (**Figure 3.10 E, F, G**). These results show that YAP/TAZ are required for sprouting of new blood vessels, and also suggest that TAZ has a more preponderant role in sprouting than YAP.

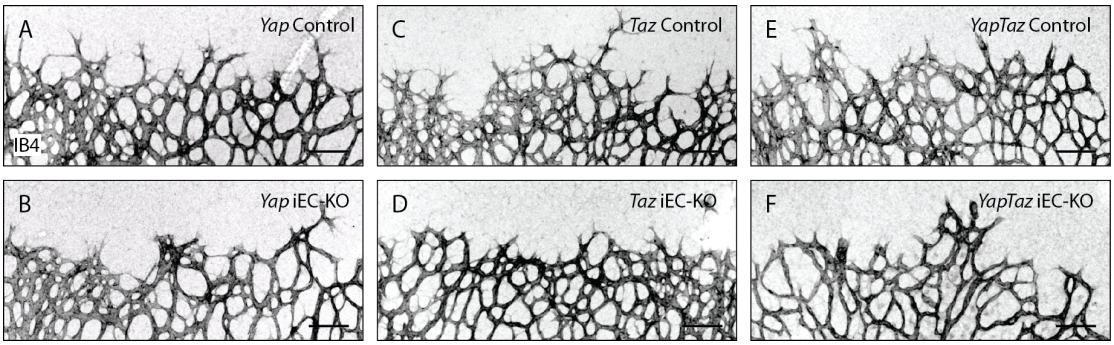

Figure 3.10. Endothelial YAP and TAZ are required for vascular sprouting

A-F, Retinas from P6 *Yap* iEC-KO (B), *Taz* iEC-KO (D) and *YapTaz* iEC-KO (F), and respective control pups (A, C, E) were stained with Isolectin B4 (IB4). Images show the sprouting front. Scale bar: 100µm.

G, Number of sprouts per surface extension in *Yap* iEC-KO, *Taz* iEC-KO and *YapTaz* iEC-KO. Results are shown as percentage of the respective littermate controls. Box and whiskers plot: whiskers show minimum to maximum value; box extends from the 25th to 75th percentiles; line shows median; +

sign shows mean. *p* values were calculated using unpaired t-test between the mutant and respective littermate control. *, $p<0.05$; **, $p<0.01$; ****, $p<0.0001$. n= 5 pups per condition.

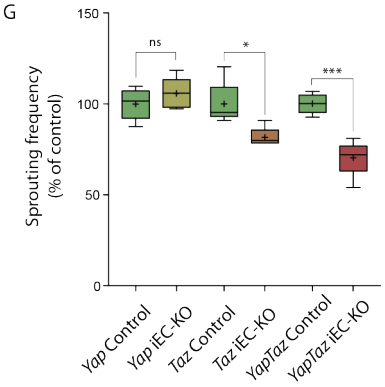

3.2. YAP/TAZ are required for endothelial cells to distribute and rearrange in sprouting vessels

Not only have *YapTaz* iEC-KO retinas less sprouts than control retinas, they also present severe morphological defects. To further analyse the shape defects and organisation of ECs in sprouting vessels, I co-stained retinas for IB4 and ERG and imaged retinas in higher resolution. Sprouts of control mice (**Figure 3.11, A, A'**) are elongated and show long cellular protrusions towards the non-vascularised front. In contrast, sprouts from *YapTaz* iEC-KO mice are rounder in shape and lack cellular protrusions (**Figure 3.11, B, B'**). Moreover, endothelial nuclei in sprouts of control mice are elongated and homogeneously distributed throughout the vessels (**Figure 3.11 A'**). In *YapTaz* iEC-KO mice however, endothelial nuclei are rounder and show irregular spacing, often appearing aggregated within the sprouts (**Figure 3.11 B'**). Together, these morphological defects suggest that ECs lacking YAP/TAZ are less able to migrate and rearrange in sprouting vessels.

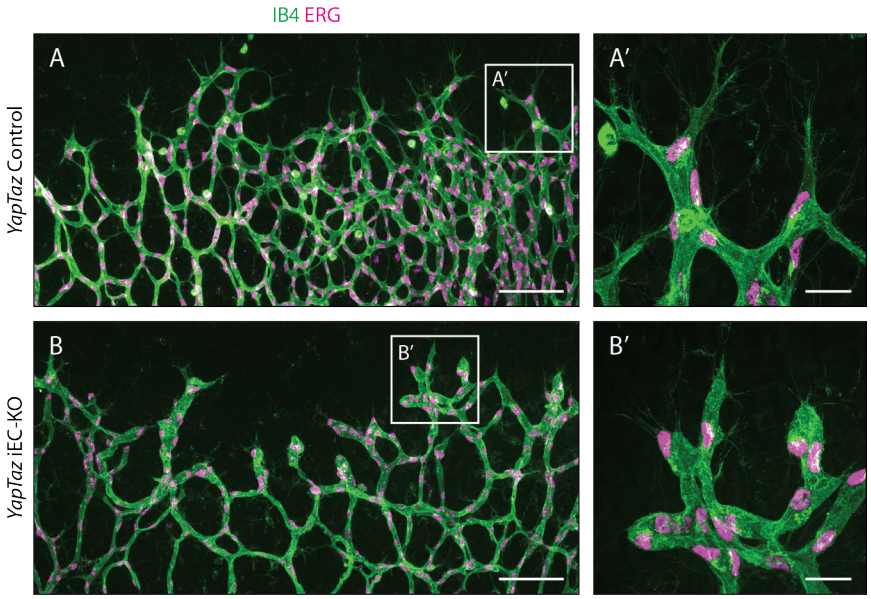

Figure 3.11. Combined loss of YAP and TAZ leads to sprouting shape defects and nuclei clumping

A, B, P6 retinal vessels labelled with Isolectin B4 (IB4, green) and stained for ERG (magenta, marking endothelial nuclei) in *YapTaz* iEC-KO (B) and littermate control mice (A). A', B', magnification of boxed areas in A and B. Scale bar: A, B 100μm, A', B' 25μm.

In order to assess the arrangement of cells within vessels, I co-stained retinas for IB4 and VE-Cadherin, the main component of vascular adherens junctions. In control retinas, ECs organise into multicellular vessel tubes, highlighted by the presence of two or more VE-Cadherin junctions running along the axis of the vessel (**Figure 3.12 A**). A few unicellular vessel segments can also be observed in control retinas but only in regressing vessels, which can be identified by their decreasing calibre (**Figure 3.12 A red arrowhead**). In contrast, in *YapTaz* iEC-KO retinas I found many unicellular vessel segments that did not localise to regressing vessels, but instead existed in vessels of normal calibre (**Figure 3.12 B**). Moreover, the appearance of adherens junctions was also affected by the loss of endothelial YAP/TAZ. In control vessels, the junctions between ECs are thin and linear (**Figure 3.12 A"**). In contrast, in *YapTaz* iEC-KO vessels I often observed tortuous junctions between ECs (**Figure 3.12 B"**), again pointing towards a defect in cell elongation and rearrangements.

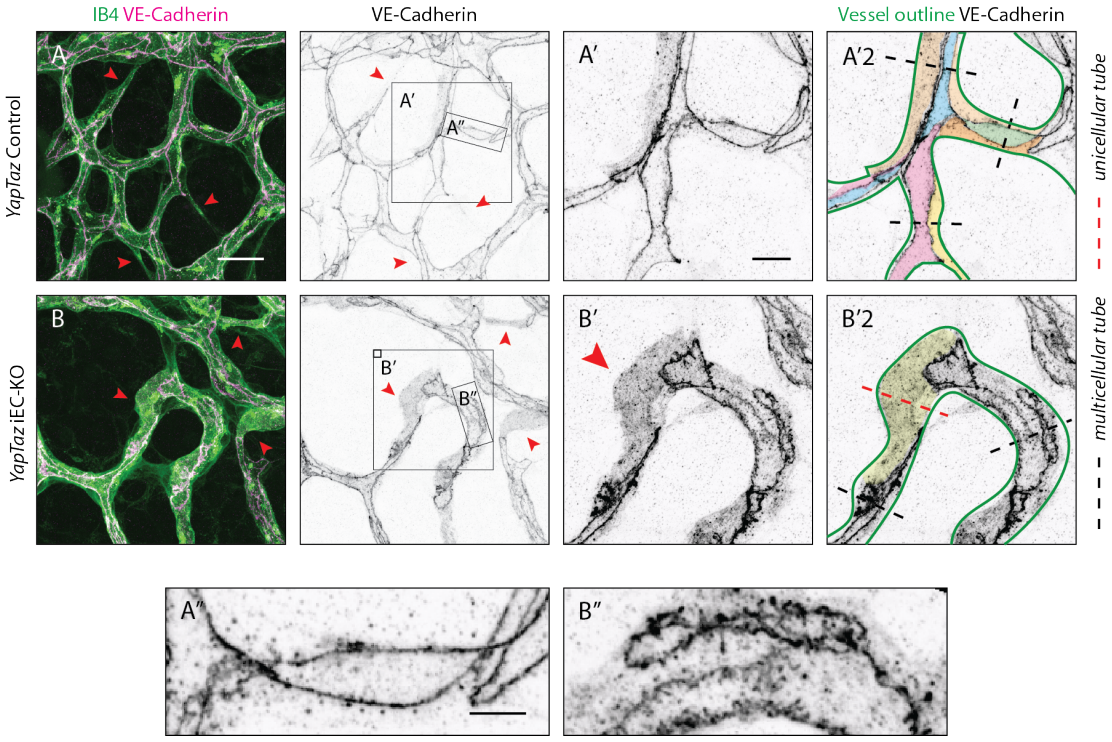

Figure 3.12. The combined loss of YAP and TAZ leads to adherens junctions' defects in vivo

A, B, P6 retinal vessels labelled with Isolectin B4 (IB4, green) and stained for VE-Cadherin (magenta) in *YapTaz* iEC-KO (B) and control mice (A). Red arrowheads, no longitudinal VE-Cadherin labelled junction along vessel axis denoting unicellular vessel segments. A', B', A'', B'', magnification of boxed areas in A and B. A'2, B'2, individual ECs are highlighted in different colours. Scale bar: A,B 25μm, A',B' 10μm, A",B" 5μm. n=4 control/4 KO pups.

Moreover, I found in *YapTaz* iEC-KO retinas aberrant vessel crosses not only in arteries and veins as I have here already reported but also in the capillaries near the sprouting front. In the control retina at P6, blood vessels grow in one single layer (**Figure 3.13 A**). However, in *YapTaz* iEC-KO retinas I found several vessel crosses in three dimensions (**Figure 3.13 B**). These suggest that vessels failed to anastomose or stabilise connections following sprouting, and instead passed each other.

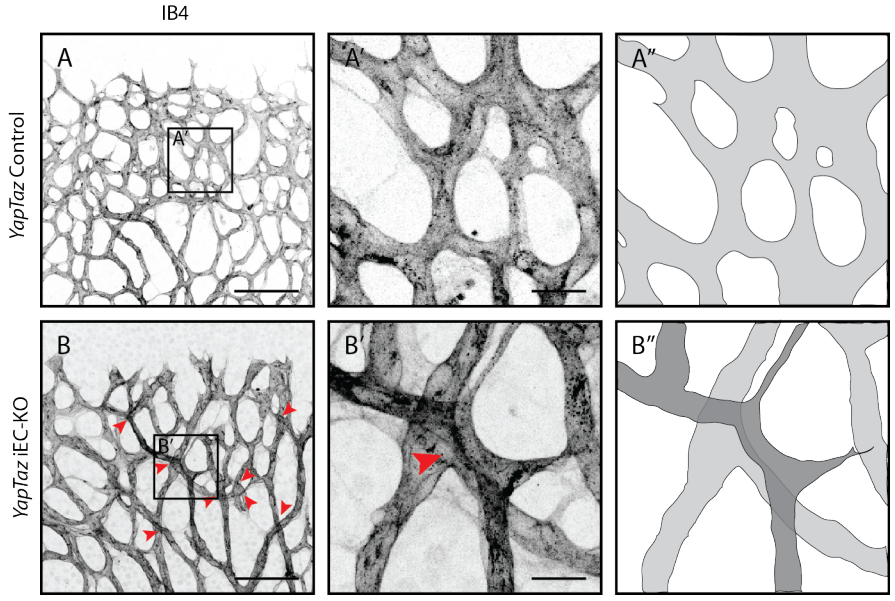

Figure 3.13. The combined loss of YAP and TAZ leads to vessel crosses *in vivo*

A, B, P6 retinal vessels labelled with Isolectin B4 (IB4) in *YapTaz* iEC-KO (B) and control mice (A). Red arrowheads, vessel crosses. A', B', magnification of boxed areas in A, B. A'',B'', depiction of vessels in A' and B', where different colours represent vessels in different 3D planes. Scale bar: A,B 100µm, A'-B' 20µm. n=4 control/4 KO pups.

3.3. *YapTaz* iEC-KO retinas present haemorrhages at the sprouting front

While dissecting retinas from *YapTaz* double mutant litters I observed that some had haemorrhages, which I had not seen while processing retinas from *Yap* or *Taz* single mutant litters. Staining for TER119, a marker of red blood cells, confirmed the presence of large haemorrhages in *YapTaz* iEC-KO retinas (**Figure 3.14**), and also their absence in the single mutants (data not shown). Interestingly, the haemorrhages in *YapTaz* iEC-KO retinas were predominantly located at the sprouting front, and rarely present in the mature plexus. *YapTaz* iEC-KO P6 brains showed no signs of haemorrhages on visual inspection (data not shown), and mice survived normally up to P28, thus excluding life-threatening haemorrhages during that period of time. These results suggest that especially actively sprouting ECs require YAP/TAZ in order to maintain the vascular barrier function.

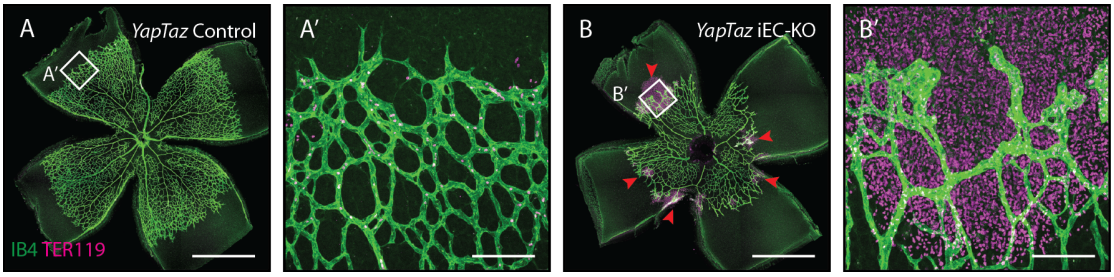

Figure 3.14. Endothelial YAP and TAZ prevent haemorrhages at the sprouting front

A, B, P6 retinal vessels labelled with Isolectin B4 (IB4, green) and stained for TER119 (magenta, marking red blood cells) in *YapTaz* iEC-KO (B) and control mice (A). Red arrowheads, haemorrhages. A', B', magnification of boxed areas in A and B. Scale bar: A,B 1000μm, A', B' 100μm. n> 4 pups.

3.4. Pericytes covering YapTaz iEC-KO vessels at the sprouting front show abnormal expression of αSMA

Deficient coverage of vessels by mural cells – pericytes and smooth muscle cells - has been associated not only with loss of barrier function (Armulik et al., 2010) but also with haemorrhages (Li et al., 2011). Furthermore, vessel coverage by mural cells has been inversely correlated with vessel diameter and vessel density (Enge et al., 2002, Bjarnegard et al., 2004, Lindahl et al., 1997, Hellstrom et al., 2001, Armulik et al., 2010), both of which are affected in *YapTaz* iEC-KO vessels. As such, I sought to address whether endothelial YAP/TAZ affects the coverage of vessels by mural cells. To do so, I co-stained *YapTaz* iEC-KO retinas for IB4, with the pericyte marker NG2 and with the vascular smooth muscle cell marker αSMA, and focused my analysis at the sprouting front, as the place of preferential haemorrhages (**Figure 3.15**). There, the extension of coverage of *YapTaz* iEC-KO vessels by NG2 positive cells is not different from control vessels (**Figure 3.15 B, D, G, I**). However, αSMA signal is present in *YapTaz* iEC-KO retinas at the sprouting front (**Figure 3.15 H, J**), where it is practically absent in control retinas (**Figure 3.15 C, E**). On closer observation (**Figure 3.15 K**), I could identify that the αSMA signal followed the same shape as the NG2 signal, with both protruding slightly outside of the IB4 marked endothelial tube. These results show that some of the pericytes in the sprouting front of *YapTaz* iEC-KO retinas abnormally express αSMA. By looking at the distribution of αSMA signal throughout the entire retina (**Figure 3.15 L-P**), I observed that its expression is not different in the mature plexus of *YapTaz* iEC-KO and controls. There, αSMA signal is restricted to arteries, labelling the smooth muscle cells there present. However, at the sprouting front the αSMA signal is distinctly different

between *YapTaz* iEC-KO and controls. In control retinas the αSMA signal is sharply lost when arteries branch into progressively smaller vessels, approximately at 2/3 of the distance between the optic nerve and the sprouting front; there is almost no αSMA signal in the distal 1/3 of the retinal vasculature. In contrast, in *YapTaz* iEC-KO retinas the αSMA signal does not stop but instead decreases when arteries divide into smaller branches, continuing until the capillaries at the sprouting front (**Figure 3.15 N, O, P**). Sprouting front capillaries upstream of a vein show less or no αSMA signal. The difference in αSMA expression by pericytes in capillaries close to an artery or to a vein suggests that local mechanisms other than the endothelial loss of YAP/TAZ could account for the phenotype. This could reflect an indirect response to altered hemodynamics in the YapTaz iEC-KO retina vasculature, or to an increased inflammatory response caused by haemorrhages. Computer simulations showed that the sprouting front vessels of the P6 WT mouse retina experience very low levels of shear stress (Bernabeu et al., 2014). Because of the severe reduction in vessel density and branches in YapTaz iEC-KO retinas, an increase in shear stress is expectable, as there is less total capacity to disperse the blood volume coming from the arteries feeding the retina. Another plausible mechanism is inflammation. Although quiescent pericytes do not express αSMA, its expression can be upregulated in inflammation (Armulik et al., 2011). Importantly, more macrophages are found surrounding YapTaz iEC-KO vessels than control vessels (data not shown), which is a common finding when haemorrhages are present, and denotes increased inflammation.

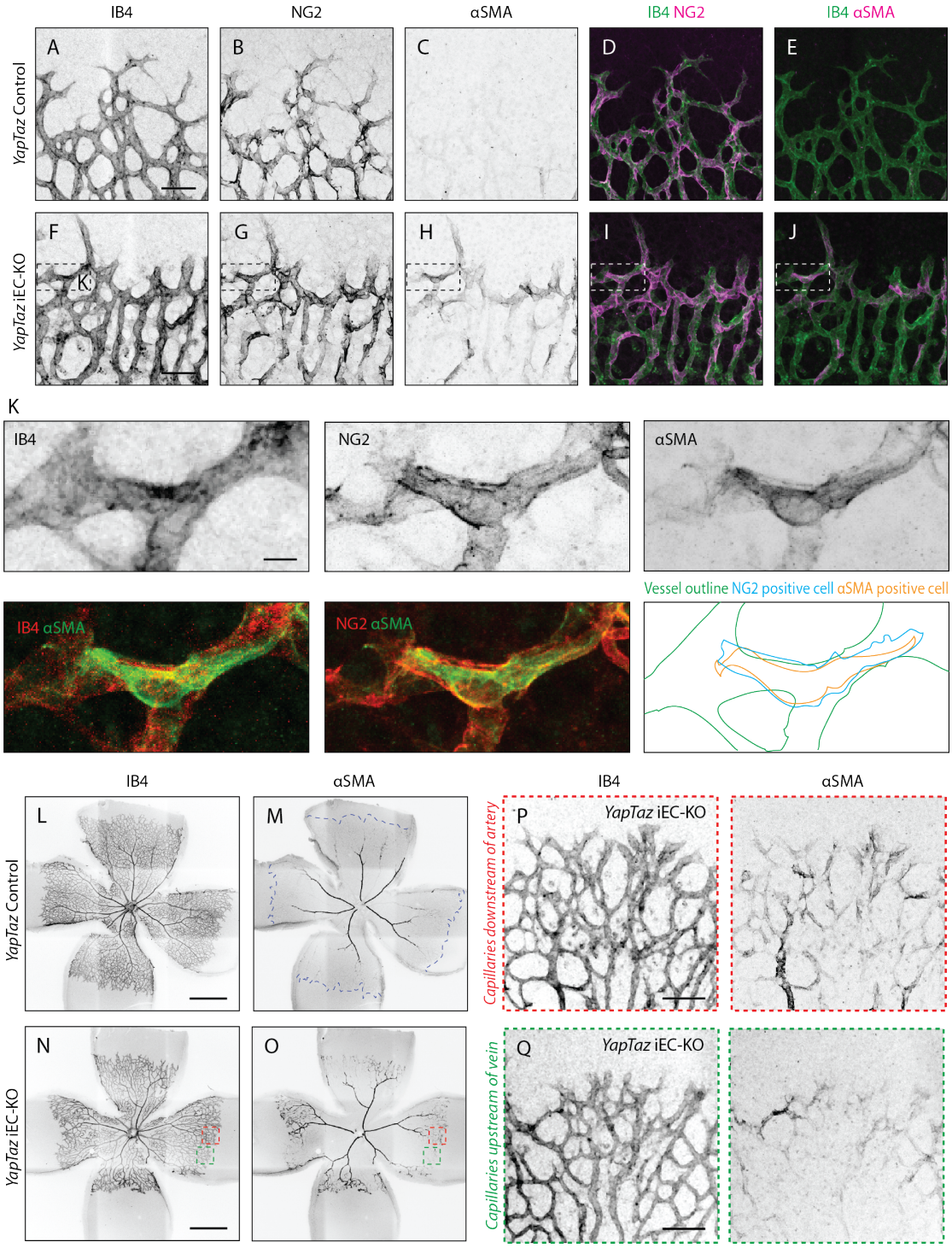

Figure 3.15. Pericytes in the sprouting front of YapTaz iEC-KO retinas ectopically express αSMA

A-J, Retinas from P6 *YapTaz* iEC-KO (F-J), and control pups (A-E) stained with Isolectin B4 (IB4), NG2 and αSMA. Scale bar: 50 µm. **K**, Magnification of boxed area in F-J. Scale bar: 10 µm.

L-O, Retinas from P6 *YapTaz* iEC-KO (N, O), and control pups (L, M) stained with Isolectin B4 (IB4) and αSMA. Blue dashed line, sprouting front of vasculature. Scale bar: 500 µm. **P, Q**, Magnification of boxes areas in N, O. **P**, sprouting front capillaries downstream of artery. **R**, sprouting front capillaries upstream of vein. Scale bar: 100 µm.

4. Summary and conclusions

In this chapter I have shown that YAP and TAZ are highly expressed by ECs of the developing vasculature, and localise to the nucleus at the sprouting front. This is especially true for TAZ; differently, YAP mostly localises to the cytoplasm of ECs.

My functional experiments using single and double mutant mice have shown that although YAP and TAZ have a great deal of redundancy (mostly evident from the mild phenotype of the single mutants and the striking phenotype of the double mutant), they do not show fully overlapping functions. For instance, only TAZ mutants show hyposprouting, AV crosses and vein defects. This signifies that although redundancy is present, some functions are still unique for YAP and TAZ.

I have shown that *YapTaz* iEC-KO retinas have decreased radial expansion, vascular density, sprouting and branching. These phenotypes could be related to a defect in getting sufficient numbers of ECs to populate the retina. It is in fact one of the best-documented functions of YAP and TAZ, that of regulating proliferation and apoptosis. However, other described phenotypes – defective integrity of vessel barrier, defective cell distribution and elongation, vessel crosses – point towards a possible role of YAP and TAZ in regulating junctional morphology and cell migration.

In the next chapter I will describe my findings relating to how YAP and TAZ control the referred cellular processes in ECs, and possible molecular mechanisms.

Chapter 4: YAP and TAZ increase JAIL formation and junctional turnover

1. YAP and TAZ increase endothelial cell proliferation downstream of mechanical stimuli

1.1. Endothelial YAP and TAZ regulate cell numbers in the mouse retina through the promotion of cell proliferation

The growth of new vessel sprouts requires endothelial proliferation. This can be readily appreciated in the developing mouse retina vasculature, where ECs at the sprouting front are highly proliferative, in contrast with the ones in more mature vessels (**Figure 4.1**).

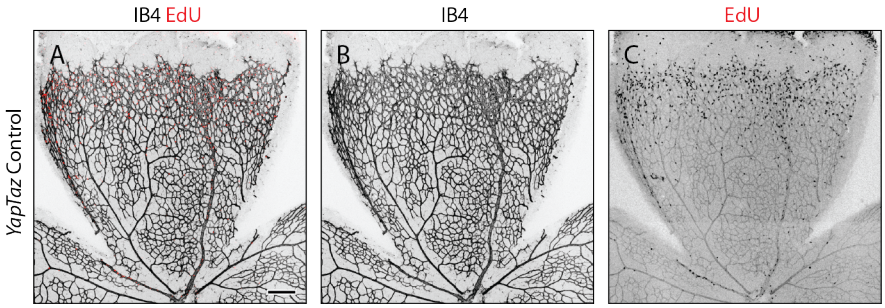

Figure 4.1. Endothelial cells at the sprouting front are highly proliferative

A-C, Retinas from P6 mice stained with Isolectin B4 (IB4) (A, B, black) and EdU marking nuclei of S-phase cells (A, C, red). Mice were injected with EdU 2 hrs prior to culling to analyse endothelial proliferation. A well-delimited proliferation area is seen at the sprouting front. Scale bar: 200µm.

When the ability of ECs to proliferate is compromised (Ubezio et al., 2016), retinal vessels show decreased radial expansion, decreased vascular density, decreased protruding tip cells and decreased branching points. As all these parameters were affected in *YapTaz* iEC-KO retinas, and nuclear YAP and TAZ are found in the same area where proliferation takes place, I investigated whether YAP and TAZ impacted cell proliferation. Moreover, and as referred to before, YAP and TAZ are critical regulators of cell proliferation in many cell types. To do so, I pulsed mutant mice with EdU, a nucleoside analog of thymidine that is incorporated into DNA during active DNA synthesis, 2 hrs before culling. I then co-stained retinas for

endothelial nuclei (ERG) and blood vessels (IB4) to make sure I evaluated endothelial proliferation and not proliferation from other cells in the retina (**Figure 4.2 A, B**). EC proliferation was 24% decreased in *Yap* iEC-KO retinas (76 +/- 10 % of the control, *p*=0.0469), but not affected in *Taz* iEC-KO (**Figure 4.2 C**). Consistent with previous observations the decrease in cell proliferation was strongest in *Yap/Taz* iEC-KO retinas, showing a 33% reduction in proliferation (67 +/- 26% of the control, *p*=0.0059) (**Figure 4.2 A, B, C**).

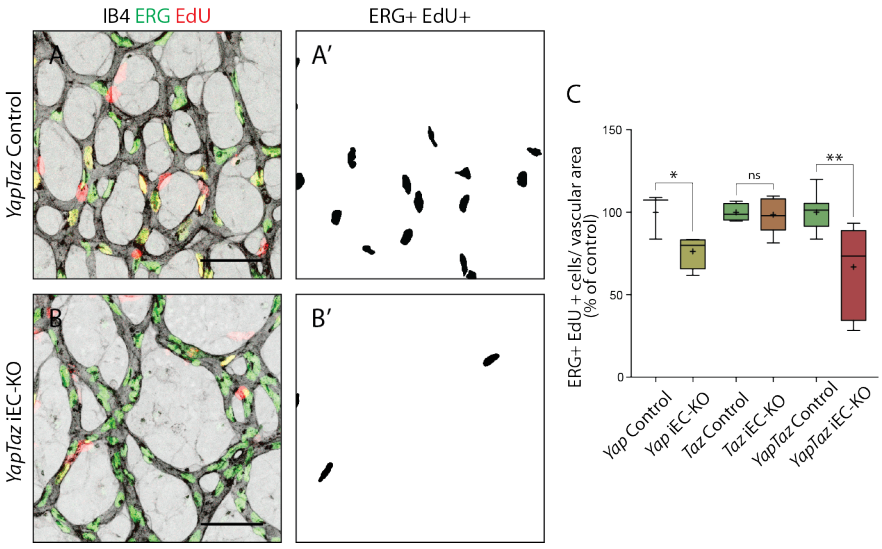

Figure 4.2. YAP/TAZ promote endothelial proliferation in the mouse retina

A, B, P6 retinal vessels labelled with Isolectin B4 (IB4, grey) and stained for EdU (red, marking S phase positive cells) and ERG (green, marking endothelial nuclei) in *YapTaz* iEC-KO (B) and littermate control mice (A). A', B', mask of Erg + and EdU + cells indicating proliferating ECs. Scale bar: 50µm.

C, Quantification of endothelial proliferation in *Yap* iEC-KO (n=3 control/4 KO pups), *Taz* iEC-KO (n=5 control/5 KO pups) and *YapTaz* iEC-KO (n=8 control/7 KO pups). Number of EdU-positive and ERG-positive cells per IB4 labelled vascular area was calculated for each genotype. Results are shown as percentage of the respective littermate controls. Box and whiskers plot: whiskers show minimum to maximum value; box extends from the 25th to 75th percentiles; line shows median; + sign shows mean. *p* values were calculated using unpaired t-test between the mutant and respective littermate control. *, $p<0.05$; **, $p<0.01$.

I also investigated if an additional cause for decreased vascularization in *YapTaz* iEC-KO retinas would be increased endothelial apoptosis. Yorkie, the YAP ortholog in the fly, is not only pro-proliferative but also anti-apoptotic (Huang et al., 2005). YAP however has been shown to be both anti (Rosenbluh et al., 2012) (Marti et al., 2015, Schwartzman et al., 2016) and pro (Tomlinson et al., 2010, Cottini et al., 2014) apoptotic depending on the cell type and context. To evaluate if YAP and TAZ

affect endothelial apoptosis in the retina vasculature I stained mutant retinas for the active form of the executioner caspase 3 (cleaved caspase 3) together with IB4 and measured the number of apoptosis events (**Figure 4.3**). By doing so, I did not observe an increase in apoptosis for any of the mouse mutants (**Figure 4.3 C**). Instead, there was a tendency for decreased apoptosis in all mutants, however not statistically significant. This clearly shows that YAP/TAZ do not inhibit endothelial apoptosis.

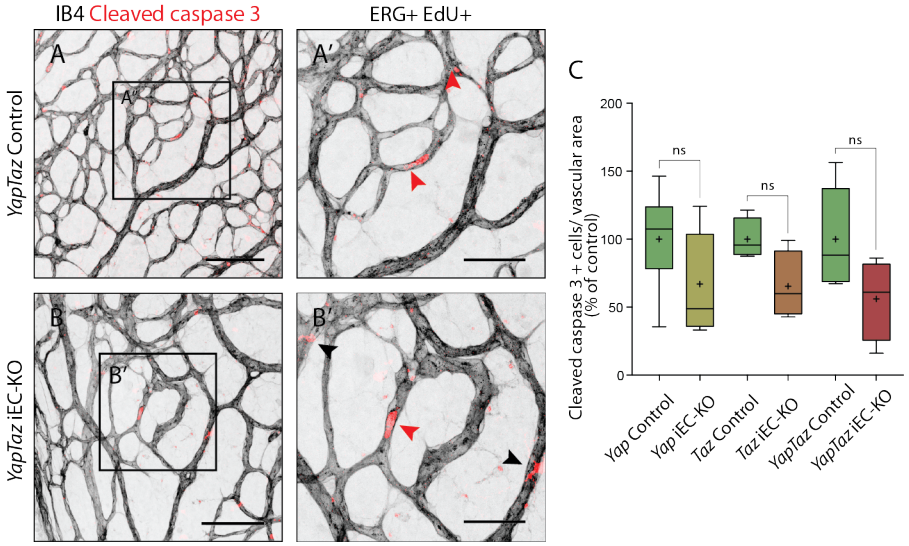

Figure 4.3. YAP/TAZ do not inhibit endothelial apoptosis in the mouse retina

A, B, P6 retinal vessels labelled with Isolectin B4 (IB4, grey) and stained for cleaved caspase 3 (red) in *YapTaz* iEC-KO (H) and littermate control mice. A', B', magnification of boxed area in A, B. Red arrowheads, cleaved caspase 3 positive endothelial cell. Black arrowheads, cleaved caspase 3 outside vessels. Scale bar: A,B 100µm, A'-B' 50µm.

C, Quantification of endothelial apoptosis in *Yap* iEC-KO (n=7 control/7 KO pups), *Taz* iEC-KO (n= 4 control/4KO pups) and *YapTaz* iEC-KO (n=5 control/4 KO pups). Results are shown as percentage of the respective littermate controls. Box and whiskers plot: whiskers show minimum to maximum value; box extends from the 25th to 75th percentiles; line shows median; + sign shows mean. *p* values were calculated using unpaired t-test between the mutant and respective littermate control. ns, $p>0.05$.

Together, my results suggest that a decrease in endothelial proliferation, but not an increase in apoptosis, can lead to the vascularisation defects in *Yap/Taz* iEC-KO retinas.

1.2. YAP is required for stretch induced proliferation, but not for VEGF induced proliferation

Endothelial proliferation is triggered by a variety of stimuli, some of which are chemical in nature, while others are mechanical (Akimoto et al., 2000, Lacolley, 2004). As YAP and TAZ are regulated both by chemical and mechanical stimuli in other cell types, I aimed to investigate which stimuli would be upstream of YAP/TAZ dependent endothelial proliferation.

To do these experiments I turned to *in vitro* culture of HUVECs and established a loss of function system by doing gene knockdown for YAP and/or TAZ using siRNAs in HUVECs. This strategy efficiently led to the loss of YAP and/or TAZ protein, as I could verify by immunofluorescence (**Figure 4.4 A-H**) and western-blot (**Figure 4.4 I**).

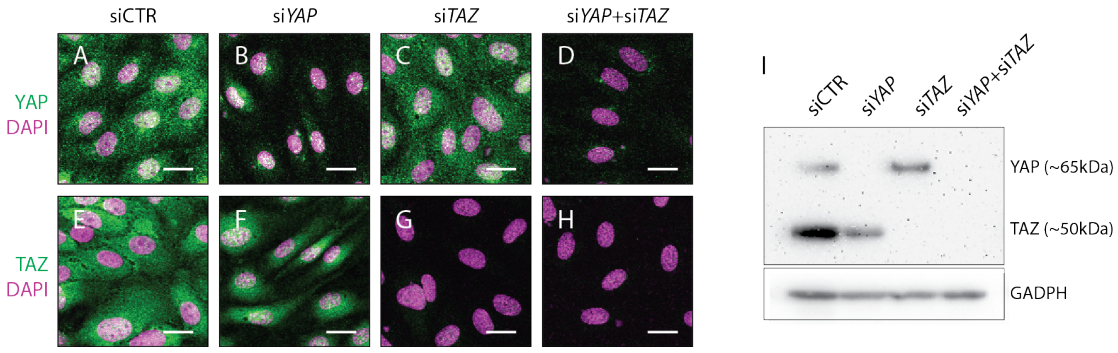

Figure 4.4. Efficient loss of YAP and TAZ protein after gene knockdown by siRNA

HUVECs treated with non-targeting siRNA (siCTR) or siRNA targeting YAP, TAZ and YAP +TAZ for 24h.

A-H, Immunofluorescence staining for YAP (green, A-D) or TAZ (green, E-H) and labelling of nuclei with DAPI (magenta) 72h after siRNA transfection. Scale bar: 10µm.

I, Western blot for YAP/TAZ and GAPDH 72h after siRNA transfection

The first stimuli I evaluated was VEGF, a critical endothelial mitogen (Hoeben et al., 2004). To understand if YAP and/or TAZ responded to VEGF with increasing proliferation, I treated confluent monolayers of HUVECs knocked down for YAP and/or TAZ with increasing dosages of VEGF and evaluated the cell cycle using flow cytometry. By plotting the fold change in % of S phase cells after VEGF stimulation, I could observe that the knockdown of YAP, TAZ and YAP/TAZ together did not abrogate the increase in proliferation with VEGF (**Figure 4.5 A**). Moreover, treating cells with VEGF did not lead to a shift in the intracellular location of YAP and TAZ,

suggesting that VEGF is not upstream of YAP and TAZ (**Figure 4.5 B-K**). These results show that YAP and TAZ are not required for VEGF induced proliferation.

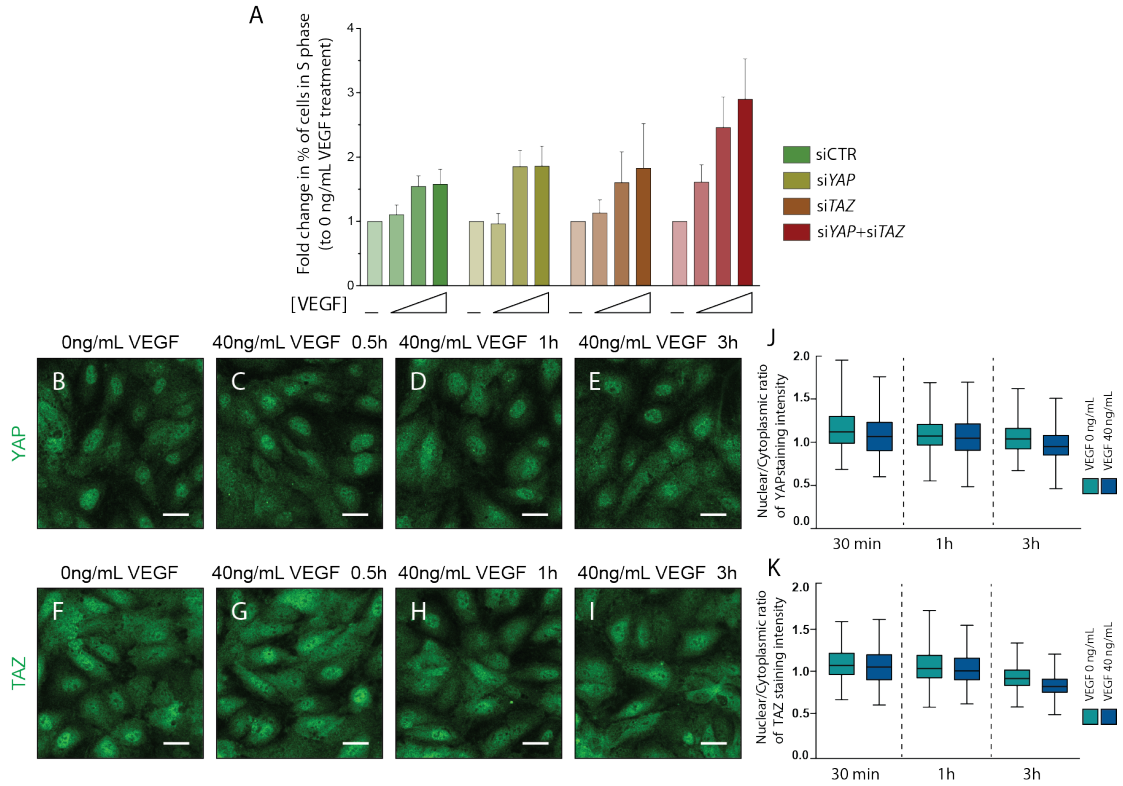

Figure 4.5. YAP and TAZ are not required for VEGF induced proliferation

A, Endothelial proliferation with increasing concentrations of VEGF treatment in YAP, TAZ and YAP/TAZ knockdown cells and control. HUVECs were treated with 0, 40, 200 or 1000 ng/mL VEGF for 24h and the percentage of cells in S phase was determined by flow cytometry. Graph shows the mean +/- SD of the fold change in percentage of S phase positive cells relative to 0 ng/mL of VEGF treatment. n= 3 independent experiments; > 50.000 cells analysed per experiment per condition.

B-I, Confluent HUVECs were treated with 40ng/mL of VEGF for 30 min (C,G), 1h (D,H) and 3h (E,I) or with no VEGF (B,F) and stained for YAP (B-E) or TAZ (F-I) and DAPI (not shown).Scale bar: 25µm.

J, K, Quantification of nuclear to cytoplasmic ratio of YAP (J) or TAZ (K) with VEGF treatment of one representative experiment. Nuclear/cytoplasmic ratio > 1, YAP/TAZ nuclear; nuclear/cytoplasmic ratio < 1, YAP/TAZ cytoplasmic. At least 200 cells quantified per condition per experiment. n= 2 independent experiments.

I then asked whether YAP and TAZ mediated endothelial proliferation in response to mechanical stretch. To do so, I subjected HUVECs to cycles of mechanical stretch for 24hrs and compared their proliferative response to cells that were not stretched, in control conditions and upon YAP, TAZ and YAP/TAZ knockdown (**Figure 4.6**). Proliferation was after assessed by EdU incorporation. Upon stretch, control cells showed a 5-fold average increase in proliferation (5+/-

2.6%), and this effect was reduced upon knockdown of VE-Cadherin, confirming previous observations (Liu et al., 2007). The knockdown of YAP, but not of TAZ, led to a significant decrease in stretch-induced proliferation (2+/-0.6%, *p*=0.0351). The knockdown of YAP/TAZ showed a tendency to decreased proliferation in response to stretch but did not reach statistical significance. Thus YAP is required for EC proliferation in response to mechanical stimulation at cell-cell junctions.

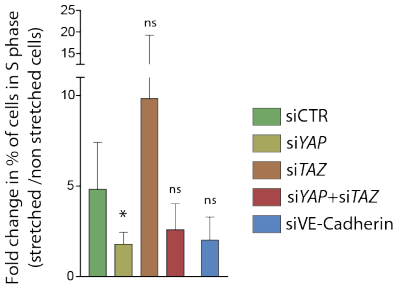

Figure 4.6. YAP is required for stretch induced proliferation

Quantification of endothelial proliferation after stretch in in YAP, TAZ, YAP/TAZ and VE-Cadherin knockdown cells and control. HUVECs were subjected to cyclic stretch for 24h and percentage of cells in S phase was determined by EdU pulsing and immunofluorescence staining. Graph shows the mean +/- SD of the fold change in percentage of S phase positive cells of stretched to non stretched cells for each knockdown condition. n= 5 independent experiments, > 100 cells counted per experiment per condition. *p* values were calculated using unpaired t-test. *, $p<0.05$.

2. YAP and TAZ promote individual endothelial cell migration

2.1. YAP/TAZ promote directional cell migration

The analysis of *Yap/Taz* iEC-KO retinas suggested that a migration defect could be at play. Specifically, sprouting ECs lacking YAP/TAZ have less elongated nuclei and form a blunted sprouting front with fewer protrusions. Moreover, clumped nuclei in sprouts also suggest deficient migration and distribution of cells in space.

To evaluate if YAP and TAZ regulate EC migration, I performed wound assays using HUVECs knocked down for YAP and/or TAZ (**Figure 4.7 A-I**). There, confluent ECs are induced to migrate towards a newly formed cell free “wound”. In control cells, the 500µm wound was always completely closed after 16hrs (**Figure 4.7 A, B, I**). At the same time point, less than 50% of the wound area was closed after knockdown of YAP (47+/- 16% wound closure, $p<0.0001$) (**Figure 4.7 C, D, I**).

The knockdown of TAZ (**Figure 4.7 E, F, I**) and YAP/TAZ combined (**Figure 4.7 G, H, I**) has a stronger impact on cell migration, with less then 20% of the wound being closed at 16hrs (17+/-24% for si*Taz*, $p<0.0001$ and 18+/- 15% for si*Yap*+si*Taz,* $p<0.0001$).

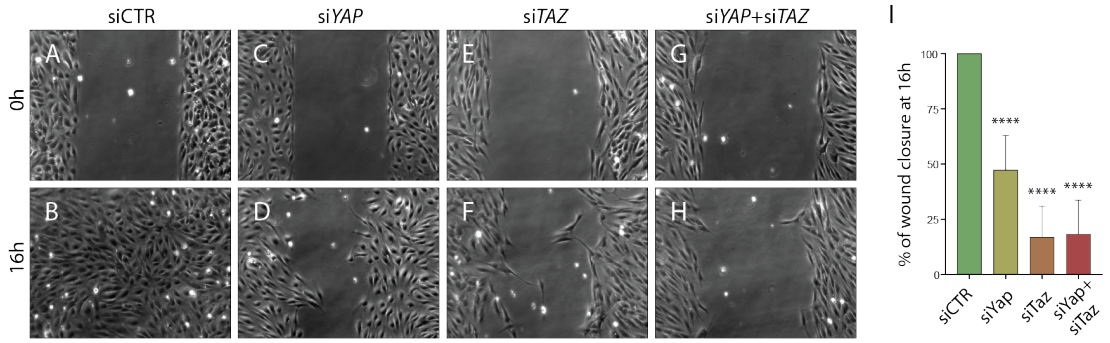

Figure 4.7. YAP/TAZ promote cell migration

A-H, Phase contrast images of YAP (C, D), TAZ (E, F) and YAP/TAZ (G, H) knockdown HUVECs and control cells (A, B) immediately after removing barrier to create a cell free space (A, C, E, G) and 16 hrs later (B, D, F, H). **I**, Wound closure at 16 hrs. Data are mean +/- SD of 3 independent experiments (8-9 biological replicates). *p* values were calculated using unpaired *t*-test between knocked down cells for YAP, TAZ or YAP/TAZ and control. ****, $p<0.0001$.

2.2. YAP/TAZ decrease cell-cell coupling with neighbouring cells, favouring positional rearrangements

While doing these experiments, I observed that at the same time as control cells displayed the classic cobblestone appearance of HUVECs, cells knocked down for YAP and TAZ combined arranged in the monolayer into swirls (**Figure 4.8 A, B**). Looking into the literature, I found recent data illustrating that collectively migrating ECs *in vitro* move in streams and swirls, displaying straight junctions along the lateral boundaries and fingers along the front and rear (Hayer et al., 2016). This suggested that the organisation of cells in the monolayer could be used as a readout for collective cell migration, in opposition to the wound assay that informed on directional cell migration. To analyse this effect I collaborated with Dr. Silvanus Alt who developed a measure of monolayer coordination based on the alignment of cells with their neighbours. As a proxy for the orientation of each cell we used the longest axis of the nucleus obtained from a DAPI staining (**Figure 4.8 C, D, C', D'**). A score of 1 would signify parallel alignment between all cells, and a score of 0 random alignment of the population (**Figure 4.8 E**). Control cells displayed higher than random

alignment with their closest neighbours, but were arranged at random when distant by more than 300µm (**Figure 4.8 F**). While the knockdown of YAP did not affect the alignment score of cells, the knockdown of TAZ led to increased alignment. The combined knockdown of YAP/TAZ led to an even higher degree of coordination, with higher alignment scores across all distances between cells. These results suggest that YAP/TAZ promote the ability of cells to distribute individually within monolayers. Although YAP showed no difference in the alignment score of cells, this approach cannot exclude that also YAP knockdown cells show a defect in rearranging positions with the neighbours. A more conclusive experiment would be to perform time-lapse imaging of live HUVECs and analysing their positions in the monolayer over time.

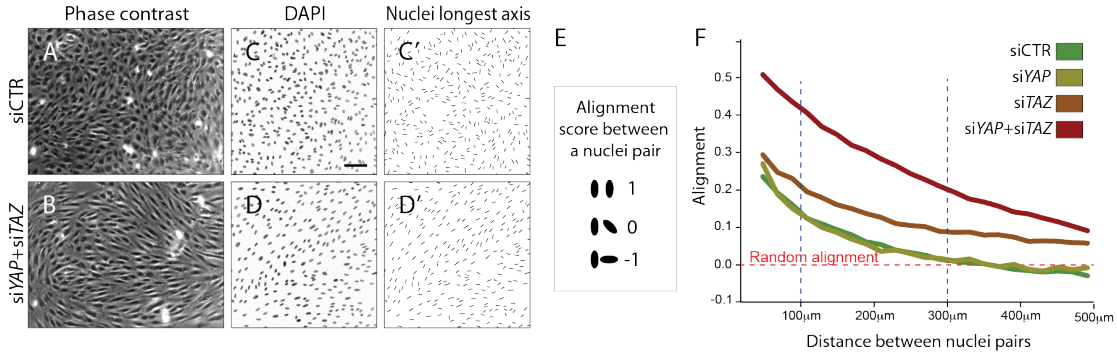

Figure 4.8. YAP/TAZ favour positional rearrangements

A, B, Phase contrast images of YAP/TAZ knockdown monolayer of HUVECs (B) and control cells (A).

C, D, Fluorescence labelling of nuclei with DAPI of YAP/TAZ knockdown monolayer of HUVECs (D) and control (C). C', D', Longest axis of nuclei in C,D. Scale bar: 100mm.

E, Alignment score between nuclei pairs used for quantification of cell coordination in F. Angles made by the nuclei longest axis of a pair of nuclei were calculated; angles of 0, 45 and 90 degrees scored 1,0 and -1 in alignment. **F**, Coordination plot of monolayers of HUVECs knocked down for YAP, TAZ, YAP and TAZ and control. Graph shows mean alignment score of all pairs of cells in the monolayer plotted against distance between them. Randomly aligned cells score 0 in mean alignment. n= 3 independent experiments, >10.000 pairs of nuclei analysed per knockdown condition per experiment.

Together, these experiments suggest that YAP/TAZ are essential for ECs to migrate in an individual way. *In vivo*, this could relate to how ECs migrate in sprouts – in the direction of the hypoxic tissue, instructed by growth factors, at the same time as shuffling positions with neighbouring ECs.

3. YAP and TAZ regulate endothelial adherens junctions

3.1. YAP/TAZ decrease endothelial permeability

As shown before, the endothelial deletion of YAP and TAZ leads in the developing vasculature to a loss of vascular integrity in the sprouting front, with large haemorrhages. The maintenance of vascular integrity highly depends on the status of junctions between ECs (Dejana et al., 2008). However, it can also be affected by reasons external to ECs, as for example deficient mural cell coverage (Armulik et al., 2010, Hellstrom et al., 2001). Although my results did not show deficient mural cell coverage in *YapTaz* iEC-KO vessels, they did show that the pericytes in *YapTaz* iEC-KO sprouting vessels abnormally express αSMA. Therefore, to directly test whether YAP and TAZ regulate endothelial permeability, I plated confluent YAP and/or TAZ knockdown cells on a semi-permeable membrane and evaluated the monolayers' permeability to 250kDa dextran molecules. By doing so, I found that only the combined knockdown of YAP/TAZ led to a significant increase in permeability in comparison to the control situation (**Figure 4.9**). These results show that YAP/TAZ are required for the barrier function of the endothelium and can compensate for each other in this particular role.

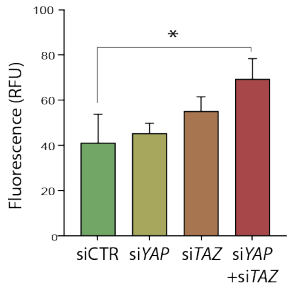

Figure 4.9. YAP/TAZ decrease endothelial permeability

Permeability of YAP, TAZ and YAP/TAZ knockdown monolayers of HUVECs to 250kDa fluorescent dextran molecules. Data are mean ± SD of 3 independent experiments. *p* values were calculated using unpaired *t*-test between knocked down cells for YAP, TAZ and YAP/TAZ and control. *, $p<0.05$.

3.2. YAP and TAZ promote the formation of junction associated intermediate lamellipodia

Several of the results shown so far suggest that YAP/TAZ regulate junctional remodelling. *Yap/Taz* iEC-KO retinas display increased unicellular vessel tubes, signifying loss of cellular rearrangements, which previous studies have shown to rely on remodelling of adherens junctions (Sauteur et al., 2014). Moreover, *Yap/Taz* iEC-KO retinas display vessel crosses at the sprouting front, suggestive of failed anastomosis, that can also be caused by junctional remodelling defects (Lenard et al., 2013). Furthermore, the loss of endothelial YAP/TAZ leads to vessel bleedings *in vivo* and increased monolayer permeability *in vitro*, a hallmark of junctional dysfunction. Finally, YAP/TAZ promote cell migration, which is deeply linked to junctional remodelling. For all these reasons, I decided to investigate if YAP and TAZ regulate adherens junctions.

To do so, I performed immunostainings for VE-Cadherin, the main component of endothelial adherens junctions, in YAP, TAZ and YAP/TAZ knockdown HUVECs. This approach revealed altered junctional morphologies in cells deficient for YAP and TAZ in comparison to control cells (**Figure 4.10 A-D**). Importantly, the morphology of adherens junctions has previously been correlated with its function. Although the earliest observations were performed *in vitro* and correlated the morphology of junctions only with permeability, later studies found similar morphologies *in vivo* and other readouts were investigated as well. In the mouse retina, straight (or linear) junctions were associated with high Notch activity and stalk cell behaviour, while VE-Cadherin fingers (or serrated junctions) were more often found in tip cells or actively rearranging cells (Bentley et al., 2014). *In vitro*, activation of EC monolayers with pro-angiogenic molecules such as VEGF increases both the appearance of fingers and the permeability between cells. For this reason, straight junctions have been associated with a quiescent endothelium, while serrated junctions bearing VE-Cadherin fingers have been associated with an activated, angiogenic endothelium, characterised by both increased migratory activity and permeability. Interestingly, VE-Cadherin fingers were also shown to steer migrating ECs and couple leader and follower cells in cell culture (Hayer et al., 2016). More recently, a newly described junction type named junction associated intermediate lamellipodia (JAIL) (Abu Taha et al., 2014), that morphologically appears as reticular and broad shaped, has been observed in the sprouting vessels of the mouse retina (Cao et al., 2017). In culture, JAILs have been linked to increased migration (Cao et al., 2017) and decreased permeability of ECs (Breslin et al., 2015).

In order to describe the immunofluorescence data in the most unbiased way possible, I defined five junctional categories that included all the morphologies I

found: straight junctions, thick junctions, thick to reticular junctions, reticular junctions and fingers (**Figure 4.10 E**). Live imaging analysis of VE-Cadherin-GFP transduced HUVECs confirmed that reticular junctions correspond to junction associated intermediate lamellipodia (JAIL), and showed that thick to reticular junctions correspond to small JAIL (**Supplementary video 4.1**). Additionally, the observation of live junctions also revealed that junction morphologies are very dynamic and the categorical junction types change between one another with time. In my static data, while control cells presented mostly reticular junctions (**Figure 4.10 A, F**), the knockdown of YAP and TAZ led respectively to an increase in straight junctions and fingers (**Figure 4.10 B, C, F**). The combined knockdown of YAP/TAZ led to an increase in both straight junctions and fingers and to a loss of reticular junctions (**Figure 4.10 D, F**). Moreover, the knockdown of YAP/TAZ led to junctional breaks in the monolayer, as seen by the presence of gaps in VE-Cadherin stainings (**Figure 4.10 D**, **red arrowheads**). Together, these observations demonstrate that YAP and TAZ together are required for the formation of JAIL and reduce the formation of straight junctions and fingers.

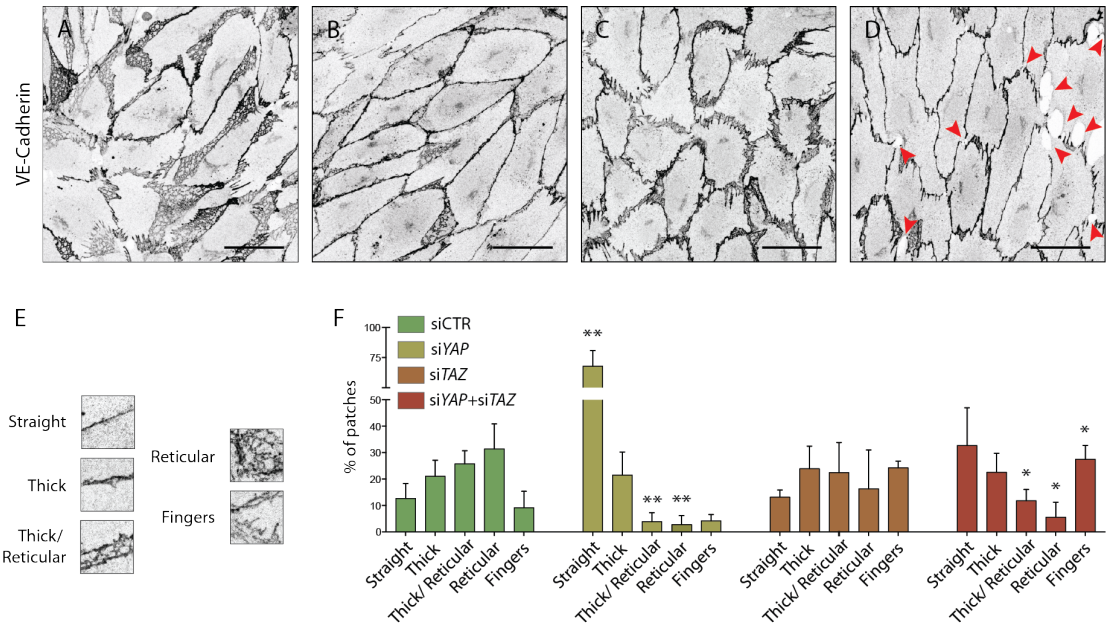

Figure 4.10. YAP/TAZ promote the formation of junction associated intermediate lamellipodia

A-D, HUVECs knocked down for YAP (C), TAZ (D) and YAP/TAZ (E) and control cells (B) stained for VE-Cadherin. Red arrowheads, discontinuous VE-Cadherin. Scale bar: 50µm.

E, Representative patches used for manual morphological classification of adherens junctions in 5 categories: straight junctions, thick junctions, thick to reticular junctions, reticular junctions and fingers.

F, Morphological classification of VE-Cadherin labelled cell junctions in HUVECs knocked down for YAP, TAZ and YAP/TAZ. Data are mean percentage ± SD of 3 independent experiments (2 for siTAZ). n> 140 patches of VE-Cadherin stained HUVECs per knockdown condition per experiment. *p* values were calculated using unpaired *t*-test between knocked down cells for YAP, TAZ and YAP/TAZ and control. *, $p<0.05$; **, $p<0.01$.

3.3. YAP and TAZ increase the turnover of endothelial adherens junctions

Sprouting ECs are extremely dynamic. They migrate, undergo cell shape changes and swap positions with neighboring cells. All these rearrangements require cell-cell junctions that allow endothelial movement but at the same time ensure the maintenance of vessel integrity, which depends on the constant assembling and disassembling of molecular bonds. To understand if YAP and TAZ regulate the turnover of cell junctions, I performed pulse chase immunofluorescence experiments (**Figure 4.11 A, B**). Briefly, I pulse-labeled VE-Cadherin molecules at the cell junctions of live cells using an antibody directly coupled to a fluorescent dye for 30 minutes (Dorland et al., 2016). Subsequently I washed out the antibody and cultured the cells for two more hours in normal conditions, allowing for the relocation of the pulsed antibody with the normal recycling of VE-Cadherin. At the end of this period I fixed the cells and stained for surface VE-Cadherin using a second fluorescent label. Comparing the two sequential VE-Cadherin labels allowed me to distinguish junctions with high, intermediate and low turnover rates (**Figure 4.11 C**). In control cells, 44% of patches were of high turnover junctions, 24% of intermediate turnover junctions and 32% of low turnover junctions (**Figure 4.11 D**). The knockdown of YAP/TAZ significantly decreased the percentage of high turnover junctions to 14% ($p=0.0387$) and increased the percentage of low turnover junctions to 58%. Interestingly, when coupling this analysis with the categorization of junction morphologies, I uncovered a correlation between the morphology of junctions and VE-Cadherin turnover rates (**Figure 4.11 E,** see pattern for siCTR). My results show that straight junctions and fingers are the junctions with lowest turnover, while reticular junctions (corresponding to JAIL) show the highest turnover. This was not surprising considering that JAIL are very dynamic junctions associated with lamellipodia activity. To understand if the different VE-Cadherin turnover observed after knockdown of YAP/TAZ was caused by a shift in morphology, I compared the turnover of VE-Cadherin within the same morphological categories (**Figure 4.11 E**).

Knockdown of YAP/TAZ decreased the percentage of high turnover junctions within all morphological categories, confirming a specific defect in VE-Cadherin turnover.

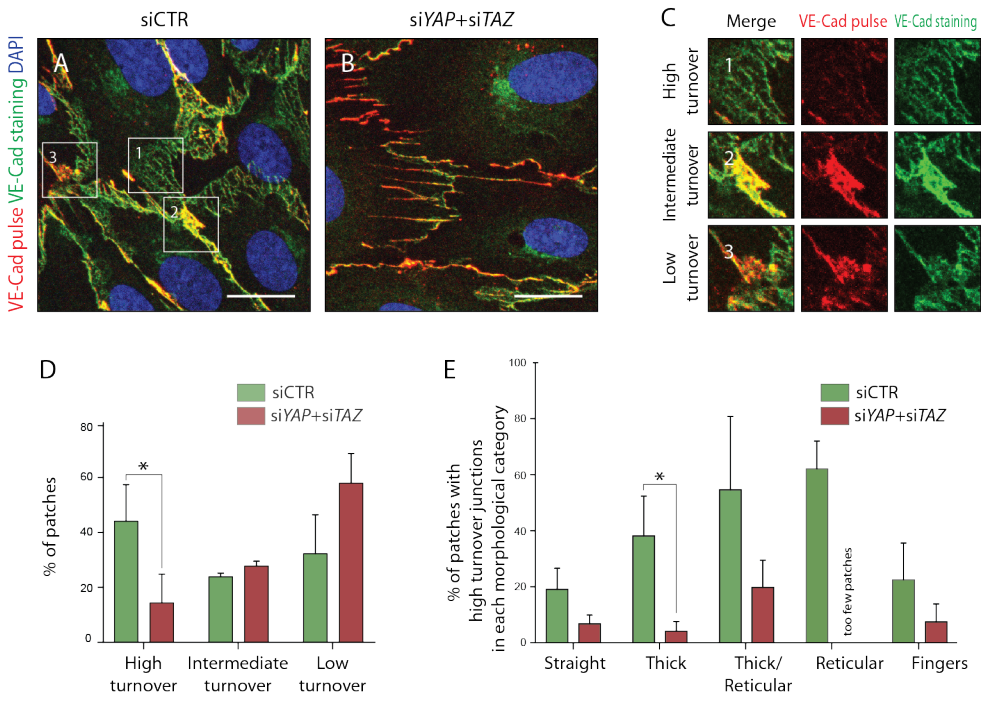

Figure 4.11. YAP/TAZ increase the turnover of adherens junctions

A, B, HUVECs knocked down for YAP/TAZ (B) and control (A) triple labelled with DAPI (blue), pulsed VE-Cadherin 55-7HI (red, VE-Cadherin pulse), and surface VE-Cadherin (green, VE-Cadherin staining). VE-Cadherin 55-7HI pulse was done for 30 minutes and cells were fixed 2 hours after end of pulse. Scale bar: 20µm. **C**, Representative patches used for manual classification of junctions into high, intermediate and low turnover. **D**, Junctional turnover in YAP/TAZ knockdown HUVECs and control cells. **E**, Percentage of high turnover junctions in each morphological category in YAP/TAZ knockdown cells and control. **D, E**, Data are mean ± SD of 3 independent experiments. n> 70 patches per knockdown condition per experiment. Fewer then 5 patches were reticular in YAP/TAZ knockdown, not allowing for reliable assessment of percentages between high, intermediate and low turnover. *p* values were calculated using unpaired t-test. *, $p<0.05$.

3.4. YAP/TAZ decrease the immobile fraction of VE-Cadherin at the cell junction

To validate these results and further investigate how YAP/TAZ affect the turnover of VE-cadherin, I used an approach similar to fluorescence recovery after photobleaching (FRAP), a well-established and quantitative method of measuring movement of molecules within the cell. In endothelial monolayers where cells are very dynamic, FRAP suffers from uncertainty caused by the movement of junctions. To overcome this limitation I used VE-Cadherin tagged with the photoconvertible molecule mEos, which allowed me to quantify the loss of fluorescence after

conversion of a subset of molecules, while monitoring the location of the junctions with the unconverted molecules (fluorescence loss after photoconversion, or FLAP). Because of the differences in turnover between junction morphologies uncovered before, only straight junctions were analysed in this experiment. Using this method, I observed an increase in the immobile fraction of VE-Cadherin at the junctions after YAP/TAZ knockdown (**Figure 4.12 A**), while no difference was seen for the half-time of fluorescence loss of the mobile fraction (**Figure 4.12 B**).

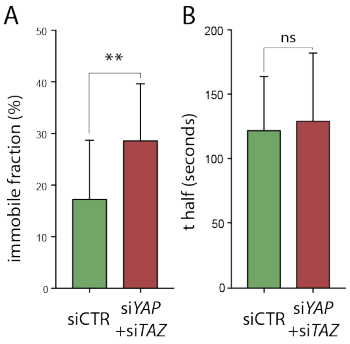

Figure 4.12. YAP/TAZ decrease the immobile fraction of VE-Cadherin at adherens junctions

A, B, Fluorescence loss after photoconversion of VE-Cadherin mEos in straight junctions of YAP/TAZ knockdown HUVECs and control HUVECs. A, VE-Cadherin mEos immobile fraction. B, VE-Cadherin mEos half-life of fluorescence loss. Data are mean ± SD of 3 independent experiments. n= 15 control cells and 16 cells YAP/TAZ knockdown cells. *p* values were calculated using unpaired *t*-test between knocked down cells for YAP/TAZ and control. ns, p>0.05; **, *p*<0.01.

Together, these results show that YAP/TAZ increase the turnover of adherens junctions by increasing the pool of mobile VE-Cadherin.

3.5. YAP/TAZ regulate the actin cytoskeleton

To investigate if YAP and TAZ regulate the actin cytoskeleton I performed immunofluorescence staining for filamentous actin (F-actin) in YAP/TAZ deficient HUVECs and control cells. While control cells present junctional actin, stress fibers and branched actin (**Figure 4.13 A, A'**), YAP/TAZ deficient cells (**Figure 4.13 B, B'**) mostly display F-actin in stress fibers, low junctional actin and no branched actin networks. This result correlates with the junctional morphologies observed before, as fingers associate with stress fibers (Abu Taha and Schnittler, 2014), while JAILs associate with branched actin (Abu Taha et al., 2014). Interestingly, the VE-Cadherin

pulse labeling experiments showed that the junction morphologies with less turnover, straight junctions and fingers, were the ones associated with bundled actin filaments, while the morphologies with higher turnover, reticular junctions, associated with branched actin networks, raising the questions as to whether f-actin association impacts the turnover of adherens junctions.

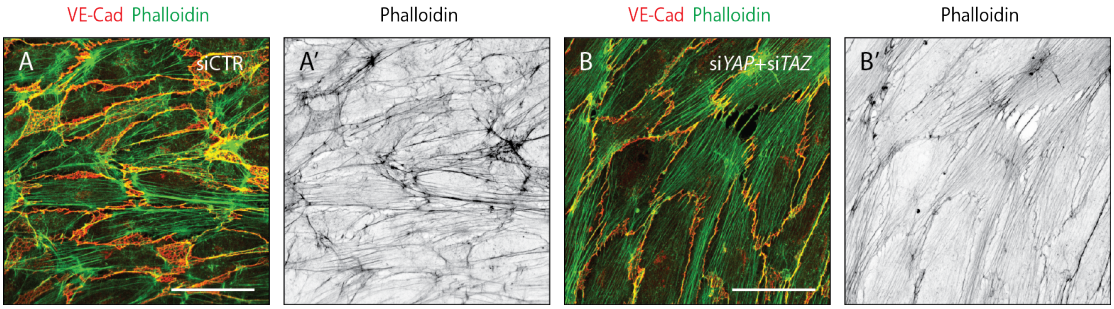

Figure 4.13. YAP/TAZ regulate the actin cytoskeleton in endothelial cells

A, B, HUVECs knocked down for YAP/TAZ (B) and control (A) double stained for VE-Cadherin (red) and f-actin (green, phalloidin). A', B', f-actin (black, phalloidin). Scale bar: 50μm.

4. Summary and conclusions

In this chapter I have shown that YAP/TAZ regulate endothelial cell numbers by promoting endothelial proliferation in response to mechanical stretch, a response depend on YAP but not on TAZ. Moreover, YAP/TAZ promote endothelial cell migration and decrease endothelial permeability. At the cell junctions, YAP/TAZ favour the presence of junction associated intermediate lamellipodia, which are the junction type showing highest turnover.

Chapter 5: Recovery of JAIL formation through BMP signalling rescue improves the migratory and permeability defects caused by YAP and TAZ deficiency

1. Introduction

In the previous chapter I presented my findings on cellular and molecular defects caused by the loss of YAP/TAZ in ECs. In this chapter I will describe how some of these defects can be attributed to abnormal BMP signalling.

2. YAP and TAZ repress BMP signalling in sprouting endothelial cells

2.1. YAP and TAZ repress BMP signalling in HUVECs

In order to investigate possible signalling pathways downstream of endothelial YAP/TAZ I used *in vitro* luciferase assays. In an attempt to mimic the different activation status of YAP/TAZ in the vasculature (more nuclear at the sprouting front and more cytoplasmic in the remaining plexus), I assayed cells in different confluency conditions. *In vitro*, ECs display more often nuclear YAP/TAZ when sparse than when confluent (**Figure 5.1** shows an example for TAZ; similar regulation is present also for YAP).

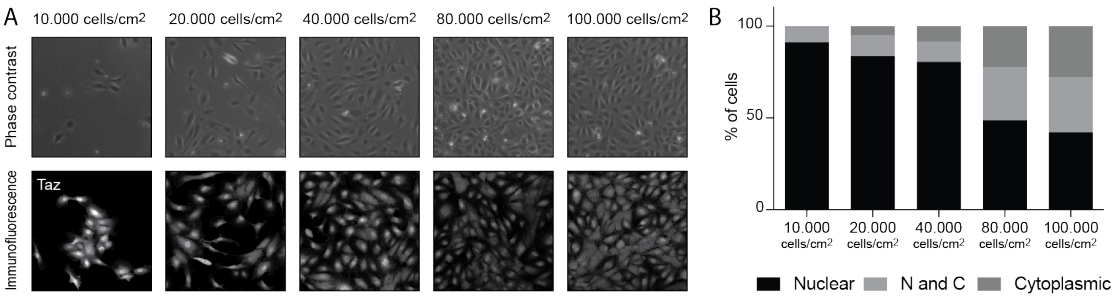

Figure 5.1. Sparse cells have increased nuclear TAZ

A, HUVECs plated at increasing cell densities were on the following day imaged by phase contrast, and fixed and stained for TAZ protein (white) by immunofluorescence and DAPI labelling (not shown). **B,** Quantification of subcellular location of TAZ protein in HUVECs seeded at increasing cell densities. Nuclear, intensity in nucleus/ intensity in cytoplasm >1.2; N and C, intensity in nucleus/

intensity in cytoplasm 0.8-1.2; Cytoplasmic, intensity in nucleus/ intensity in cytoplasm <0.8. Results are from one representative experiment.

Because of toxicity, it was not possible to achieve a fully confluent monolayer after double transfection with siRNAs and luciferase reporters; nonetheless, this approach was sensitive enough to pick up differences in signalling between sparse and subconfluent cells. The co-transfection of cells with siRNAs targeting YAP, TAZ or YAP/TAZ together with the TEAD luciferase reporter confirmed the applicability of this approach, showing a decrease in TEAD reporter activity in YAP, TAZ and YAP/TAZ knockdown HUVECs both in sparse and in subconfluent culture conditions (**Figure 5.2 A, B**). Canonical Wnt signalling, which promotes endothelial cell proliferation (Masckauchan et al., 2005) and vessel development (Phng et al., 2009), is not regulated by YAP/TAZ in HUVECs (**Figure 5.2 C, D**). Notch signalling on the other hand, which regulates tip-stalk cell specification and sprouting (Kofler et al., 2011), is affected by the loss of YAP/TAZ, and curiously in opposite ways in sparse and subconfluent cells. While in sparse cells the knockdown of YAP/TAZ causes a ~ 6 fold increase in RBP-J reporter activity (**Figure 5.2 E**), in subconfluent cells it leads to a ~3 fold decrease in RBP-J reporter activity (**Figure 5.2 F**). Finally, BMP signalling, another key pathway regulating sprouting angiogenesis (Dyer et al., 2014, Garcia de Vinuesa et al., 2016), was investigated using a BRE reporter. In sparse cells, the knockdown of YAP, TAZ and YAP/TAZ leads respectively to a ~6, ~10 and ~50 fold increase in BRE reporter activity (**Figure 5.2 G**). In subconfluent cells the same direction of effect is seen, but approximately 5 times weaker than in sparse cells (~1.3, ~3 and ~9 fold increase in BRE reporter activity in YAP, TAZ and YAP/TAZ knockdown cells respectively) (**Figure 5.2 H**).

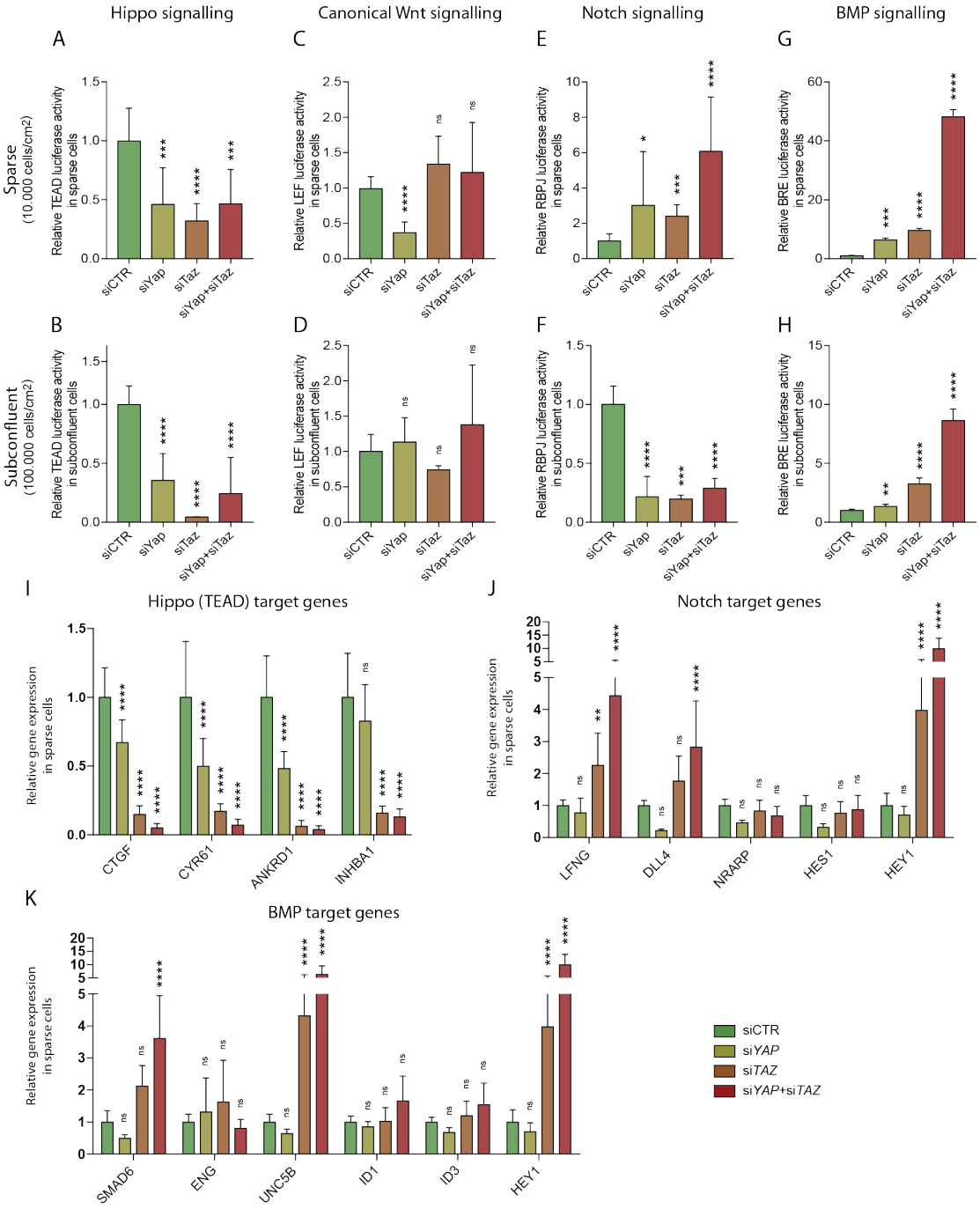

Figure 5.2. Endothelial YAP and TAZ repress BMP signalling in HUVECs

A-H, Luciferase reporter assays in YAP, TAZ and YAP/TAZ knockdown HUVECs and controls. Assays were performed using Hippo (A, B), Wnt (C, D), Notch (E, F) and BMP (G, H) reporters both in sparse (A, C, E, G) and subconfluent (B, D, F, H) culture conditions. Data are mean +/- SD. *p* values were calculated using unpaired t-test. n≥ 6 experiments for Hippo reporter, ≥ 3 experiments for Wnt reporter (except for siTAZ, were n=2), ≥ 3 experiments for Notch reporter, 3 experiments for BMP reporter. *, $p<0.05$; **, $p<0.01$; ***, $p<0.001$; ****, $p<0.0001$.

I-K, Reverse transcriptase quantitative PCR in YAP, TAZ and YAP/TAZ knockdown HUVECs and control HUVECs for TEAD (I), Notch (J) and BMP (K) target genes. Results are relative to siCTR. RT-PCR normalisation was performed with HPRT expression. Data are mean +/- SD of 3 independent

experiments. *p* values were calculated using unpaired *t*-test. ns, non significant, $p>0.05$; *, $p<0.05$; **, $p<0.01$; ***, $p<0.001$; ****, $p<0.0001$.

The results with the BRE reporter were confirmed by RT-qPCR in sparse YAP/TAZ knockdown cells. As expected, YAP/TAZ knockdown cells show decreased expression of the TEAD target genes *CTGF*, *CYR61* and *ANKRD1* and *INHBA1* (**Figure 5.2 I**). As for Notch target genes, YAP/TAZ knockdown cells express more *LFNG*, *DLL4* and *HEY1*; the expression of *NRARP* and *HES1* is not changed (**Figure 5.2 J**). Finally, YAP/TAZ knockdown cells express more of the BMP target genes *SMAD6 and UNC5B,* but not *ID1* or *ID3* (**Figure 5.2 K**). Importantly, significant crosstalk between Notch and BMP signalling exists in the vasculature (Beets et al., 2013). Specifically, the transcription of *HEY1* can also be induced by BMPs independently of Notch in ECs (Woltje et al., 2015), thus it is also here shown as a BMP target gene.

2.2. YAP and TAZ repress BMP signalling in the sprouting front of the mouse retina

To understand if similar regulation was present *in vivo* I performed immunofluorescence stainings in *Yap/Taz* iEC-KO retinas. I evaluated Wnt signalling by staining for the Wnt/b-catenin nuclear effector LEF-1 (**Figure 5.3 A, B**). In both control and *Yap/Taz* iEC-KO retinas, LEF-1 signal is lowest at tip cells and in arteries, and highest in the remaining ECs. I found no difference between LEF-1 signal intensity or location between control and *Yap/Taz* iEC-KO retinas, in line with the previous luciferase results. Evaluation of Notch signalling by immunofluorescence is hindered by the absence of a working NICD antibody, which would be the best readout for Notch activity. As DLL4 was upregulated in the qRT-PCR analysis in YAP/TAZ knockdown HUVECs, I used this protein as the readout to assess Notch signalling *in vivo* (**Figure 5.3 C, D**). In the vasculature of the developing retina, DLL4 typically labels tip cells and arteries, and is absent from veins. A similar pattern of staining is present in *Yap/Taz* iEC-KO retinas, however the drop in intensity in DLL4 signal from tip to stalk cells is not as sharp as in control retinas, with a broader DLL4 signal area. Finally, I stained retinas for the BMP nuclear effector pSMAD1/5/8 (**Figure 5.3 E, F**). In control retinas, very little pSMAD1/5/8 signal is seen throughout the entire vasculature. In contrast, *Yap/Taz* iEC-KO retinas show increased pSMAD1/5/8 signal especially at the sprouting front.

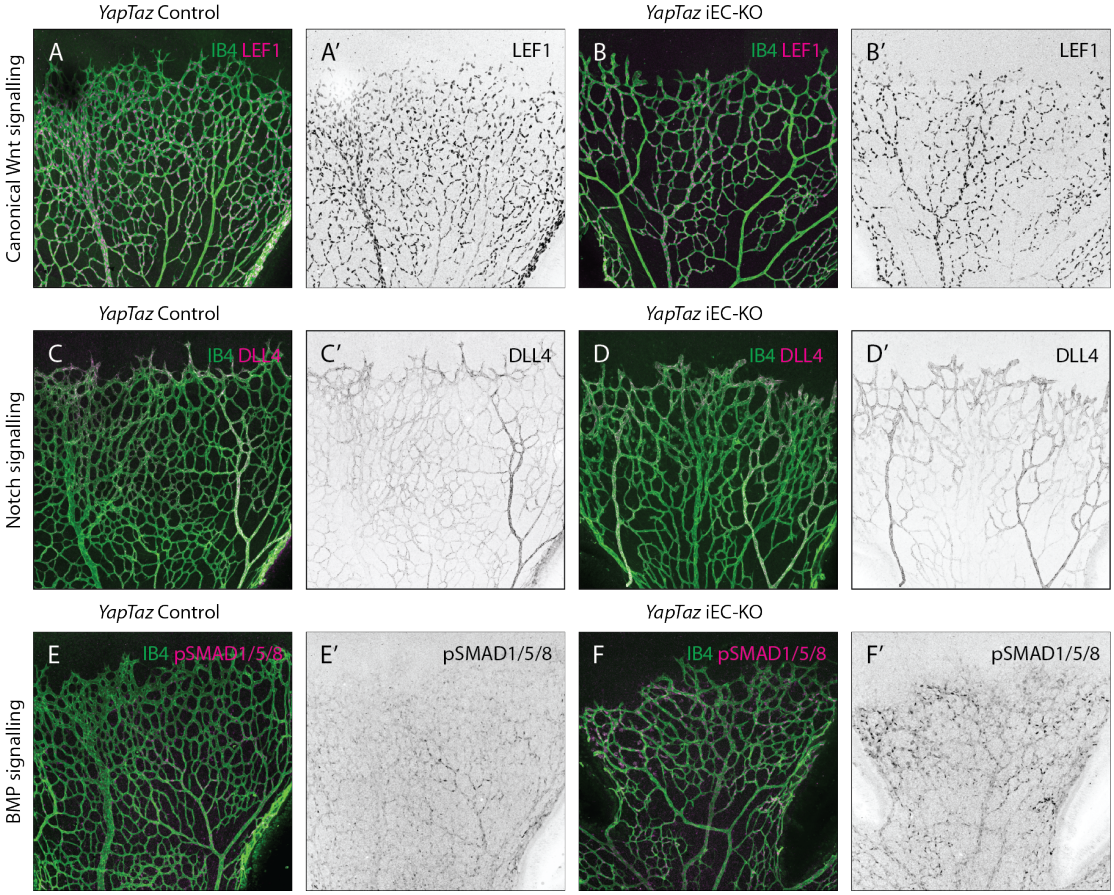

Figure 5.3. pSMAD 1/5/8 is increased in YAP/TAZ iEC-KO retinas

A-F, Retinas from P6 *YapTaz* iEC-KO (B,D,F) and respective control pups (A,C,E) were stained with Isolectin B4 (A-F, IB4) and with LEF1 (A,B magenta, A', B' grey), DLL4 (C,D magenta, C', D' grey) or pSMAD1/5/8 (E,F magenta, E', F' grey). Scale bar: 200µm.

To confirm that this increase was endothelial I co-stained retinas for pSMAD1/5/8 together with the endothelial nuclear marker ERG and imaged retinas at higher resolution (**Figure 5.4 A, B**). Both in control and in *Yap/Taz* iEC-KO retinas pSMAD1/5/8 positive nuclei are found adjacent to the vasculature in ERG negative, non-ECs (**Figure 5.4 A1, B1, yellow arrowheads**). At the sprouting front of control retinas, 5 +/- 2.5% of ECs are positive for pSMAD1/5/8 (**Figure 5.4 A2, C**). In contrast, in *Yap/Taz* iEC-KO retinas 52+/-0.6%, of ECs are positive for pSMAD1/5/8 (**Figure 5.4 B2, C**). Moreover, this effect is likely underestimated by the binary quantification that I performed, as the intensity of pSMAD1/5/8 in the nuclei of *Yap/Taz* iEC-KO ECs is also much higher than in control ECs. Together, the *in vitro* and *in vivo* results here presented clearly show that YAP/TAZ strongly repress BMP signalling in ECs at the sprouting front.

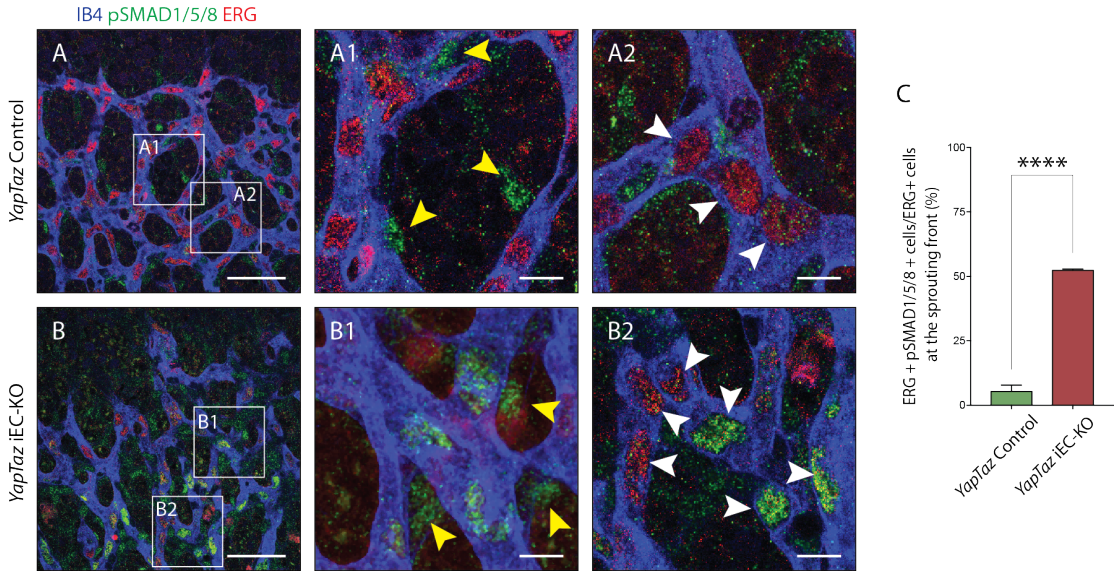

Figure 5.4. YAP/TAZ repress BMP signalling in sprouting endothelial cells

A, B, P6 retinal vessels labelled with IB4 (blue) and stained for ERG (red, marking endothelial nuclei) and pSMAD1/5/8 (green) in *YapTaz* iEC-KO (B) and littermate control mice (A). Images correspond to single confocal planes. A1, A2, B1, B2, magnification of boxed areas in A and B. Yellow arrowheads, perivascular cells. White arrowheads, endothelial nuclei. Scale bar: A, B 50μm, A1, A2, B1, B2, 10μm.

C, Percentage of ECs positive for pSMAD1/5/8 at the sprouting front of the P6 retina in *YapTaz* iEC-KO and littermate control mice (n=3 pups per condition). Data are mean ± SD. *p* values were calculated using unpaired *t*-test. ****, $p<0.0001$.

BMPs (bone morphogenetic proteins) were first identified in the 1960s as inducers of ectopic bone formation, when demineralised bone matrix implanted in rabbit muscle gave rise to bone (Urist, 1965). Their recognised spectrum of action has since expanded, and nowadays BMPs are known to exert fundamental roles during the embryonic developmental of many organs and maintenance of homeostasis in the adult, so much so that some authors suggested their renaming as body morphogenetic proteins (Wagner et al., 2010).

BMPs, or BMP ligands, are secreted proteins that belong to the TGFβ superfamily. Based both on their amino acid and nucleotide similarities and on affinities for different receptors they can be categorised into four subgroups: BMP 2/4 subgroup, the BMP 5/6/7/8 subgroup, the BMP 9/10 subgroup and the BMP 12,13,14 (or growth and differentiation factors 5,6,7) subgroup. BMP receptors have a short extracellular domain, a single transmembrane domain, and an intracellular domain with serine/threonine kinase activity. There are a total of seven type I receptors (ALK1-7) for the TGFβ family, four of which bind BMPs: type 1A BMP receptor

(BMPR-1A or ALK3), type 1B BMP receptor (BMPR-1B or ALK6), type 1A activin receptor (ActR-1A or ALK2) and ALK1. There are four type II receptors, three of which bind BMPs: type 2 BMP receptor (BMPR-2), type 2 activin receptor (ActR-2A), and type 2B activin receptor (ActR-2B). While BMPR-1A/ALK3, BMPR-1B/ALK6, and BMPR-2 are specific to BMPs, ALK1, ActR-1A, ActR-2A, and ActR-2B can function as receptors for activins, which are also members of the TGFβ superfamily. Most receptors are not specific for individual BMPs, which causes great combinatorial complexity of BMP ligand – receptor partners (Townson et al., 2012).

In the canonical BMP signalling pathway, BMPs bind BMP receptors comprised of two type I receptor subunits and two type II receptor subunits. Upon ligand binding, the type II receptor trans phosphorylates the type I receptor, which then phosphorylates the immediate downstream substrate proteins known as receptor regulated Smads (R-Smad), Smad1, Smad5 and Smad8 (Smad1/5/8). Activated pSMAD1/5/8 complexes with the co-mediator Smad (co-Smad) Smad4 translocating to the nucleus. There, together with other transcription factors, co-activators and co-repressors, pSMAD1/5/8-Smad4 activate or repress target genes. Inhibitory Smads (I-Smads), Smad6 and Smad7 (Smad6/7), are involved in feedback inhibition of the signaling pathway. They inhibit the activation of R-Smads by competing for type I receptor interaction and by recruiting ubiquitin ligases or phosphatases to the activated receptor complex thereby targeting it for proteosomal degradation or dephosphorylation, respectively. BMP signaling can also occur through not canonical pathway, in which BMPs signal through MAPK kinases, PI3 kinase/AKT, PKC and others (Zhang, 2009).

Regulation of BMP signaling is achieved by a diverse number of extracellular, intracellular and membrane modulators. Extracellular modulators can be agonists or antagonists of BMP signaling; BMP antagonists bind BMPs thus preventing them from binding their cognate receptors (Walsh et al., 2010). Some BMP antagonists are the CAN (Cerberus and DAN) family of proteins, Twisted gastrulation, Chordin and Crossveinless 2, and Noggin. Intracellular regulators of BMP signaling include microRNAs, I-SMADS, phosphatases that dephosphorylate the BMP receptors and R-Smad, and FK506-binding protein 1A that binds type I receptors to inhibit receptor internalization. Co-receptors in the plasma membrane that interact with type I and type II receptors further add a level of regulation. Of particular interest for vascular biology, Endoglin is a co-receptor that has been shown to be important in vascular growth and disease (ten Dijke et al., 2008). Finally, crosstalk with other signaling

pathways, such as Notch, Wnt and Sonic hedgehog signaling, likely adds another layer of control.

3. Partial rescue of BMP signaling in YAP/TAZ deficient cells improves cellular defects

3.1. Ldn193187 treatment partially rescues the BMP signalling defect in vitro

Notch signalling plays a key role in the determination of tip and stalk cell identities in developing vessels. Too little Notch signalling, as seen in DLL4 or Notch 1 mutants or by DAPT treatment, favours tip cell specification, leading to a hypersprouting phenotype with consequent increased vascular density (Suchting et al., 2007, Hellstrom et al., 2007, Lobov et al., 2007, Tammela et al., 2008). In contrast, too much Notch signaling reduces the number of tip cells and leads to a hyposprouting phenotype, with reduced branch points and vascular density (Benedito et al., 2009, Hellstrom et al., 2007). As the loss of YAP/TAZ causes a hyposprouting phenotype *in vivo* and increases Notch signaling in sparse cells *in vitro*, I hypothesized that too much Notch signaling could be driving the phenotype in *Yap/Taz* iEC-KO retinas. This hypothesis was however proven wrong by Gou Young Koh's group, who showed that Notch inhibition in *Yap/Taz* iEC-KO retinas does not rescue the vascular defects (Kim et al., 2017). Moreover, the *in vitro* cellular phenotypes I unveiled were present in confluent YAP/TAZ knockdown cells, where the luciferase data shows a decrease instead of an increase in Notch signalling. This reason also suggests that the cellular defects of YAP/TAZ loss are not driven by an increase in Notch signalling.

In contrast to Notch, the effect of YAP/TAZ on BMP signalling was much clearer and stronger. How BMP signalling affects the development of blood vessels is however not as straightforward. As presented before, there are multiple BMP ligands and receptors that can combine in different ways. Depending on the specific ligands and receptors involved, BMP signalling can either be pro or antiangiogenic. In the vasculature, the BMP9/BMP10-ALK1 axis supresses sprouting (Ricard et al., 2012), thus, an increase in the activity of this axis could be a cause for the hyposprouting phenotype of YAP/TAZ mutant retinas. On the other hand, BMP2/BMP4 are considered pro-angiogenic molecules (Mishina et al., 2002), as well

as signalling through the Alk2 and Alk3 receptors (Lee et al., 2017). For this reason, an increase of BMP signalling through these ligands/receptors was not expected.

To understand the contribution of the BMP signalling increase for the cellular defects caused by YAP/TAZ loss I attempted to rescue the signalling defect in YAP/TAZ knockdown cells. To do so, I treated cells with a panel of BMP inhibitors targeting different ligands or receptors (**Figure 5.5 A**). Moreover, this strategy presented the added benefit of dissecting the axis through with BMP signalling was increased in YAP/TAZ knockdown cells. Of all the drugs tested only Ldn193187, an Alk2/3/1 kinase inhibitor, significantly decreased the BMP reporter activity after YAP and TAZ knockdown (**Figure 5.5 B**). This decrease was however not a complete rescue: in YAP/TAZ knockdown cells the BMP reporter activity dropped from 12 times higher when treated with DMSO to 7 times higher when treated with Ldn193187, in comparison to control cells. Contrary to the expectations, the use of ALK1-Fc and ENG-ecd, which primarily bind to and inhibit BMP9 and BMP10, did not affect the BMP signaling increase in YAP/TAZ knockdown cells.

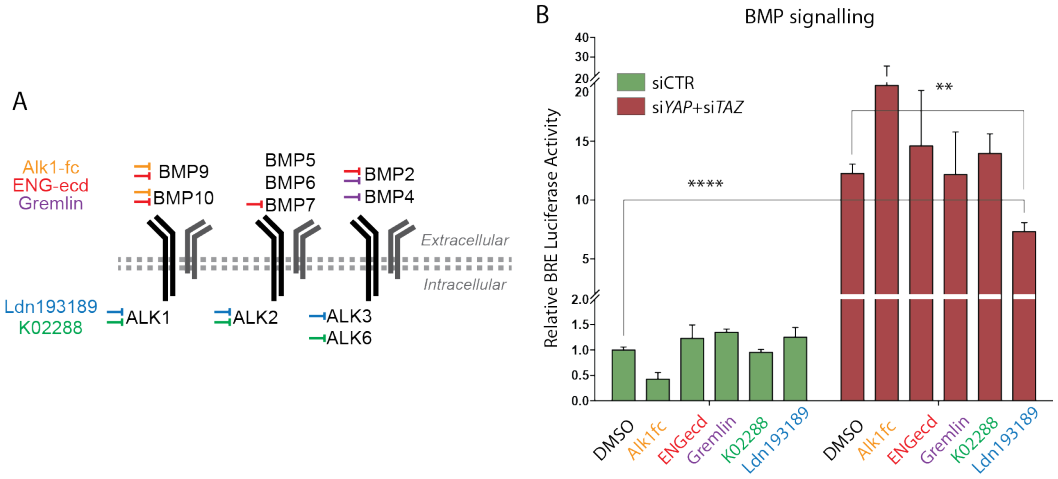

Figure 5.5. Ldn193187 treatment partially rescues the BMP signalling increase in YAP/TAZ deficient endothelial cells.

A, Schematic of the BMP inhibitors used depicting preferential sites of inhibition. Alk1fc, ENGecd and Gremlin bind extracellular BMPs. K02288 and Ldn193189 are kinase inhibitors acting intracellularly.

B, Luciferase reporter assay for BMP activity in YAP/TAZ knockdown HUVECs and controls treated with 25 ng/mL Alk1fc, 0.25µg/mL ENGecd, 0.1 µg/mL Gremlin, 1µM K02288, 1µM Ldn193189 and DMSO. Data are mean ± SEM. *p* values were calculated using unpaired *t*-test. **, $p<0.01$; ****, $p<0.0001$. n≥3 biological replicates.

3.2. Ldn193187 treatment increases the frequency of junction associated intermediate lamellipodia in YAPTAZ knockdown cells and improves the migration and permeability defects

Although Ldn193187 treatment only partially rescued the increase in BMP signalling in YAP/TAZ knockdown HUVECs, I investigated whether this was sufficient to affect the morphology of adherens junctions. To do so, I treated YAP/TAZ knockdown cells with Ldn193187 or DMSO and compared the morphology of VE-Cadherin (**Figure 5.6 A, B**). Ldn193187 treatment decreased the frequency of finger junctions and increased the frequency of reticular junctions in YAP/TAZ deficient cells (**Figure 5.6 A', B'**). Quantification of junction morphologies by blind analysis of patches revealed that Ldn193187 treatment decreased the frequency of finger junctions in YAP/TAZ deficient cells to levels comparable to control cells (**Figure 5.6 C** and **Figure 4.10 A, F**) (% of fingers: siYAP/TAZ DMSO, 25+/-5%, siYAP/TAZ Ldn193187 12+/-0.6%, siCTR: 9+/-4%). Ldn193187 treatment also led to a 3-fold increase in thick to reticular and reticular junctions in YAP/TAZ knockdown cells. The frequency of straight junctions was also significantly decreased, although still remaining high in comparison to control cells.

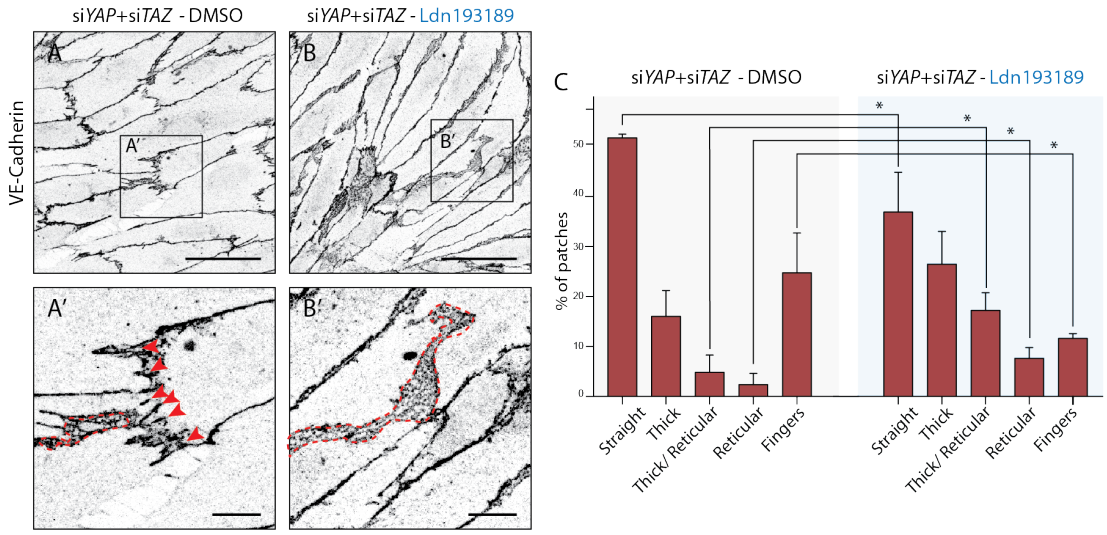

Figure 5.6. Ldn193187 treatment increases the frequency of junction associated intermediate lamellipodia in YAP/TAZ knockdown endothelial cells

A, B, HUVECs knocked down for YAP/TAZ and treated with 1 μM Ldn193189 (B) or DMSO (A) were stained for VE-Cadherin. A', B', magnification of boxed areas in A, B. Red arrowheads, fingers. Red dashed line, reticular junction. Scale bar A, B, 50μm. Scale bar A', B', 10μm.

C, Morphological analysis of VE-Cadherin labelled cell junctions in HUVECs knocked down for YAP/TAZ and treated with 1μM Ldn193189 or DMSO control. Data are mean ± SD. *p* values were

calculated using unpaired *t*-test. n= 3 biological replicates; n≥ 45 patches of VE-Cadherin stained HUVECs per condition per replicate.

I then investigated whether Ldn193187 treatment affected the migratory capacity of YAP/TAZ knockdown HUVECs, as well as the barrier function of the monolayer. Ldn193187 treatment improves the migration defect of YAP/TAZ knockdown cells: in the scratch wound assay, the wound closure increases from 33+/- 3% in DMSO treated cells to 56+/-5% in Ldn193187 treated cells (**Figure 5.7 A**). Moreover, Ldn193187 treatment completely rescues the barrier defect of YAP/TAZ knockdown cells (**Figure 5.7 B**). These results show that at least partially the cellular and molecular defects of YAP/TAZ knockdown cells are caused by an increase in BMP signalling. As Ldn193187 treatment did not completely rescue the signalling defect it was not possible to completely understand how much of the cellular defects are in fact caused by increased BMP signalling.

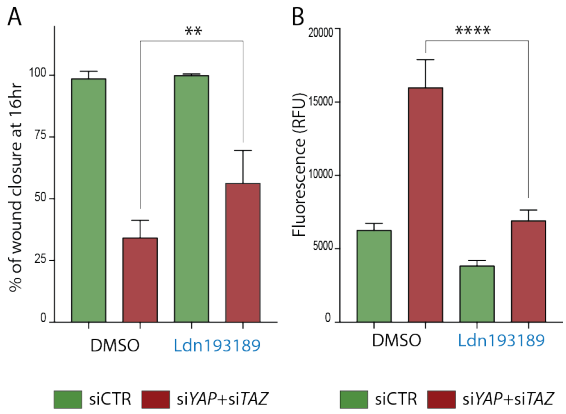

Figure 5.7. Ldn193187 treatment improves the migration and decreases the permeability in YAP/TAZ knockdown endothelial cells

A, Wound closure at 16hrs for HUVECs knocked down for YAP/TAZ and treated with 1mM Ldn193189 or DMSO. Data are mean +/- SD. *p* values were calculated using unpaired *t*-test. **, $p<0.01$. n= 6-7 biological replicates.

B, Permeability of HUVECs knocked down for YAP/TAZ and treated with 1μM Ldn193189 or DMSO to 250kDa fluorescent dextran molecules. Data are mean +/- SD. RFU, relative fluorescence units. *p* values were calculated using unpaired *t*-test. ****, $p<0.0001$. n = 6 biological replicates.

4. YAP/TAZ increase the transcription of BMP inhibitors

An increase in BMP signaling can be a consequence of an increase in BMPs, BMP receptors/co-receptors or a decrease in BMP antagonists (**Figure 5.8 A**). To understand at what level of regulation YAP/TAZ affect BMP signaling I investigated

the expression of these components in YAP/TAZ knockdown cells. The knockdown of YAP/TAZ causes a decrease in the expression of BMP4 in ECs, which however cannot be the cause for the increased BMP signaling (**Figure 5.8 B**). The expression of BMP2 and BMP6 is not affected and that of BMP7 and BMP9 is too low for detection in HUVECs. The knockdown of YAP/TAZ does not affect the expression of the BMP receptors *ALK1*, *ALK2*, *ALK5*, *ALK6*, *BMPR2* and of the co-receptor *ENG* (**Figure 5.8 C**); the expression of *ALK3* is too low for detection in HUVECs. Interestingly, the knockdown of YAP/TAZ leads to a strong decrease in the expression of the BMP antagonists *CTGF*, *NOG* and *FST*, and to a milder but also significant decrease in the expression of *FSTL1*, *SMURF1* and *SMURF2* (**Figure 5.8 D**). Other BMP antagonists as *BMPER* and *BAMBI* are not affected by YAP/TAZ loss in HUVECs. These results suggest that the increase in BMP signaling in the context of YAP/TAZ loss of function can be due to a loss of BMP antagonists. Furthermore, as YAP/TAZ act as transcriptional co-activators when in the nucleus, meaning that they promote the transcription of genes and do not act as transcriptional repressors, this results fits with the possibility of a direct transcriptional effect of YAP/TAZ on BMP antagonists.

Together, these results suggest that YAP and TAZ repress BMP signalling in ECs by increasing the expression of BMP inhibitors.

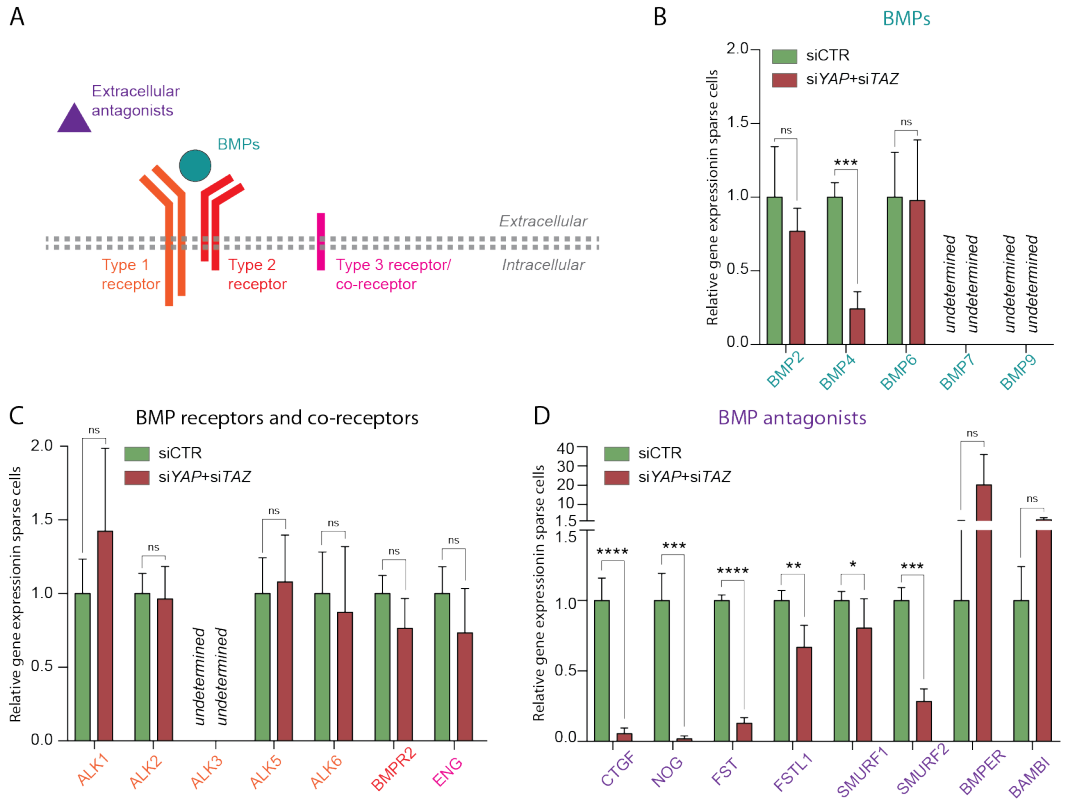

Figure 5.8. YAP/TAZ increase the expression of BMP antagonists in endothelial cells

A, Schematic of the main BMP signaling components.

B-D, RT-qPCR in YAP/TAZ knockdown HUVECs and control cells for BMPs (B), BMP receptors and co-receptors (C) and BMP antagonists (D). Results are relative to siCTR. Normalisation was performed with GAPDH expression. No amplification of the cDNA of BMP7, BMP9 and ALK3 was obtained. Data are mean ± SD of 7 biological replicates from 3 independent experiments. *p* values were calculated using unpaired *t*-test. ns, $p>0.05$; *, $p<0.05$; **, $p<0.01$; ***, $p<0.001$; ****, $p<0.0001$.

5. Summary and conclusions

In this chapter I have shown that endothelial YAP/TAZ repress BMP signaling in sprouting ECs likely by increasing the expression of secreted BMP antagonists such as *CTGF* and *NOG*. In ECs, the repression of BMP signaling increases the formation of JAILs, promotes cell migration and decreases permeability.

Chapter 6 – Discussion and future perspectives

When this study started very little was known of the role of the Hippo pathway effectors YAP and TAZ on the biology of ECs, and particularly during sprouting angiogenesis. Because of the critical roles discovered for YAP and TAZ in the development of other tissues and organs, a lot of attention from the angiogenesis community was put into unravelling their roles in the endothelium. These efforts culminated with the publication of a series of papers in the last half of 2017 – first half of 2018, including my own paper. Here, I will discuss the results of my discoveries and place them in the overall field of YAP/TAZ in endothelial biology and angiogenesis.

4. Summary of the findings

YAP and TAZ are both expressed in ECs. While in quiescent vessels they are only present in the cytoplasm, they are nuclear in a few ECs of actively sprouting vessels. This pattern of expression is accompanied by a functional role during sprouting angiogenesis. YAP/TAZ are necessary for the new blood vessels to grow and cover the hypoxic tissue. Without YAP/TAZ fewer sprouts are formed; the sprouts are rounder, lack cellular protrusions and are haemorrhagic. The vasculature formed is smaller, less dense, with fewer connections and less homogeneous, and abnormal crosses between arteries and veins and between capillaries are formed. YAP and TAZ show a high degree of redundancy, which is better illustrated by the striking phenotype of the double mutant in comparison with the single mutants. Nonetheless, they also show unique characteristics. *In vivo*, while YAP preferentially locates to the cytoplasm, TAZ preferentially locates in the nucleus. Only TAZ single mutants show hyposprouting, AV crosses and vein defects.

I found several cellular functions of YAP and TAZ that seem to account for the phenotype of the YAP/TAZ iEC-KO mutants. First, YAP/TAZ promote endothelial cell proliferation, which is essential to provide new cells to the growing vascular tissue. Specifically, I found that YAP is necessary for stretch-induced proliferation of ECs, but not for VEGF-induced proliferation. I propose that this represents a cell intrinsic way of controlling cell densities, in contrast to the more widespread

proliferation that happens in response to growth factor signalling. Second, YAP/TAZ promote cell migration and rearrangements of cells, necessary during the formation of new sprouts and anastomosis of vessels. Third, YAP/TAZ decrease endothelial permeability, thereby preventing haemorrhages. Molecularly, YAP/TAZ regulate the architecture and turnover of VE-Cadherin adherens junctions, promoting the formation of JAILs. In this way, YAP/TAZ not only are required to provide the correct number of ECs for the growing vasculature, they also ensure that ECs are correctly distributed, thereby achieving the right number of ECs in the right place.

YAP/TAZ strongly repress BMP signalling in actively sprouting ECs likely by promoting the transcription of secreted BMP inhibitors. In particular, I show that BMP signalling repression is required to limit endothelial permeability and for ECs to form JAILs.

5. Regulation of YAP and TAZ in the endothelium

YAP/TAZ are commonly found in the nucleus of epithelial cells located in actively proliferating areas of developed and developing tissues. In contrast, quiescent tissues display cytoplasmic, transcriptionally inactive YAP/TAZ, and frequently in those the re-location of YAP/TAZ to the nucleus is seen and plays a role during inflammation or neoplastic transformation. Through my work I have found that a similar regulation is present in ECs of developing blood vessels: more mature, quiescent vessels uniformly display inactive YAP/TAZ, while actively sprouting vessels show a more dynamic expression of active YAP/TAZ.

How this is regulated in ECs is not entirely clear. ECs at the sprouting front and in quiescent vessels show various differences that could account for this regulation. Distinct adherens junctions, basement membrane and coverage by pericytes; distinct levels of signalling from secreted angiogenic molecules; different levels of shear stress by blood flow; different levels of pulling and pushing forces from migrating neighbouring cells.

In vitro, endothelial YAP and TAZ relocate to the nucleus upon disruption of cell junctions or loss of VE-Cadherin (Choi et al., 2015). In the mouse retina vasculature, it was recently shown that ECs at the sprouting front display reduced VE-Cadherin concentration than more mature vessels (Cao et al., 2017). In addition to the concentration of VE-Cadherin being different, adherens junctions at the sprouting front are activated, more permeable, and displaying increased finger junctions (Bentley et al., 2014) and JAILs (Cao et al., 2017). These differences nicely

correlate with my data showing the sprouting front as the area of preferential nuclear YAP/TAZ, and suggest that similarly to other cell types the subcellular location of YAP/TAZ is regulated by the status of adherens junctions.

Some studies point to YAP/TAZ being regulated by shear stress. Nakajima and colleagues (Nakajima et al., 2017) showed that in the zebrafish YAP nuclear relocation correlated with lumenisation of sprouting vessels, which was attributed to the effect of shear stress on YAP. In the mouse retina, hemodynamic fluid laws predict that vessels at the sprouting front experience very low levels of shear (Bernabeu et al., 2014), arguing against YAP and TAZ being activated by shear in this model. Additionally, I found no difference in the subcellular localisation of YAP or TAZ between arteries and veins, i.e. vessels that experience distinct shear stress levels. However, it is possible that local and fast changes in shear stress levels are more relevant to regulate YAP and TAZ than sustained shear. In support of this idea, YAP and TAZ appear not to respond to 12 or 24h of laminar shear (Wang et al., 2016), but translocate to the nucleus after only 10 minutes of laminar shear (Nakajima et al., 2017). In addition to shear, ECs are subjected to pushing and pulling forces from neighbouring cells, especially at the sprouting front where they undergo cell migration towards the source of pro-angiogenic molecules. In this regard, I have shown that YAP is required for stretch induced proliferation, highlighting this mechanical stimuli as a regulator for the function of YAP. In epithelial cells, YAP was further shown to relocate to the nucleus upon application of cyclic stretch(Benham-Pyle et al., 2015), suggesting that a similar mechanism could be present in ECs.

As YAP/TAZ are also regulated by growth factors in other cell types, I tested if VEGF, a crucial driver of endothelial proliferation and migration, was upstream of YAP/TAZ in ECs. Although I found no evidence for this, four independent labs (Kim et al., 2017, Wang et al., 2017, Azad et al., 2018, He et al., 2018) published evidence for VEGF-VEGFR2 signalling being upstream of YAP/TAZ activation, including one unbiased screen for upstream regulators of the Hippo pathway from one non-angiogenesis lab. Their combined data thus support a model in which VEGF signalling critically regulates YAP/TAZ subcellular location, and because VEGF is produced ahead of the growing vessels, it fits with the nuclear location of YAP/TAZ at the sprouting front. Differently, my proliferation experiments suggest that cells deficient for YAP/TAZ are even more sensitive to VEGF. Interestingly, CTGF, a secreted molecule downstream of YAP/TAZ-TEAD signalling, was shown to directly bind extracellular VEGF thereby preventing its downstream signalling (Inoki et al., 2002), which could explain the apparent increased sensitivity of YAP/TAZ deficient

cells to VEGF. Apart from VEGF, the effect of other pro-angiogenic molecules, either locally produced or blood-borne, was not yet addressed, and could prove in the future to regulate endothelial YAP and TAZ during development. Future work will help clarify these questions and how different chemical and mechanical stimuli come together to regulate YAP and TAZ.

6. The balance between migration and permeability during the sprouting of new vessels

Among all the pro-angiogenic molecules known, VEGF is arguably the most critical. The requirement of VEGF for blood vessel development is readily illustrated by the early embryonic lethality and abnormal vessel formation of even the heterozygous VEGF deletion (Carmeliet et al., 1996, Ferrara et al., 1996). VEGF is produced and secreted by the hypoxic tissue and upon binding to its cognate receptors on ECs activates them to start sprouting new vessels. Importantly, during sprouting angiogenesis, VEGF increases both EC migration and permeability. These well-established roles of VEGF have contributed to the concept of inactive and active junctions in the endothelium: while stable, quiescent blood vessels display inactive adherens junctions that limit endothelial motility and maintain the vessel impermeable, ECs undergoing angiogenesis display activated adherens junctions that allow increased endothelial motility and are characterized by increased permeability. Thus, my results showing that YAP/TAZ increase both migration and decrease permeability were at first surprising. However, it is conceivable that YAP/TAZ at the sprouting front is necessary to balance the VEGF induced increased permeability of new sprouts. Interestingly, data from recent years has revealed that sprouting ECs do not migrate in a head to toe fashion, but instead can swap positions with their neighbours (Jakobsson et al., 2010). While doing so, ECs maintain cell-cell contacts, which requires the formation of new junctions and resolution of the old ones(Blum et al., 2008, Jakobsson et al., 2010, Lenard et al., 2013). Additionally, observations in the zebrafish and mouse showed that a perfused lumen is already present in the nascent sprout reaching the tip cell, propelled by the pressure of blood (Gebala et al., 2016) – unlike the previous idea that tip cells were not subjected to the effect of blood pressure. These new findings illustrate the importance of tightly balancing the permeability while allowing the migration of the very dynamic, pressure subjected ECs in sprouts, so that bleedings can be prevented.

The opposite effects on endothelial permeability between VEGF and YAP/TAZ seem to be explained by the type of adherens junctions they promote: while VEGF induces the formation of finger junctions (Monaghan-Benson and Burridge, 2009), YAP/TAZ induce the formation of JAILs, which were previously shown to decrease endothelial permeability (Breslin et al., 2015).

JAILs were first described in cultured ECs in 2014(Abu Taha et al., 2014), and they were first observed in ECs *in vivo* at the sprouting front, suggesting an important role there (Cao et al., 2017). Interestingly, JAILs both decrease permeability and increase migration. I suggest that the reason for this relies on the organisation and fast half-life of JAILs and on the fast turnover of the VE-Cadherin molecules within JAILs. When two ECs are connected via finger junctions in culture, a long extension of contacting cell membrane is devoid of VE-Cadherin; gaps between the cell bodies can also occur – all this accounting for increased paracellular permeability. In contrast, when two ECs are connected by JAILs, their cell bodies are connected by many VE-Cadherin molecules covering the large extension of the lamellipodia – thus decreasing permeability. While this is so, the JAIL is very short-lived and VE-Cadherin molecules show fast turnover, which means that the molecular bonds between touching cells are quickly formed and resolved – allowing for increased cell movements.

7. YAP/TAZ and adhesive junctions

In addition to nuclear and cytoplasmic YAP and TAZ, I also observed junctional localization of these proteins in retinal vessels. A previous study by Giampietro and colleagues (Giampietro et al., 2015) has shown that endothelial YAP associates with adherens junction proteins at stable junctions and that this prevents its nuclear accumulation and transcriptional activity. Similarly, the disorganisation of VE-Cadherin bonds by calcium chelation or the loss of VE-Cadherin protein by gene knockdown were shown to cause the relocation of YAP to the nucleus (Choi et al., 2015). Curiously, a recent publication reported that, in the mouse retina, sprouts have relatively less VE-Cadherin than more mature vessels with stable junctions (Cao et al., 2017), which fits with the area of nuclear YAP/TAZ. Moreover, I did not find junctional YAP or TAZ at the sprouting front, suggesting that activated junctions fail to sequester YAP/TAZ. Conceptually, these data support the hypothesis that the subcellular location of YAP/TAZ in the vasculature is at least in part regulated by the maturation of adherens junctions. Importantly, my work now adds that, in turn, YAP/TAZ also regulate adherens junctions. YAP/TAZ promote the formation of

JAILs, which are very dynamic and fast turnover adherens junctions. This is mediated through BMP signalling repression via transcription of YAP/TAZ antagonists, therefore represents a nuclear role of YAP/TAZ. Interestingly, this finding corroborates recent findings in mouse hepatocytes where YAP antagonises adherens junction stability (Bai et al., 2016). The authors showed that YAP regulates hepatocyte adherens junctions in response to increased actomyosin contractility by increasing myosin II light chain gene expression (Bai et al., 2016). Also there, the transcriptional, nuclear role of YAP was required for junctional regulation, although the described mechanism was different. However also in ECs YAP/TAZ regulate actomyosin contraction (Kim et al., 2017), so possibly both mechanisms act together in regulating junctional proteins. Together, these findings indicate the existence of a positive feedback loop where stable junctions sequester YAP and TAZ from the nucleus, therefore maintaining less junctional turnover, while remodelling junctions allow YAP and TAZ to relocate to the nucleus where they increase VE-Cadherin turnover.

In addition to the regulation of adherens junctions, Kim and colleagues found decreased levels of the tight junction proteins ZO-1 and Claudin-5 in retinas from YAP/TAZ iEC-KO mice (Kim et al., 2017). Although in my model I did not observe brain haemorrhages at P6, other labs did report them, perhaps in connection to the use of a different Cre line to induce YAP/TAZ deletion in ECs (*VE-Cadherin Cre*)(Kim et al., 2017, Wang et al., 2017).

8. YAP/TAZ, migration and the actin cytoskeleton

I analysed the directional cell migration using the scratch wound assay and inferred the non-directional rearrangements of cells by their position in the monolayer, and concluded that YAP/TAZ both increase the directional cell migration and the individual rearrangements of cells. Interestingly, my conclusions are supported by Wang and colleagues that analysed the migration tracts of live cells and similarly observed that the loss of YAP/TAZ decreases the random movement of ECs (Wang et al., 2017). Mechanistically, I showed that YAP/TAZ promotes actin branching and the formation of JAILs, which are necessary for cell migration. In a complementary way, other labs focusing on the actomyosin cytoskeleton reported on YAP/TAZ being required for the formation of filopodia (Kim et al., 2017), lamellipodia (Wang et al., 2017, Sakabe et al., 2017) and contractility (Kim et al., 2017).

Transcriptome analysis of isolated brain ECs from YAP/TAZ iEC-KO pups and chromatin immunoprecipitation sequencing analysis showed that YAP/TAZ directly up-regulate genes linked to cytoskeletal remodelling (*MACF1*, *FLNB*, *MICAL3*, *CTGF*) (Wang et al., 2017). My data shows that BMP signalling repression, which is caused by the transcription of BMP inhibitors, is partially responsible for the migration defect. Together, these results suggest that the nuclear, transcriptional role of YAP/TAZ, are required for cell migration. Curiously, Sakabe and colleagues found that cytoplasmic but not nuclear YAP increases Cdc42 activity in lamellipodia and phosphorylation of N-WASP (Sakabe et al., 2017), an actin binding protein that promotes branching of actin through the activation of the Arp2/3. They also showed partial rescue of the migration defect by expressing a constitutively active form of Cdc42. It is thus likely that YAP/TAZ promote endothelial cell migration by more than one molecular mechanism.

9. YAP/TAZ and the regulation of BMP signalling

It was previously known that YAP/TAZ could be regulated by BMP signalling (Yu and Guan, 2013). However, that YAP/TAZ can in turn regulate BMP signalling had not been appreciated before, and this in spite of the classical YAP/TAZ target gene CTGF being a known BMP antagonist (Abreu et al., 2002). Here, I clearly show that YAP/TAZ modulate BMP signalling in ECs and that some of the cellular functions of YAP/TAZ are dependent on BMP signalling repression. In particular, the increased permeability of YAP/TAZ knockdown cells is completely rescued by decreasing BMP signalling. This result is in accordance with previous data showing that BMP2 (Hussein et al., 2014) and BMP6 (Benn et al., 2016) increase EC permeability. In ECs, YAP/TAZ promote the transcription of the BMP signalling antagonists *CTGF*, *NOG, FST* and others. In particular, CTGF directly binds to BMP4 decreasing its binding to BMP receptors (Abreu et al., 2002). In ECs, CTGF increases the migration of cells *in vitro* and promotes the extension of filopodia and the growth of the vascular plexus in the mouse retina (Pi et al., 2011), so at least part of the YAP/TAZ loss of function phenotype might be caused by the lack of CTGF expression. *In vivo* rescue experiments using CTGF and other BMP antagonists will be required to determine if one or several of them cause, and to what extent, the YAP/TAZ loss of function phenotype.

In addition to the precise relevant BMP antagonist being undetermined, further research will need to clarify the specific ligands/ receptors involved, and what

their roles are in the context of YAP/TAZ loss. While my *in vitro* results suggest an increase in the BMP2/4 – ALK3 pathway, this pathway was previously shown to be pro-angiogenic (Lee et al., 2017), which goes against the antiangiogenic phenotype of YAP/TAZ loss.

10. Unique and redundant roles of YAP and TAZ during blood vessel formation

Unlike certain organs where the single deletion of YAP leads to dramatic developmental defects (for example, the skin (Schlegelmilch et al., 2011), kidneys (Reginensi et al., 2013) and lung (Lin et al., 2017)), ECs require both YAP and TAZ during blood vessel development.

YAP and TAZ show some redundant and some unique roles. The nature of this partial redundancy is most likely explained by the high degree of structural similarity between the two proteins. In ECs, it seems that TAZ evolved to play a more important role as a nuclear transcriptional co-activator in sprouting ECs, while YAP seems to be more relevant in the cytoplasm of all ECs. My stainings in *WT* retinas support this idea, as do the luciferase assays and qPCR data that in general show a higher transcriptional effect for TAZ. Furthermore, my experiments with *Yap* EC-KO mice suggest that TAZ has a preferential nuclear location: when increasing the expression of TAZ by deleting YAP, nuclear expression of TAZ is seen not only at the sprouting front, where it is increased, but also in veins, where no nuclear YAP or TAZ are present in WT conditions. Moreover, only the single deletion of TAZ, but not of YAP, decreases the number of sprouts. This does not mean that YAP is not required for sprouting ECs – the results with the double mutants show the contrary, but the function of YAP in the endothelium might be different and not restricted to sprouting. Curiously, I found that in the single mutants only the deletion of YAP, but not of TAZ, led to decreased endothelial proliferation. However, experiments with gain of function forms of YAP and TAZ showed opposite results. While the expression of a constitutively active form of YAP in ECs did not increase endothelial proliferation (Sakabe et al., 2017), the constitutively active form of TAZ did (Neto et al., 2018). It is possible that YAP and TAZ increase EC proliferation by different mechanisms – that of YAP in transducing signals from mechanical stimulation and of TAZ by promoting pro-proliferatory genes. YAP is, unlike TAZ, much more expressed in the cytoplasm of ECs *in vivo* and is not only in sprouting vessels, but also in more mature, quiescent vessels. This suggests on the one hand that YAP plays a

cytoplasmic role, and on the other hand that it is required during vessel maintenance. Interestingly, Sakabe and colleagues showed that cytoplasmic YAP, but not nuclear YAP, is required for endothelial cell migration as it activates Cdc42 (Sakabe et al., 2017). *In vivo*, they showed that while YAP/TAZ iEC-KO retinas display signs of proliferation and migration defects, the LATS1/2 iEC-KO, that causes nuclear YAP and TAZ accumulation, only showed proliferation but not migration defects (Sakabe et al., 2017). In the zebrafish vasculature, the deletion of YAP leads not to sprouting defects but to vessel collapse (Nakajima et al., 2017), suggesting a role for vessel maintenance in that system.

11. Future work and perspectives

Here, I have uncovered an important role of YAP and TAZ during blood vessel development in the mouse retina. Future research will determine how much these functions are maintained in other vascular tissues and during maintenance, response to injury and pathological angiogenesis. Interestingly, YAP and TAZ are in other cells heavily regulated by the mechanical stiffness of the tissue they contact. If ECs can perceive the stiffness of the tissue through the basement membrane is not known, as also if YAP and TAZ are differently expressed in tissues in different stiffness. It will definitely be interesting to investigate if because of this YAP and TAZ are involved in tissue specific vasculature differences. In the same line of thought, it will be interesting to investigate if conditions that affect vascular stiffness, as atherosclerosis and vascular calcification, affect endothelial YAP/TAZ and if YAP/TAZ are involved in the pathogenesis process. On this regard, a previous study showed increased nuclear localization and activation of YAP/TAZ in atheroprone areas of the endothelium in mouse arteries, and a reduction in the size of atherosclerotic lesions after targeting YAP/TAZ by morpholinos (Wang et al., 2016), suggesting that YAP/TAZ may be a promising target in atherosclerosis. Finally, another remaining question is if YAP and TAZ impact tumour angiogenesis. Data showing nuclear YAP/TAZ in glioblastoma tumour vessels in comparison with their normal cytoplasmic location in cortical vessels suggests that YAP/TAZ may be involved in pathological angiogenesis (Wang et al., 2017). Importantly, clinically targeting YAP/TAZ requires the use of inhibitors or activators of the pathway. As upstream regulators and molecular mechanisms are uncovered, various drugs targeting different areas of the pathway are being tested (Zanconato et al., 2016). To those, I here add the possibility of targeting BMP antagonists as a way to modify YAP/TAZ functions. More research, especially in the *in vivo* situation, will evaluate

how much these drugs are applicable and can change disease progression and outcomes.

References

ABREU, J. G., KETPURA, N. I., REVERSADE, B. & DE ROBERTIS, E. M. 2002. Connective-tissue growth factor (CTGF) modulates cell signalling by BMP and TGF-beta. *Nat Cell Biol,* 4**,** 599-604.

ABU TAHA, A. & SCHNITTLER, H. J. 2014. Dynamics between actin and the VE-cadherin/catenin complex: novel aspects of the ARP2/3 complex in regulation of endothelial junctions. *Cell Adh Migr,* 8**,** 125-35.

ABU TAHA, A., TAHA, M., SEEBACH, J. & SCHNITTLER, H. J. 2014. ARP2/3-mediated junction-associated lamellipodia control VE-cadherin-based cell junction dynamics and maintain monolayer integrity. *Mol Biol Cell,* 25**,** 245-56.

AKIMOTO, S., MITSUMATA, M., SASAGURI, T. & YOSHIDA, Y. 2000. Laminar shear stress inhibits vascular endothelial cell proliferation by inducing cyclin-dependent kinase inhibitor p21(Sdi1/Cip1/Waf1). *Circ Res,* 86**,** 185-90.

ARDESTANI, A., LUPSE, B. & MAEDLER, K. 2018. Hippo Signaling: Key Emerging Pathway in Cellular and Whole-Body Metabolism. *Trends Endocrinol Metab*.

ARMULIK, A., GENOVE, G. & BETSHOLTZ, C. 2011. Pericytes: developmental, physiological, and pathological perspectives, problems, and promises. *Dev Cell,* 21**,** 193-215.

ARMULIK, A., GENOVE, G., MAE, M., NISANCIOGLU, M. H., WALLGARD, E., NIAUDET, C., HE, L., NORLIN, J., LINDBLOM, P., STRITTMATTER, K., JOHANSSON, B. R. & BETSHOLTZ, C. 2010. Pericytes regulate the blood-brain barrier. *Nature,* 468**,** 557-61.

ATTWELL, D., BUCHAN, A. M., CHARPAK, S., LAURITZEN, M., MACVICAR, B. A. & NEWMAN, E. A. 2010. Glial and neuronal control of brain blood flow. *Nature,* 468**,** 232-43.

AZAD, T., JANSE VAN RENSBURG, H. J., LIGHTBODY, E. D., NEVEU, B., CHAMPAGNE, A., GHAFFARI, A., KAY, V. R., HAO, Y., SHEN, H., YEUNG, B., CROY, B. A., GUAN, K. L., POULIOT, F., ZHANG, J., NICOL, C. J. B. & YANG, X. 2018. A LATS biosensor screen identifies VEGFR as a regulator of the Hippo pathway in angiogenesis. *Nat Commun,* 9**,** 1061.

AZZOLIN, L., PANCIERA, T., SOLIGO, S., ENZO, E., BICCIATO, S., DUPONT, S., BRESOLIN, S., FRASSON, C., BASSO, G., GUZZARDO, V., FASSINA, A., CORDENONSI, M. & PICCOLO, S. 2014. YAP/TAZ incorporation in the beta-catenin destruction complex orchestrates the Wnt response. *Cell,* 158**,** 157-70.

AZZOLIN, L., ZANCONATO, F., BRESOLIN, S., FORCATO, M., BASSO, G., BICCIATO, S., CORDENONSI, M. & PICCOLO, S. 2012. Role of TAZ as mediator of Wnt signaling. *Cell,* 151**,** 1443-56.

BAI, H., ZHU, Q., SURCEL, A., LUO, T., REN, Y., GUAN, B., LIU, Y., WU, N., JOSEPH, N. E., WANG, T. L., ZHANG, N., PAN, D., ALPINI, G., ROBINSON, D. N. & ANDERS, R. A. 2016. Yes-associated protein impacts adherens junction assembly through regulating actin cytoskeleton organization. *Am J Physiol Gastrointest Liver Physiol,* 311**,** G396-411.

BASU, S., TOTTY, N. F., IRWIN, M. S., SUDOL, M. & DOWNWARD, J. 2003. Akt phosphorylates the Yes-associated protein, YAP, to induce interaction with 14-3-3 and attenuation of p73-mediated apoptosis. *Mol Cell,* 11**,** 11-23.

BAUMGARTNER, R., POERNBACHER, I., BUSER, N., HAFEN, E. & STOCKER, H. 2010. The WW domain protein Kibra acts upstream of Hippo in Drosophila. *Dev Cell,* 18**,** 309-16.

BEETS, K., HUYLEBROECK, D., MOYA, I. M., UMANS, L. & ZWIJSEN, A. 2013. Robustness in angiogenesis: notch and BMP shaping waves. *Trends Genet,* 29**,** 140-9.

BENEDITO, R., ROCA, C., SORENSEN, I., ADAMS, S., GOSSLER, A., FRUTTIGER, M. & ADAMS, R. H. 2009. The notch ligands Dll4 and Jagged1 have opposing effects on angiogenesis. *Cell,* 137**,** 1124-35.

BENHAM-PYLE, B. W., PRUITT, B. L. & NELSON, W. J. 2015. Cell adhesion. Mechanical strain induces E-cadherin-dependent Yap1 and beta-catenin activation to drive cell cycle entry. *Science,* 348**,** 1024-7.

BENN, A., BREDOW, C., CASANOVA, I., VUKICEVIC, S. & KNAUS, P. 2016. VE-cadherin facilitates BMP-induced endothelial cell permeability and signaling. *J Cell Sci,* 129**,** 206-18.

BENTLEY, K., FRANCO, C. A., PHILIPPIDES, A., BLANCO, R., DIERKES, M., GEBALA, V., STANCHI, F., JONES, M., ASPALTER, I. M., CAGNA, G., WESTROM, S., CLAESSON-WELSH, L., VESTWEBER, D. & GERHARDT, H. 2014. The role of differential VE-cadherin dynamics in cell rearrangement during angiogenesis. *Nat Cell Biol,* 16**,** 309-21.

BERNABEU, M. O., JONES, M. L., NIELSEN, J. H., KRUGER, T., NASH, R. W., GROEN, D., SCHMIESCHEK, S., HETHERINGTON, J., GERHARDT, H., FRANCO, C. A. & COVENEY, P. V. 2014. Computer simulations reveal complex distribution of haemodynamic forces in a mouse retina model of angiogenesis. *J R Soc Interface,* 11.

BEYER, T. A., WEISS, A., KHOMCHUK, Y., HUANG, K., OGUNJIMI, A. A., VARELAS, X. & WRANA, J. L. 2013. Switch enhancers interpret TGF-beta and Hippo signaling to control cell fate in human embryonic stem cells. *Cell Rep,* 5**,** 1611-24.

BJARNEGARD, M., ENGE, M., NORLIN, J., GUSTAFSDOTTIR, S., FREDRIKSSON, S., ABRAMSSON, A., TAKEMOTO, M., GUSTAFSSON, E., FASSLER, R. & BETSHOLTZ, C. 2004. Endothelium-specific ablation of PDGFB leads to pericyte loss and glomerular, cardiac and placental abnormalities. *Development,* 131**,** 1847-57.

BLUM, Y., BELTING, H. G., ELLERTSDOTTIR, E., HERWIG, L., LUDERS, F. & AFFOLTER, M. 2008. Complex cell rearrangements during intersegmental vessel sprouting and vessel fusion in the zebrafish embryo. *Dev Biol,* 316**,** 312-22.

BRESLIN, J. W., ZHANG, X. E., WORTHYLAKE, R. A. & SOUZA-SMITH, F. M. 2015. Involvement of local lamellipodia in endothelial barrier function. *PLoS One,* 10**,** e0117970.

CAO, J., EHLING, M., MARZ, S., SEEBACH, J., TARBASHEVICH, K., SIXTA, T., PITULESCU, M. E., WERNER, A. C., FLACH, B., MONTANEZ, E., RAZ, E., ADAMS, R. H. & SCHNITTLER, H. 2017. Polarized actin and VE-cadherin dynamics regulate junctional remodelling and cell migration during sprouting angiogenesis. *Nat Commun,* 8**,** 2210.

CARMELIET, P., FERREIRA, V., BREIER, G., POLLEFEYT, S., KIECKENS, L., GERTSENSTEIN, M., FAHRIG, M., VANDENHOECK, A., HARPAL, K., EBERHARDT, C., DECLERCQ, C., PAWLING, J., MOONS, L., COLLEN, D., RISAU, W. & NAGY, A. 1996. Abnormal blood vessel development and lethality in embryos lacking a single VEGF allele. *Nature,* 380**,** 435-9.

CARPENTER, A. E., JONES, T. R., LAMPRECHT, M. R., CLARKE, C., KANG, I. H., FRIMAN, O., GUERTIN, D. A., CHANG, J. H., LINDQUIST, R. A., MOFFAT, J., GOLLAND, P. & SABATINI, D. M. 2006. CellProfiler: image analysis

software for identifying and quantifying cell phenotypes. *Genome Biol,* 7**,** R100.

CASTONGUAY, R., WERNER, E. D., MATTHEWS, R. G., PRESMAN, E., MULIVOR, A. W., SOLBAN, N., SAKO, D., PEARSALL, R. S., UNDERWOOD, K. W., SEEHRA, J., KUMAR, R. & GRINBERG, A. V. 2011. Soluble endoglin specifically binds bone morphogenetic proteins 9 and 10 via its orphan domain, inhibits blood vessel formation, and suppresses tumor growth. *J Biol Chem,* 286**,** 30034-46.

CHEN, C. L., GAJEWSKI, K. M., HAMARATOGLU, F., BOSSUYT, W., SANSORES-GARCIA, L., TAO, C. & HALDER, G. 2010. The apical-basal cell polarity determinant Crumbs regulates Hippo signaling in Drosophila. *Proc Natl Acad Sci U S A,* 107**,** 15810-5.

CHOI, H. J., ZHANG, H., PARK, H., CHOI, K. S., LEE, H. W., AGRAWAL, V., KIM, Y. M. & KWON, Y. G. 2015. Yes-associated protein regulates endothelial cell contact-mediated expression of angiopoietin-2. *Nat Commun,* 6**,** 6943.

CLAXTON, S. & FRUTTIGER, M. 2004. Periodic Delta-like 4 expression in developing retinal arteries. *Gene Expr Patterns,* 5**,** 123-7.

CLAXTON, S., KOSTOUROU, V., JADEJA, S., CHAMBON, P., HODIVALA-DILKE, K. & FRUTTIGER, M. 2008. Efficient, inducible Cre-recombinase activation in vascular endothelium. *Genesis,* 46**,** 74-80.

COTTINI, F., HIDESHIMA, T., XU, C., SATTLER, M., DORI, M., AGNELLI, L., TEN HACKEN, E., BERTILACCIO, M. T., ANTONINI, E., NERI, A., PONZONI, M., MARCATTI, M., RICHARDSON, P. G., CARRASCO, R., KIMMELMAN, A. C., WONG, K. K., CALIGARIS-CAPPIO, F., BLANDINO, G., KUEHL, W. M., ANDERSON, K. C. & TONON, G. 2014. Rescue of Hippo coactivator YAP1 triggers DNA damage-induced apoptosis in hematological cancers. *Nat Med,* 20**,** 599-606.

DAVIS, G. E. & BAYLESS, K. J. 2003. An integrin and Rho GTPase-dependent pinocytic vacuole mechanism controls capillary lumen formation in collagen and fibrin matrices. *Microcirculation,* 10**,** 27-44.

DEJANA, E., ORSENIGO, F. & LAMPUGNANI, M. G. 2008. The role of adherens junctions and VE-cadherin in the control of vascular permeability. *J Cell Sci,* 121**,** 2115-22.

DEJANA, E., TOURNIER-LASSERVE, E. & WEINSTEIN, B. M. 2009. The control of vascular integrity by endothelial cell junctions: molecular basis and pathological implications. *Dev Cell,* 16**,** 209-21.

DONG, J., FELDMANN, G., HUANG, J., WU, S., ZHANG, N., COMERFORD, S. A., GAYYED, M. F., ANDERS, R. A., MAITRA, A. & PAN, D. 2007. Elucidation of a universal size-control mechanism in Drosophila and mammals. *Cell,* 130**,** 1120-33.

DORLAND, Y. L., MALINOVA, T. S., VAN STALBORCH, A. M., GRIEVE, A. G., VAN GEEMEN, D., JANSEN, N. S., DE KREUK, B. J., NAWAZ, K., KOLE, J., GEERTS, D., MUSTERS, R. J., DE ROOIJ, J., HORDIJK, P. L. & HUVENEERS, S. 2016. The F-BAR protein pacsin2 inhibits asymmetric VE-cadherin internalization from tensile adherens junctions. *Nat Commun,* 7**,** 12210.

DUPONT, S., MORSUT, L., ARAGONA, M., ENZO, E., GIULITTI, S., CORDENONSI, M., ZANCONATO, F., LE DIGABEL, J., FORCATO, M., BICCIATO, S., ELVASSORE, N. & PICCOLO, S. 2011. Role of YAP/TAZ in mechanotransduction. *Nature,* 474**,** 179-83.

DYER, L. A., PI, X. & PATTERSON, C. 2014. The role of BMPs in endothelial cell function and dysfunction. *Trends Endocrinol Metab,* 25**,** 472-80.

ELBEDIWY, A., VINCENT-MISTIAEN, Z. I., SPENCER-DENE, B., STONE, R. K., BOEING, S., WCULEK, S. K., CORDERO, J., TAN, E. H., RIDGWAY, R., BRUNTON, V. G., SAHAI, E., GERHARDT, H., BEHRENS, A., MALANCHI,

I., SANSOM, O. J. & THOMPSON, B. J. 2016. Integrin signalling regulates YAP and TAZ to control skin homeostasis. *Development,* 143**,** 1674-87.

ENGE, M., BJARNEGARD, M., GERHARDT, H., GUSTAFSSON, E., KALEN, M., ASKER, N., HAMMES, H. P., SHANI, M., FASSLER, R. & BETSHOLTZ, C. 2002. Endothelium-specific platelet-derived growth factor-B ablation mimics diabetic retinopathy. *EMBO J,* 21**,** 4307-16.

FERNANDEZ, L. A., NORTHCOTT, P. A., DALTON, J., FRAGA, C., ELLISON, D., ANGERS, S., TAYLOR, M. D. & KENNEY, A. M. 2009. YAP1 is amplified and up-regulated in hedgehog-associated medulloblastomas and mediates Sonic hedgehog-driven neural precursor proliferation. *Genes Dev,* 23**,** 2729-41.

FERRARA, N., CARVER-MOORE, K., CHEN, H., DOWD, M., LU, L., O'SHEA, K. S., POWELL-BRAXTON, L., HILLAN, K. J. & MOORE, M. W. 1996. Heterozygous embryonic lethality induced by targeted inactivation of the VEGF gene. *Nature,* 380**,** 439-42.

FRANCO, C. A., JONES, M. L., BERNABEU, M. O., GEUDENS, I., MATHIVET, T., ROSA, A., LOPES, F. M., LIMA, A. P., RAGAB, A., COLLINS, R. T., PHNG, L. K., COVENEY, P. V. & GERHARDT, H. 2015. Dynamic endothelial cell rearrangements drive developmental vessel regression. *PLoS Biol,* 13**,** e1002125.

FRITZMANN, J., MORKEL, M., BESSER, D., BUDCZIES, J., KOSEL, F., BREMBECK, F. H., STEIN, U., FICHTNER, I., SCHLAG, P. M. & BIRCHMEIER, W. 2009. A colorectal cancer expression profile that includes transforming growth factor beta inhibitor BAMBI predicts metastatic potential. *Gastroenterology,* 137**,** 165-75.

FU, V., PLOUFFE, S. W. & GUAN, K. L. 2017. The Hippo pathway in organ development, homeostasis, and regeneration. *Curr Opin Cell Biol,* 49**,** 99-107.

FUJII, M., TOYODA, T., NAKANISHI, H., YATABE, Y., SATO, A., MATSUDAIRA, Y., ITO, H., MURAKAMI, H., KONDO, Y., KONDO, E., HIDA, T., TSUJIMURA, T., OSADA, H. & SEKIDO, Y. 2012. TGF-beta synergizes with defects in the Hippo pathway to stimulate human malignant mesothelioma growth. *J Exp Med,* 209**,** 479-94.

GARCIA DE VINUESA, A., ABDELILAH-SEYFRIED, S., KNAUS, P., ZWIJSEN, A. & BAILLY, S. 2016. BMP signaling in vascular biology and dysfunction. *Cytokine Growth Factor Rev,* 27**,** 65-79.

GEBALA, V., COLLINS, R., GEUDENS, I., PHNG, L. K. & GERHARDT, H. 2016. Blood flow drives lumen formation by inverse membrane blebbing during angiogenesis in vivo. *Nat Cell Biol,* 18**,** 443-50.

GENEVET, A., WEHR, M. C., BRAIN, R., THOMPSON, B. J. & TAPON, N. 2010. Kibra is a regulator of the Salvador/Warts/Hippo signaling network. *Dev Cell,* 18**,** 300-8.

GERHARDT, H., GOLDING, M., FRUTTIGER, M., RUHRBERG, C., LUNDKVIST, A., ABRAMSSON, A., JELTSCH, M., MITCHELL, C., ALITALO, K., SHIMA, D. & BETSHOLTZ, C. 2003. VEGF guides angiogenic sprouting utilizing endothelial tip cell filopodia. *J Cell Biol,* 161**,** 1163-77.

GEUDENS, I., COXAM, B., V., G., ALT, S., VION, A. C., ROSA, A. & GERHARDT, H. 2018. Arterio-venous remodeling in the zebrafish trunk is controlled by genetic programming and flow-mediated fine-tuning. *(Manuscript in preparation)*.

GEUDENS, I., HERPERS, R., HERMANS, K., SEGURA, I., RUIZ DE ALMODOVAR, C., BUSSMANN, J., DE SMET, F., VANDEVELDE, W., HOGAN, B. M., SIEKMANN, A., CLAES, F., MOORE, J. C., PISTOCCHI, A. S., LOGES, S., MAZZONE, M., MARIGGI, G., BRUYERE, F., COTELLI, F., KERJASCHKI, D., NOEL, A., FOIDART, J. M., GERHARDT, H., NY, A., LANGENBERG, T., LAWSON, N. D., DUCKERS, H. J., SCHULTE-MERKER, S., CARMELIET, P.

& DEWERCHIN, M. 2010. Role of delta-like-4/Notch in the formation and wiring of the lymphatic network in zebrafish. *Arterioscler Thromb Vasc Biol,* 30**,** 1695-702.

GIAMPIETRO, C., DISANZA, A., BRAVI, L., BARRIOS-RODILES, M., CORADA, M., FRITTOLI, E., SAVORANI, C., LAMPUGNANI, M. G., BOGGETTI, B., NIESSEN, C., WRANA, J. L., SCITA, G. & DEJANA, E. 2015. The actin-binding protein EPS8 binds VE-cadherin and modulates YAP localization and signaling. *J Cell Biol,* 211**,** 1177-92.

GRILLO, E., RAVELLI, C., CORSINI, M., BALLMER-HOFER, K., ZAMMATARO, L., ORESTE, P., ZOPPETTI, G., TOBIA, C., RONCA, R., PRESTA, M. & MITOLA, S. 2016. Monomeric gremlin is a novel vascular endothelial growth factor receptor-2 antagonist. *Oncotarget,* 7**,** 35353-68.

GRUBER, R., PANAYIOTOU, R., NYE, E., SPENCER-DENE, B., STAMP, G. & BEHRENS, A. 2016. YAP1 and TAZ Control Pancreatic Cancer Initiation in Mice by Direct Up-regulation of JAK-STAT3 Signaling. *Gastroenterology,* 151**,** 526-39.

GRZESCHIK, N. A., PARSONS, L. M., ALLOTT, M. L., HARVEY, K. F. & RICHARDSON, H. E. 2010. Lgl, aPKC, and Crumbs regulate the Salvador/Warts/Hippo pathway through two distinct mechanisms. *Curr Biol,* 20**,** 573-81.

HALDER, G. & JOHNSON, R. L. 2011. Hippo signaling: growth control and beyond. *Development,* 138**,** 9-22.

HAMARATOGLU, F., WILLECKE, M., KANGO-SINGH, M., NOLO, R., HYUN, E., TAO, C., JAFAR-NEJAD, H. & HALDER, G. 2006. The tumour-suppressor genes NF2/Merlin and Expanded act through Hippo signalling to regulate cell proliferation and apoptosis. *Nat Cell Biol,* 8**,** 27-36.

HAMPF, M. & GOSSEN, M. 2006. A protocol for combined Photinus and Renilla luciferase quantification compatible with protein assays. *Anal Biochem,* 356**,** 94-9.

HARVEY, K. F., PFLEGER, C. M. & HARIHARAN, I. K. 2003. The Drosophila Mst ortholog, hippo, restricts growth and cell proliferation and promotes apoptosis. *Cell,* 114**,** 457-67.

HARVEY, K. F., ZHANG, X. & THOMAS, D. M. 2013. The Hippo pathway and human cancer. *Nat Rev Cancer,* 13**,** 246-57.

HAYER, A., SHAO, L., CHUNG, M., JOUBERT, L. M., YANG, H. W., TSAI, F. C., BISARIA, A., BETZIG, E. & MEYER, T. 2016. Engulfed cadherin fingers are polarized junctional structures between collectively migrating endothelial cells. *Nat Cell Biol,* 18**,** 1311-1323.

HE, J., BAO, Q., ZHANG, Y., LIU, M., LV, H., LIU, Y., YAO, L., LI, B., ZHANG, C., HE, S., ZHAI, G., ZHU, Y., LIU, X., ZHANG, K., WANG, X. J., ZOU, M. H., ZHU, Y. & AI, D. 2018. Yes-Associated Protein Promotes Angiogenesis via Signal Transducer and Activator of Transcription 3 in Endothelial Cells. *Circ Res,* 122**,** 591-605.

HEALLEN, T., ZHANG, M., WANG, J., BONILLA-CLAUDIO, M., KLYSIK, E., JOHNSON, R. L. & MARTIN, J. F. 2011. Hippo pathway inhibits Wnt signaling to restrain cardiomyocyte proliferation and heart size. *Science,* 332**,** 458-61.

HELLSTROM, M., GERHARDT, H., KALEN, M., LI, X., ERIKSSON, U., WOLBURG, H. & BETSHOLTZ, C. 2001. Lack of pericytes leads to endothelial hyperplasia and abnormal vascular morphogenesis. *J Cell Biol,* 153**,** 543-53.

HELLSTROM, M., PHNG, L. K., HOFMANN, J. J., WALLGARD, E., COULTAS, L., LINDBLOM, P., ALVA, J., NILSSON, A. K., KARLSSON, L., GAIANO, N., YOON, K., ROSSANT, J., IRUELA-ARISPE, M. L., KALEN, M., GERHARDT, H. & BETSHOLTZ, C. 2007. Dll4 signalling through Notch1 regulates formation of tip cells during angiogenesis. *Nature,* 445**,** 776-80.

HIEMER, S. E. & VARELAS, X. 2013. Stem cell regulation by the Hippo pathway. *Biochim Biophys Acta,* 1830**,** 2323-34.

HILMAN, D. & GAT, U. 2011. The evolutionary history of YAP and the hippo/YAP pathway. *Mol Biol Evol,* 28**,** 2403-17.

HOEBEN, A., LANDUYT, B., HIGHLEY, M. S., WILDIERS, H., VAN OOSTEROM, A. T. & DE BRUIJN, E. A. 2004. Vascular endothelial growth factor and angiogenesis. *Pharmacol Rev,* 56**,** 549-80.

HOSSAIN, Z., ALI, S. M., KO, H. L., XU, J., NG, C. P., GUO, K., QI, Z., PONNIAH, S., HONG, W. & HUNZIKER, W. 2007. Glomerulocystic kidney disease in mice with a targeted inactivation of Wwtr1. *Proc Natl Acad Sci U S A,* 104**,** 1631-6.

HUANG, J., WU, S., BARRERA, J., MATTHEWS, K. & PAN, D. 2005. The Hippo signaling pathway coordinately regulates cell proliferation and apoptosis by inactivating Yorkie, the Drosophila Homolog of YAP. *Cell,* 122**,** 421-34.

HUSSEIN, K. A., CHOKSI, K., AKEEL, S., AHMAD, S., MEGYERDI, S., EL-SHERBINY, M., NAWAZ, M., ABU EL-ASRAR, A. & AL-SHABRAWEY, M. 2014. Bone morphogenetic protein 2: a potential new player in the pathogenesis of diabetic retinopathy. *Exp Eye Res,* 125**,** 79-88.

INOKI, I., SHIOMI, T., HASHIMOTO, G., ENOMOTO, H., NAKAMURA, H., MAKINO, K., IKEDA, E., TAKATA, S., KOBAYASHI, K. & OKADA, Y. 2002. Connective tissue growth factor binds vascular endothelial growth factor (VEGF) and inhibits VEGF-induced angiogenesis. *FASEB J,* 16**,** 219-21.

JAKOBSSON, L., FRANCO, C. A., BENTLEY, K., COLLINS, R. T., PONSIOEN, B., ASPALTER, I. M., ROSEWELL, I., BUSSE, M., THURSTON, G., MEDVINSKY, A., SCHULTE-MERKER, S. & GERHARDT, H. 2010. Endothelial cells dynamically compete for the tip cell position during angiogenic sprouting. *Nat Cell Biol,* 12**,** 943-53.

JARRIAULT, S., BROU, C., LOGEAT, F., SCHROETER, E. H., KOPAN, R. & ISRAEL, A. 1995. Signalling downstream of activated mammalian Notch. *Nature,* 377**,** 355-8.

JIA, J., ZHANG, W., WANG, B., TRINKO, R. & JIANG, J. 2003. The Drosophila Ste20 family kinase dMST functions as a tumor suppressor by restricting cell proliferation and promoting apoptosis. *Genes Dev,* 17**,** 2514-9.

JOYNER, M. J. & CASEY, D. P. 2015. Regulation of increased blood flow (hyperemia) to muscles during exercise: a hierarchy of competing physiological needs. *Physiol Rev,* 95**,** 549-601.

JUSTICE, R. W., ZILIAN, O., WOODS, D. F., NOLL, M. & BRYANT, P. J. 1995. The Drosophila tumor suppressor gene warts encodes a homolog of human myotonic dystrophy kinase and is required for the control of cell shape and proliferation. *Genes Dev,* 9**,** 534-46.

KAMEI, M., SAUNDERS, W. B., BAYLESS, K. J., DYE, L., DAVIS, G. E. & WEINSTEIN, B. M. 2006. Endothelial tubes assemble from intracellular vacuoles in vivo. *Nature,* 442**,** 453-6.

KANAI, F., MARIGNANI, P. A., SARBASSOVA, D., YAGI, R., HALL, R. A., DONOWITZ, M., HISAMINATO, A., FUJIWARA, T., ITO, Y., CANTLEY, L. C. & YAFFE, M. B. 2000. TAZ: a novel transcriptional co-activator regulated by interactions with 14-3-3 and PDZ domain proteins. *EMBO J,* 19**,** 6778-91.

KIM, J., KIM, Y. H., KIM, J., PARK, D. Y., BAE, H., LEE, D. H., KIM, K. H., HONG, S. P., JANG, S. P., KUBOTA, Y., KWON, Y. G., LIM, D. S. & KOH, G. Y. 2017. YAP/TAZ regulates sprouting angiogenesis and vascular barrier maturation. *J Clin Invest,* 127**,** 3441-3461.

KIM, N. G., KOH, E., CHEN, X. & GUMBINER, B. M. 2011. E-cadherin mediates contact inhibition of proliferation through Hippo signaling-pathway components. *Proc Natl Acad Sci U S A,* 108**,** 11930-5.

KOFLER, N. M., SHAWBER, C. J., KANGSAMAKSIN, T., REED, H. O., GALATIOTO, J. & KITAJEWSKI, J. 2011. Notch signaling in developmental and tumor angiogenesis. *Genes Cancer,* 2**,** 1106-16.

KORCHYNSKYI, O. & TEN DIJKE, P. 2002. Identification and functional characterization of distinct critically important bone morphogenetic protein-specific response elements in the Id1 promoter. *J Biol Chem,* 277**,** 4883-91.

KORINEK, V., BARKER, N., MORIN, P. J., VAN WICHEN, D., DE WEGER, R., KINZLER, K. W., VOGELSTEIN, B. & CLEVERS, H. 1997. Constitutive transcriptional activation by a beta-catenin-Tcf complex in APC-/- colon carcinoma. *Science,* 275**,** 1784-7.

KROCK, B. L., SKULI, N. & SIMON, M. C. 2011. Hypoxia-induced angiogenesis: good and evil. *Genes Cancer,* 2**,** 1117-33.

LACOLLEY, P. 2004. Mechanical influence of cyclic stretch on vascular endothelial cells. *Cardiovasc Res,* 63**,** 577-9.

LAI, E. C. 2004. Notch signaling: control of cell communication and cell fate. *Development,* 131**,** 965-73.

LAMMERT, E., CLEAVER, O. & MELTON, D. 2003. Role of endothelial cells in early pancreas and liver development. *Mech Dev,* 120**,** 59-64.

LAPI, E., DI AGOSTINO, S., DONZELLI, S., GAL, H., DOMANY, E., RECHAVI, G., PANDOLFI, P. P., GIVOL, D., STRANO, S., LU, X. & BLANDINO, G. 2008. PML, YAP, and p73 are components of a proapoptotic autoregulatory feedback loop. *Mol Cell,* 32**,** 803-14.

LARRIVEE, B., PRAHST, C., GORDON, E., DEL TORO, R., MATHIVET, T., DUARTE, A., SIMONS, M. & EICHMANN, A. 2012. ALK1 signaling inhibits angiogenesis by cooperating with the Notch pathway. *Dev Cell,* 22**,** 489-500.

LAWSON, N. D., SCHEER, N., PHAM, V. N., KIM, C. H., CHITNIS, A. B., CAMPOS-ORTEGA, J. A. & WEINSTEIN, B. M. 2001. Notch signaling is required for arterial-venous differentiation during embryonic vascular development. *Development,* 128**,** 3675-83.

LAWSON, N. D., VOGEL, A. M. & WEINSTEIN, B. M. 2002. sonic hedgehog and vascular endothelial growth factor act upstream of the Notch pathway during arterial endothelial differentiation. *Dev Cell,* 3**,** 127-36.

LE NOBLE, F., MOYON, D., PARDANAUD, L., YUAN, L., DJONOV, V., MATTHIJSEN, R., BREANT, C., FLEURY, V. & EICHMANN, A. 2004. Flow regulates arterial-venous differentiation in the chick embryo yolk sac. *Development,* 131**,** 361-75.

LEE, H. W., CHONG, D. C., OLA, R., DUNWORTH, W. P., MEADOWS, S., KA, J., KAARTINEN, V. M., QYANG, Y., CLEAVER, O., BAUTCH, V. L., EICHMANN, A. & JIN, S. W. 2017. Alk2/ACVR1 and Alk3/BMPR1A Provide Essential Function for Bone Morphogenetic Protein-Induced Retinal Angiogenesis. *Arterioscler Thromb Vasc Biol,* 37**,** 657-663.

LENARD, A., ELLERTSDOTTIR, E., HERWIG, L., KRUDEWIG, A., SAUTEUR, L., BELTING, H. G. & AFFOLTER, M. 2013. In vivo analysis reveals a highly stereotypic morphogenetic pathway of vascular anastomosis. *Dev Cell,* 25**,** 492-506.

LI, F., LAN, Y., WANG, Y., WANG, J., YANG, G., MENG, F., HAN, H., MENG, A., WANG, Y. & YANG, X. 2011. Endothelial Smad4 maintains cerebrovascular integrity by activating N-cadherin through cooperation with Notch. *Dev Cell,* 20**,** 291-302.

LIN, C., YAO, E., ZHANG, K., JIANG, X., CROLL, S., THOMPSON-PEER, K. & CHUANG, P. T. 2017. YAP is essential for mechanical force production and epithelial cell proliferation during lung branching morphogenesis. *Elife,* 6.

LINDAHL, P., JOHANSSON, B. R., LEVEEN, P. & BETSHOLTZ, C. 1997. Pericyte loss and microaneurysm formation in PDGF-B-deficient mice. *Science,* 277**,** 242-5.

LING, C., ZHENG, Y., YIN, F., YU, J., HUANG, J., HONG, Y., WU, S. & PAN, D. 2010. The apical transmembrane protein Crumbs functions as a tumor suppressor that regulates Hippo signaling by binding to Expanded. *Proc Natl Acad Sci U S A,* 107**,** 10532-7.

LIU, C. Y., ZHA, Z. Y., ZHOU, X., ZHANG, H., HUANG, W., ZHAO, D., LI, T., CHAN, S. W., LIM, C. J., HONG, W., ZHAO, S., XIONG, Y., LEI, Q. Y. & GUAN, K. L. 2010. The hippo tumor pathway promotes TAZ degradation by phosphorylating a phosphodegron and recruiting the SCF{beta}-TrCP E3 ligase. *J Biol Chem,* 285**,** 37159-69.

LIU, W. F., NELSON, C. M., TAN, J. L. & CHEN, C. S. 2007. Cadherins, RhoA, and Rac1 are differentially required for stretch-mediated proliferation in endothelial versus smooth muscle cells. *Circ Res,* 101**,** e44-52.

LOBOV, I. B., RAO, S., CARROLL, T. J., VALLANCE, J. E., ITO, M., ONDR, J. K., KURUP, S., GLASS, D. A., PATEL, M. S., SHU, W., MORRISEY, E. E., MCMAHON, A. P., KARSENTY, G. & LANG, R. A. 2005. WNT7b mediates macrophage-induced programmed cell death in patterning of the vasculature. *Nature,* 437**,** 417-21.

LOBOV, I. B., RENARD, R. A., PAPADOPOULOS, N., GALE, N. W., THURSTON, G., YANCOPOULOS, G. D. & WIEGAND, S. J. 2007. Delta-like ligand 4 (Dll4) is induced by VEGF as a negative regulator of angiogenic sprouting. *Proc Natl Acad Sci U S A,* 104**,** 3219-24.

LU, X., LE NOBLE, F., YUAN, L., JIANG, Q., DE LAFARGE, B., SUGIYAMA, D., BREANT, C., CLAES, F., DE SMET, F., THOMAS, J. L., AUTIERO, M., CARMELIET, P., TESSIER-LAVIGNE, M. & EICHMANN, A. 2004. The netrin receptor UNC5B mediates guidance events controlling morphogenesis of the vascular system. *Nature,* 432**,** 179-86.

MAHONEY, W. M., JR., HONG, J. H., YAFFE, M. B. & FARRANCE, I. K. 2005. The transcriptional co-activator TAZ interacts differentially with transcriptional enhancer factor-1 (TEF-1) family members. *Biochem J,* 388**,** 217-25.

MAKITA, R., UCHIJIMA, Y., NISHIYAMA, K., AMANO, T., CHEN, Q., TAKEUCHI, T., MITANI, A., NAGASE, T., YATOMI, Y., ABURATANI, H., NAKAGAWA, O., SMALL, E. V., COBO-STARK, P., IGARASHI, P., MURAKAMI, M., TOMINAGA, J., SATO, T., ASANO, T., KURIHARA, Y. & KURIHARA, H. 2008. Multiple renal cysts, urinary concentration defects, and pulmonary emphysematous changes in mice lacking TAZ. *Am J Physiol Renal Physiol,* 294**,** F542-53.

MARTI, P., STEIN, C., BLUMER, T., ABRAHAM, Y., DILL, M. T., PIKIOLEK, M., ORSINI, V., JURISIC, G., MEGEL, P., MAKOWSKA, Z., AGARINIS, C., TORNILLO, L., BOUWMEESTER, T., RUFFNER, H., BAUER, A., PARKER, C. N., SCHMELZLE, T., TERRACCIANO, L. M., HEIM, M. H. & TCHORZ, J. S. 2015. YAP promotes proliferation, chemoresistance, and angiogenesis in human cholangiocarcinoma through TEAD transcription factors. *Hepatology,* 62**,** 1497-510.

MASCKAUCHAN, T. N., SHAWBER, C. J., FUNAHASHI, Y., LI, C. M. & KITAJEWSKI, J. 2005. Wnt/beta-catenin signaling induces proliferation, survival and interleukin-8 in human endothelial cells. *Angiogenesis,* 8**,** 43-51.

MATHESON, P. J., WILSON, M. A. & GARRISON, R. N. 2000. Regulation of intestinal blood flow. *J Surg Res,* 93**,** 182-96.

MEESON, A. P., ARGILLA, M., KO, K., WITTE, L. & LANG, R. A. 1999. VEGF deprivation-induced apoptosis is a component of programmed capillary regression. *Development,* 126**,** 1407-15.

MILLER, E., YANG, J., DERAN, M., WU, C., SU, A. I., BONAMY, G. M., LIU, J., PETERS, E. C. & WU, X. 2012. Identification of serum-derived sphingosine-1-phosphate as a small molecule regulator of YAP. *Chem Biol,* 19**,** 955-62.

MISHINA, Y., HANKS, M. C., MIURA, S., TALLQUIST, M. D. & BEHRINGER, R. R. 2002. Generation of Bmpr/Alk3 conditional knockout mice. *Genesis,* 32**,** 69-72.

MITCHELL, D., POBRE, E. G., MULIVOR, A. W., GRINBERG, A. V., CASTONGUAY, R., MONNELL, T. E., SOLBAN, N., UCRAN, J. A., PEARSALL, R. S., UNDERWOOD, K. W., SEEHRA, J. & KUMAR, R. 2010. ALK1-Fc inhibits multiple mediators of angiogenesis and suppresses tumor growth. *Mol Cancer Ther,* 9**,** 379-88.

MITOLA, S., RAVELLI, C., MORONI, E., SALVI, V., LEALI, D., BALLMER-HOFER, K., ZAMMATARO, L. & PRESTA, M. 2010. Gremlin is a novel agonist of the major proangiogenic receptor VEGFR2. *Blood,* 116**,** 3677-80.

MO, J. S., YU, F. X., GONG, R., BROWN, J. H. & GUAN, K. L. 2012. Regulation of the Hippo-YAP pathway by protease-activated receptors (PARs). *Genes Dev,* 26**,** 2138-43.

MONAGHAN-BENSON, E. & BURRIDGE, K. 2009. The regulation of vascular endothelial growth factor-induced microvascular permeability requires Rac and reactive oxygen species. *J Biol Chem,* 284**,** 25602-11.

MONAHAN-EARLEY, R., DVORAK, A. M. & AIRD, W. C. 2013. Evolutionary origins of the blood vascular system and endothelium. *J Thromb Haemost,* 11 Suppl 1**,** 46-66.

MORIN-KENSICKI, E. M., BOONE, B. N., HOWELL, M., STONEBRAKER, J. R., TEED, J., ALB, J. G., MAGNUSON, T. R., O'NEAL, W. & MILGRAM, S. L. 2006. Defects in yolk sac vasculogenesis, chorioallantoic fusion, and embryonic axis elongation in mice with targeted disruption of Yap65. *Mol Cell Biol,* 26**,** 77-87.

MOROISHI, T., HANSEN, C. G. & GUAN, K. L. 2015. The emerging roles of YAP and TAZ in cancer. *Nat Rev Cancer,* 15**,** 73-79.

MOYON, D., PARDANAUD, L., YUAN, L., BREANT, C. & EICHMANN, A. 2001. Plasticity of endothelial cells during arterial-venous differentiation in the avian embryo. *Development,* 128**,** 3359-70.

NAKAJIMA, H., YAMAMOTO, K., AGARWALA, S., TERAI, K., FUKUI, H., FUKUHARA, S., ANDO, K., MIYAZAKI, T., YOKOTA, Y., SCHMELZER, E., BELTING, H. G., AFFOLTER, M., LECAUDEY, V. & MOCHIZUKI, N. 2017. Flow-Dependent Endothelial YAP Regulation Contributes to Vessel Maintenance. *Dev Cell,* 40**,** 523-536 e6.

NETO, F., KLAUS-BERGMANN, A., ONG, Y. T., ALT, S., VION, A. C., SZYMBORSKA, A., CARVALHO, J. R., HOLLFINGER, I., BARTELS-KLEIN, E., FRANCO, C. A., POTENTE, M. & GERHARDT, H. 2018. YAP and TAZ regulate adherens junction dynamics and endothelial cell distribution during vascular development. *Elife,* 7.

NISHIOKA, N., INOUE, K., ADACHI, K., KIYONARI, H., OTA, M., RALSTON, A., YABUTA, N., HIRAHARA, S., STEPHENSON, R. O., OGONUKI, N., MAKITA, R., KURIHARA, H., MORIN-KENSICKI, E. M., NOJIMA, H., ROSSANT, J., NAKAO, K., NIWA, H. & SASAKI, H. 2009. The Hippo signaling pathway components Lats and Yap pattern Tead4 activity to distinguish mouse trophectoderm from inner cell mass. *Dev Cell,* 16**,** 398-410.

OTHMAN-HASSAN, K., PATEL, K., PAPOUTSI, M., RODRIGUEZ-NIEDENFUHR, M., CHRIST, B. & WILTING, J. 2001. Arterial identity of endothelial cells is controlled by local cues. *Dev Biol,* 237**,** 398-409.

PANTALACCI, S., TAPON, N. & LEOPOLD, P. 2003. The Salvador partner Hippo promotes apoptosis and cell-cycle exit in Drosophila. *Nat Cell Biol,* 5**,** 921-7.

PASSANITI, A., BRUSGARD, J. L., QIAO, Y., SUDOL, M. & FINCH-EDMONDSON, M. 2017. Roles of RUNX in Hippo Pathway Signaling. *Adv Exp Med Biol,* 962**,** 435-448.

PHNG, L. K., POTENTE, M., LESLIE, J. D., BABBAGE, J., NYQVIST, D., LOBOV, I., ONDR, J. K., RAO, S., LANG, R. A., THURSTON, G. & GERHARDT, H. 2009. Nrarp coordinates endothelial Notch and Wnt signaling to control vessel density in angiogenesis. *Dev Cell,* 16**,** 70-82.

PI, L., XIA, H., LIU, J., SHENOY, A. K., HAUSWIRTH, W. W. & SCOTT, E. W. 2011. Role of connective tissue growth factor in the retinal vasculature during development and ischemia. *Invest Ophthalmol Vis Sci,* 52**,** 8701-10.

POTENTE, M., GERHARDT, H. & CARMELIET, P. 2011. Basic and therapeutic aspects of angiogenesis. *Cell,* 146**,** 873-87.

RAMASAMY, S. K., KUSUMBE, A. P. & ADAMS, R. H. 2015. Regulation of tissue morphogenesis by endothelial cell-derived signals. *Trends Cell Biol,* 25**,** 148-57.

RAMOS, A. & CAMARGO, F. D. 2012. The Hippo signaling pathway and stem cell biology. *Trends Cell Biol,* 22**,** 339-46.

REGINENSI, A., SCOTT, R. P., GREGORIEFF, A., BAGHERIE-LACHIDAN, M., CHUNG, C., LIM, D. S., PAWSON, T., WRANA, J. & MCNEILL, H. 2013. Yap- and Cdc42-dependent nephrogenesis and morphogenesis during mouse kidney development. *PLoS Genet,* 9**,** e1003380.

RICARD, N., CIAIS, D., LEVET, S., SUBILEAU, M., MALLET, C., ZIMMERS, T. A., LEE, S. J., BIDART, M., FEIGE, J. J. & BAILLY, S. 2012. BMP9 and BMP10 are critical for postnatal retinal vascular remodeling. *Blood,* 119**,** 6162-71.

RIDGWAY, J., ZHANG, G., WU, Y., STAWICKI, S., LIANG, W. C., CHANTHERY, Y., KOWALSKI, J., WATTS, R. J., CALLAHAN, C., KASMAN, I., SINGH, M., CHIEN, M., TAN, C., HONGO, J. A., DE SAUVAGE, F., PLOWMAN, G. & YAN, M. 2006. Inhibition of Dll4 signalling inhibits tumour growth by deregulating angiogenesis. *Nature,* 444**,** 1083-7.

RISAU, W. 1997. Mechanisms of angiogenesis. *Nature,* 386**,** 671-4.

ROSENBLUH, J., NIJHAWAN, D., COX, A. G., LI, X., NEAL, J. T., SCHAFER, E. J., ZACK, T. I., WANG, X., TSHERNIAK, A., SCHINZEL, A. C., SHAO, D. D., SCHUMACHER, S. E., WEIR, B. A., VAZQUEZ, F., COWLEY, G. S., ROOT, D. E., MESIROV, J. P., BEROUKHIM, R., KUO, C. J., GOESSLING, W. & HAHN, W. C. 2012. beta-Catenin-driven cancers require a YAP1 transcriptional complex for survival and tumorigenesis. *Cell,* 151**,** 1457-73.

SAKABE, M., FAN, J., ODAKA, Y., LIU, N., HASSAN, A., DUAN, X., STUMP, P., BYERLY, L., DONALDSON, M., HAO, J., FRUTTIGER, M., LU, Q. R., ZHENG, Y., LANG, R. A. & XIN, M. 2017. YAP/TAZ-CDC42 signaling regulates vascular tip cell migration. *Proc Natl Acad Sci U S A,* 114**,** 10918-10923.

SANVITALE, C. E., KERR, G., CHAIKUAD, A., RAMEL, M. C., MOHEDAS, A. H., REICHERT, S., WANG, Y., TRIFFITT, J. T., CUNY, G. D., YU, P. B., HILL, C. S. & BULLOCK, A. N. 2013. A new class of small molecule inhibitor of BMP signaling. *PLoS One,* 8**,** e62721.

SAUTEUR, L., KRUDEWIG, A., HERWIG, L., EHRENFEUCHTER, N., LENARD, A., AFFOLTER, M. & BELTING, H. G. 2014. Cdh5/VE-cadherin promotes endothelial cell interface elongation via cortical actin polymerization during angiogenic sprouting. *Cell Rep,* 9**,** 504-13.

SCHINDELIN, J., ARGANDA-CARRERAS, I., FRISE, E., KAYNIG, V., LONGAIR, M., PIETZSCH, T., PREIBISCH, S., RUEDEN, C., SAALFELD, S., SCHMID, B., TINEVEZ, J. Y., WHITE, D. J., HARTENSTEIN, V., ELICEIRI, K., TOMANCAK, P. & CARDONA, A. 2012. Fiji: an open-source platform for biological-image analysis. *Nat Methods,* 9**,** 676-82.

SCHLEGELMILCH, K., MOHSENI, M., KIRAK, O., PRUSZAK, J., RODRIGUEZ, J. R., ZHOU, D., KREGER, B. T., VASIOUKHIN, V., AVRUCH, J., BRUMMELKAMP, T. R. & CAMARGO, F. D. 2011. Yap1 acts downstream of alpha-catenin to control epidermal proliferation. *Cell,* 144**,** 782-95.

SCHWARTZMAN, M., REGINENSI, A., WONG, J. S., BASGEN, J. M., MELIAMBRO, K., NICHOLAS, S. B., D'AGATI, V., MCNEILL, H. & CAMPBELL, K. N. 2016. Podocyte-Specific Deletion of Yes-Associated Protein Causes FSGS and Progressive Renal Failure. *J Am Soc Nephrol,* 27**,** 216-26.

SHEN, Z. & STANGER, B. Z. 2015. YAP regulates S-phase entry in endothelial cells. *PLoS One,* 10**,** e0117522.

SILVIS, M. R., KREGER, B. T., LIEN, W. H., KLEZOVITCH, O., RUDAKOVA, G. M., CAMARGO, F. D., LANTZ, D. M., SEYKORA, J. T. & VASIOUKHIN, V. 2011. alpha-catenin is a tumor suppressor that controls cell accumulation by regulating the localization and activity of the transcriptional coactivator Yap1. *Sci Signal,* 4**,** ra33.

SUCHTING, S., FREITAS, C., LE NOBLE, F., BENEDITO, R., BREANT, C., DUARTE, A. & EICHMANN, A. 2007. The Notch ligand Delta-like 4 negatively regulates endothelial tip cell formation and vessel branching. *Proc Natl Acad Sci U S A,* 104**,** 3225-30.

SWIFT, M. R. & WEINSTEIN, B. M. 2009. Arterial-venous specification during development. *Circ Res,* 104**,** 576-88.

TAMMELA, T., ZARKADA, G., WALLGARD, E., MURTOMAKI, A., SUCHTING, S., WIRZENIUS, M., WALTARI, M., HELLSTROM, M., SCHOMBER, T., PELTONEN, R., FREITAS, C., DUARTE, A., ISONIEMI, H., LAAKKONEN, P., CHRISTOFORI, G., YLA-HERTTUALA, S., SHIBUYA, M., PYTOWSKI, B., EICHMANN, A., BETSHOLTZ, C. & ALITALO, K. 2008. Blocking VEGFR-3 suppresses angiogenic sprouting and vascular network formation. *Nature,* 454**,** 656-60.

TEN DIJKE, P., GOUMANS, M. J. & PARDALI, E. 2008. Endoglin in angiogenesis and vascular diseases. *Angiogenesis,* 11**,** 79-89.

TOMLINSON, V., GUDMUNDSDOTTIR, K., LUONG, P., LEUNG, K. Y., KNEBEL, A. & BASU, S. 2010. JNK phosphorylates Yes-associated protein (YAP) to regulate apoptosis. *Cell Death Dis,* 1**,** e29.

TOTARO, A., CASTELLAN, M., BATTILANA, G., ZANCONATO, F., AZZOLIN, L., GIULITTI, S., CORDENONSI, M. & PICCOLO, S. 2017. YAP/TAZ link cell mechanics to Notch signalling to control epidermal stem cell fate. *Nat Commun,* 8**,** 15206.

TOWNSON, S. A., MARTINEZ-HACKERT, E., GREPPI, C., LOWDEN, P., SAKO, D., LIU, J., UCRAN, J. A., LIHARSKA, K., UNDERWOOD, K. W., SEEHRA, J., KUMAR, R. & GRINBERG, A. V. 2012. Specificity and structure of a high affinity activin receptor-like kinase 1 (ALK1) signaling complex. *J Biol Chem,* 287**,** 27313-25.

UBEZIO, B., BLANCO, R. A., GEUDENS, I., STANCHI, F., MATHIVET, T., JONES, M. L., RAGAB, A., BENTLEY, K. & GERHARDT, H. 2016. Synchronization of endothelial Dll4-Notch dynamics switch blood vessels from branching to expansion. *Elife,* 5.

UDAN, R. S., KANGO-SINGH, M., NOLO, R., TAO, C. & HALDER, G. 2003. Hippo promotes proliferation arrest and apoptosis in the Salvador/Warts pathway. *Nat Cell Biol,* 5**,** 914-20.

URIST, M. R. 1965. Bone: formation by autoinduction. *Science,* 150**,** 893-9.

VARELAS, X., MILLER, B. W., SOPKO, R., SONG, S., GREGORIEFF, A., FELLOUSE, F. A., SAKUMA, R., PAWSON, T., HUNZIKER, W., MCNEILL, H., WRANA, J. L. & ATTISANO, L. 2010. The Hippo pathway regulates Wnt/beta-catenin signaling. *Dev Cell,* 18**,** 579-91.

VASSILEV, A., KANEKO, K. J., SHU, H., ZHAO, Y. & DEPAMPHILIS, M. L. 2001. TEAD/TEF transcription factors utilize the activation domain of YAP65, a Src/Yes-associated protein localized in the cytoplasm. *Genes Dev,* 15**,** 1229-41.

VION, A. C., ALT, S., KLAUS-BERGMANN, A., SZYMBORSKA, A., ZHENG, T., PEROVIC, T., HAMMOUTENE, A., OLIVEIRA, M. B., BARTELS-KLEIN, E., HOLLFINGER, I., RAUTOU, P. E., BERNABEU, M. O. & GERHARDT, H. 2018. Primary cilia sensitize endothelial cells to BMP and prevent excessive vascular regression. *J Cell Biol*.

WADA, K., ITOGA, K., OKANO, T., YONEMURA, S. & SASAKI, H. 2011. Hippo pathway regulation by cell morphology and stress fibers. *Development,* 138**,** 3907-14.

WAGNER, D. O., SIEBER, C., BHUSHAN, R., BORGERMANN, J. H., GRAF, D. & KNAUS, P. 2010. BMPs: from bone to body morphogenetic proteins. *Sci Signal,* 3**,** mr1.

WALSH, D. W., GODSON, C., BRAZIL, D. P. & MARTIN, F. 2010. Extracellular BMP-antagonist regulation in development and disease: tied up in knots. *Trends Cell Biol,* 20**,** 244-56.

WANG, H. U., CHEN, Z. F. & ANDERSON, D. J. 1998. Molecular distinction and angiogenic interaction between embryonic arteries and veins revealed by ephrin-B2 and its receptor Eph-B4. *Cell,* 93**,** 741-53.

WANG, K. C., YEH, Y. T., NGUYEN, P., LIMQUECO, E., LOPEZ, J., THOROSSIAN, S., GUAN, K. L., LI, Y. J. & CHIEN, S. 2016. Flow-dependent YAP/TAZ activities regulate endothelial phenotypes and atherosclerosis. *Proc Natl Acad Sci U S A,* 113**,** 11525-11530.

WANG, X., FREIRE VALLS, A., SCHERMANN, G., SHEN, Y., MOYA, I. M., CASTRO, L., URBAN, S., SOLECKI, G. M., WINKLER, F., RIEDEMANN, L., JAIN, R. K., MAZZONE, M., SCHMIDT, T., FISCHER, T., HALDER, G. & RUIZ DE ALMODOVAR, C. 2017. YAP/TAZ Orchestrate VEGF Signaling during Developmental Angiogenesis. *Dev Cell,* 42**,** 462-478 e7.

WOLTJE, K., JABS, M. & FISCHER, A. 2015. Serum induces transcription of Hey1 and Hey2 genes by Alk1 but not Notch signaling in endothelial cells. *PLoS One,* 10**,** e0120547.

WU, S., HUANG, J., DONG, J. & PAN, D. 2003. hippo encodes a Ste-20 family protein kinase that restricts cell proliferation and promotes apoptosis in conjunction with salvador and warts. *Cell,* 114**,** 445-56.

XU, T., WANG, W., ZHANG, S., STEWART, R. A. & YU, W. 1995. Identifying tumor suppressors in genetic mosaics: the Drosophila lats gene encodes a putative protein kinase. *Development,* 121**,** 1053-63.

YOU, L. R., LIN, F. J., LEE, C. T., DEMAYO, F. J., TSAI, M. J. & TSAI, S. Y. 2005. Suppression of Notch signalling by the COUP-TFII transcription factor regulates vein identity. *Nature,* 435**,** 98-104.

YU, F. X. & GUAN, K. L. 2013. The Hippo pathway: regulators and regulations. *Genes Dev,* 27**,** 355-71.

YU, F. X., ZHAO, B. & GUAN, K. L. 2015. Hippo Pathway in Organ Size Control, Tissue Homeostasis, and Cancer. *Cell,* 163**,** 811-28.

YU, F. X., ZHAO, B., PANUPINTHU, N., JEWELL, J. L., LIAN, I., WANG, L. H., ZHAO, J., YUAN, H., TUMANENG, K., LI, H., FU, X. D., MILLS, G. B. & GUAN, K. L. 2012. Regulation of the Hippo-YAP pathway by G-protein-coupled receptor signaling. *Cell,* 150**,** 780-91.

YU, J., ZHENG, Y., DONG, J., KLUSZA, S., DENG, W. M. & PAN, D. 2010. Kibra functions as a tumor suppressor protein that regulates Hippo signaling in conjunction with Merlin and Expanded. *Dev Cell,* 18**,** 288-99.

ZANCONATO, F., BATTILANA, G., CORDENONSI, M. & PICCOLO, S. 2016. YAP/TAZ as therapeutic targets in cancer. *Curr Opin Pharmacol,* 29**,** 26-33.

ZHANG, H., LIU, C. Y., ZHA, Z. Y., ZHAO, B., YAO, J., ZHAO, S., XIONG, Y., LEI, Q. Y. & GUAN, K. L. 2009. TEAD transcription factors mediate the function of TAZ in cell growth and epithelial-mesenchymal transition. *J Biol Chem,* 284**,** 13355-62.

ZHANG, H., VON GISE, A., LIU, Q., HU, T., TIAN, X., HE, L., PU, W., HUANG, X., HE, L., CAI, C. L., CAMARGO, F. D., PU, W. T. & ZHOU, B. 2014. Yap1 is required for endothelial to mesenchymal transition of the atrioventricular cushion. *J Biol Chem,* 289**,** 18681-92.

ZHANG, M., CHANG, H., ZHANG, Y., YU, J., WU, L., JI, W., CHEN, J., LIU, B., LU, J., LIU, Y., ZHANG, J., XU, P. & XU, T. 2012. Rational design of true monomeric and bright photoactivatable fluorescent proteins. *Nat Methods,* 9**,** 727-9.

ZHANG, Y. E. 2009. Non-Smad pathways in TGF-beta signaling. *Cell Res,* 19**,** 128-39.

ZHAO, B., LI, L., TUMANENG, K., WANG, C. Y. & GUAN, K. L. 2010. A coordinated phosphorylation by Lats and CK1 regulates YAP stability through SCF(beta-TRCP). *Genes Dev,* 24**,** 72-85.

ZHAO, B., LI, L., WANG, L., WANG, C. Y., YU, J. & GUAN, K. L. 2012. Cell detachment activates the Hippo pathway via cytoskeleton reorganization to induce anoikis. *Genes Dev,* 26**,** 54-68.

ZHONG, T. P., CHILDS, S., LEU, J. P. & FISHMAN, M. C. 2001. Gridlock signalling pathway fashions the first embryonic artery. *Nature,* 414**,** 216-20.